TECHNISCHE UNIVERSITÄT WIEN
Vienna University of Technology

Organic Rankine Cycle

for

Waste Heat Recovery

A 30 credit units Master's thesis under supervision of

Ao. Univ. Prof. Dipl.-Ing. Dr. techn. Andreas WERNER

Institute for Energy Systems and Thermodynamics

A Master's thesis is completed at the Vienna University of Technology

for

Faculty of Mechanical Engineering and Science of Management

Martin Knoglinger

0526979 (E700)

Vienna, September 11 _____

Abstract

This essay describes the possibility to generate electricity by Organic Rankine Cycle (ORC) technology from so far unused waste heat in terms of hot flue gas. The so called ORC technology is able to produce electric power from low grade heat sources. A computer program was developed in PYTHON to calculate the electricity output by given heat source data. The program considers two different plant designs, one with and the other without internal heat exchanger. In the simulation hot flue gas and thermal oil represent the heat sources and cooling water was assumed to be the heat sink. This thesis describes how to apply the program and how to evaluate the results from calculations. Furthermore some parameter studies have been carried out in order to get a first rough magnitude of order about power output and thermal efficiency for given heat source data. Seven different organic fluids have been investigated and implemented into the program. Basically four different fluids (Isobutane, Isopentane, Pentane and Cyclopentane) show ideal performance for flue gas temperatures up to 300℃ (573.15K) in both plant designs. The developed program considers the interaction of heat source fluids with ORC plant. The program also calculates heat transfer properties from heat exchangers. These data could also be used for further economic studies but this is not content of this essay.

Preface

In the past decades economic growth and wealth forced the whole energy consumption worldwide to increase significantly. The impact on the environment, for instance due to CO_2 emissions, was not focused by the energy market in the past years. Nowadays, the importance of keeping climate as stable as possible has forced the politics to set new standards and frames for companies operating their core business in power generation. Furthermore research on how to increase the efficiency of energy consuming processes became very popular. The Organic Rankine Cycle offers an interesting opportunity to produce electric power from low grade heat sources. It is already used more than 30 years with a proven record of success. ORC plants use heat sources like geothermal water, biomass or solar heat and other heat sources. In recent years the application of ORC for waste heat recovery also became standard. The on-going rise of electricity prices forces companies to improve the efficiency of their industrial processes in order to save expenses. Thermal energy consuming processes are analysed and ORC modules are applied to improve the total process efficiency.

The traditional approach to design a power plant relies on thermodynamics and aims in maximising fuel utilisation efficiency. Hence such a method that is commonly applied for fossil fuel power plants is not suitable for ORC units used for waste heat recovery. Therefore the optimisation of the power output is more suitable as the available heat is for free. Thus the generation of heat supply is out of focus. This thesis focuses on how much electricity production is possible, when the temperature and mass flow rate of hot flue gases with a certain composition are given. Some restrictions like flue gas dew point and cooling water temperature have great impact on electricity output produced by ORC plants. Those limitations will be discussed later in this paper.

Acknowledgements

This work would not have been possible without supervision and guidance of my advisor Ao. Univ. Prof. Dipl.-Ing. Dr. techn. Andreas Werner. He gave me some advice and support especially in the early stage of modelling. The freedom of choosing the programming language and style made me feel like a respected colleague. As a result the Institute for Energy Systems and Thermodynamics obtains this work for further research.

My acknowledgement for cordial support is send to my Icelandic mentors Skúli Jóhannsson and Valdimar K. Jónsson, Professor Emeritus from the University of Iceland. During my stay in Iceland they offered me to work within their small geothermal company where I experienced my excitement in this field as well as in Organic Rankine Cycle technology.

I met many people during the study period at the university and I became very close with some of them. Therefore I would like to thank all of my friends, especially those who have shared their thoughts and incitations with me all the time. I will miss the conversations with them in the upcoming future and hope the contact will keep as close as in the past years.

I am deepest thankful to my family, especially to my parents Gertraud and August. Their financial support offered me the opportunity to study at the Vienna University of Technology. My parents, my sister as well as my brothers always gave some moral support during incurrence of this thesis. My devout thanks addresses to this great family.

Finally I would like to express my deepest appreciation to my girlfriend, Daniela, whose love and encouragement enabled me to complete this work. Many thanks for her efforts in proofreading this essay.

Table of Contents

List of Tables

List of Figures

1 Introduction

The temperatures of the exhaust from most industrial processes and power plants are less than 400 ℃ (643.15 K). These heat sources are clas sified as low grade heat sources. Waste heat from industrial processes, for instance in steel, glass or cement production as well as in oil and gas industry or from internal combustion engines, causes large thermal pollution. The potential of this heat is enormous and further usage is strongly recommended. Waste heat recovery maximises the total efficiency of manufacturing processes and results in economical benefit for companies.

One opportunity to capture wasted heat and convert it into high grade energy in terms of electricity provides the so called Organic Rankine Cycle (ORC). It is a similar cycle process as it is in traditional power cycle of fossil or nuclear power plants, but differs mainly due to its working fluid. The used working fluids in ORC units are organic substances, for instance hydrocarbons or siloxane, with considerable different thermo-physical properties as water. Basically the lower critical points and boiling temperatures are the crucial characteristics of such refrigerants and makes conversion of low grade heat into electricity feasible and economical.

Many studies already exist related to ORC. The papers mainly summarise research on different working fluids. Drescher [1] did some research for ORC in biomass plants by suggesting a model using more than one thermal oil circuit between flue gas and ORC. He found highest efficiencies within the family of alkylbenzenes. Ngoc Ahn Lai, Wendland and Fischer [2] investigated working fluids for high temperature ORC. They used BACKONE equations for working fluids and obtained in their research best performance by using Cyclopentane for heat carrier inlet temperatures of 280 up to 350℃. Cyclopentane is even used in this essay. The recent research of Roy, Mishra and Misra [3] considered R-12, R-123 and R134 as working fluids for power generation based on ORC. They developed a MATLAB program for optimisation of work output and thermal efficiency and investigated the influence of superheating in a similar way as in this paper. Borsukewicz-Gozdur [4] analysed the influence of heat recuperation for exhaust gases with the temperature of 350℃. He used Toluene in his research and evaluated a 5% increase of efficiency when an internal heat exchanger (IHE) was applied. Furthermore he studied supercritical ORC plants which generally promise higher power as well as efficiency output. They are not considered in this thesis either as nowadays they are not utilised due to safety issues. Other investigations concerning performance analysis and optimisation for ORC have been made from Wei [5] or even Declaye [6]. All of the previous mentioned studies have either considered a basic ORC or an ORC with internal heat exchanger plant design. This essay provides results of both plant configurations.

However, Table 1 (see below) shows critical point data and molar mass of different candidate working fluids in comparison with water. These data as well as the used Equations of States (EoS) in further calculations have been taken from REFPROP, a thermo-physical fluid database, provided by the National Institute of Standards and Technology (NIST) [7].

	CAS number	**Molar mass [kg/kmol]**	**Tcrit [K]**	**pcrit [kPa]**	**Equation of States (EoS)**	**max. Temp. by EoS [K]**
Isopentane	78-78-4	72.149	460.39	3369.6	[8]	589
Isobutane	75-28-5	58.122	407.81	3629	[9]	575
Octamethyl-trisiloxane	107-51-7	236.53	564.09	1415	[10]	673
Toluene	108-88-3	92.138	591.75	4126.3	[11]	700
Cyclohexane	110-82-7	84.161	553.64	4075	[12]	700
Cyclopentane	287-92-3	70.133	511.69	4515	[13]	600
Pentane	109-66-0	72.149	469.7	3370	[14]	600
Water	7732-18-5	18.015	647.1	22064	[15]	2000

Table 1: Thermodynamic properties and identification of candidate working fluids for ORC

As it is shown, ORC fluids have rather high molar mass and lower critical temperatures than water. The high molar mass of working fluid leads to small sized units (see Appendix 11.1 as well as Fig. 25) and basically low installation costs. Isopentane, Isobutane and Pentane have relative small critical temperatures in comparison to other listed fluids in Table 1. Therefore those fluids are classified as ‘low critical point fluids’ within this paper. Furthermore the substances can be classified into three different types depending on their slope of the saturated vapour line in the Temperature (T) – Entropy (s) diagram. Generally organic fluids can have positive, negative or almost isentropic inclinations. The slope of the saturated vapour curve in the T-s diagram is negative for water. Thus, limitations of expansion in the turbine are given due to accruing droplets which cause blade erosions. Therefore, superheating in conventional steam cycle processes is mostly applied. Using organic fluids with positive slope allows expansion to the superheated steam area starting from the saturated steam state. The problem of blade erosions is eliminated and superheating is not absolutely essential. Fig. 1 shows the T-s diagram of the listed fluids in Table 1.

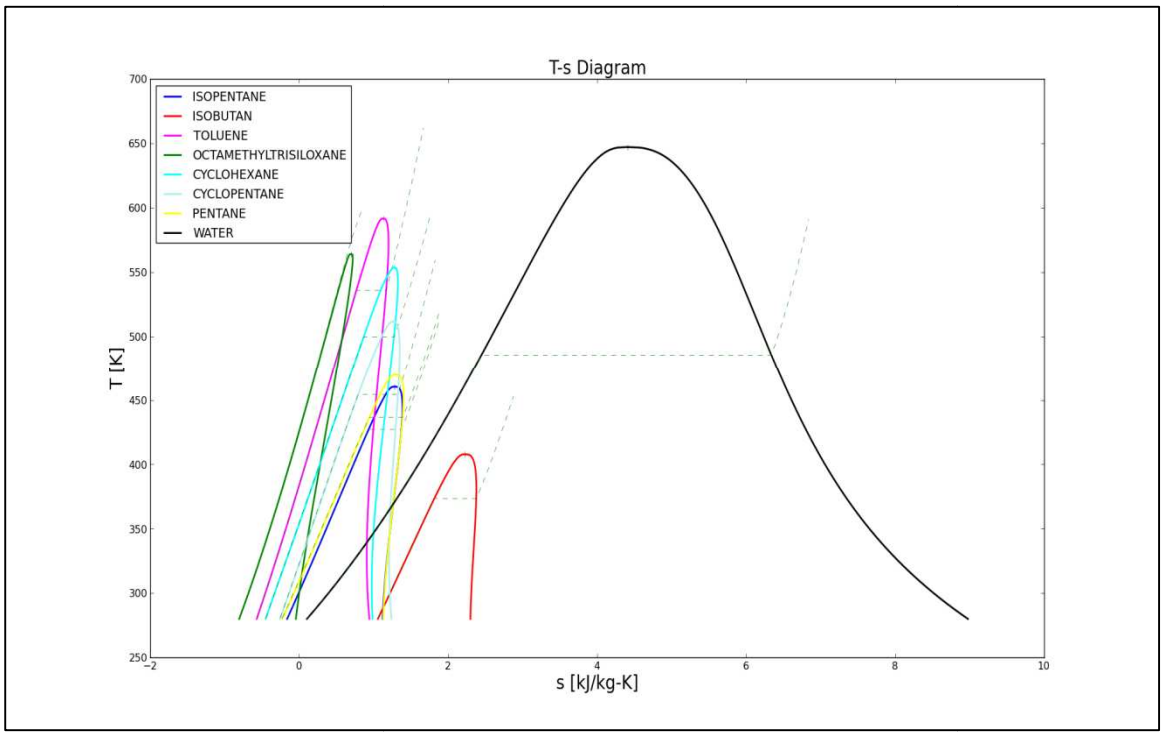

Fig. 1: T-s Diagram for different working fluids

Fig. 1 illustrates the different critical points and the dashed line within each fluid curve represents the isoline of constant pressure at 20 bars. Only the isobar line of Octamethyltrisiloxane (MDM in REFPROP) is in the supercritical region. If a fluid has positive inclination of its dew line, it is called a dry fluid. Additionally, it should be mentioned that organic fluids do have smaller latent heat in comparison to water. The proper choice of EoS-model is essential because in the calculation procedure thermo physical properties of working fluids are required for temperature ranges up to 280 ℃ (553 K). Beside the distinctive thermo-physical behaviour of each working fluid, other aspects such as health, safety and environmental impact have to be taken into account for selection [16].

1.1 Scope and target of the thesis

This essay suggests a model for an Organic Rankine Cycle whereas it is supposed that the ORC is powered by hot flue gas with certain composition. In between of flue gas and ORC a thermal oil circuit (considered in this model) is commonly used. Usually a thermal oil loop is implemented to ensure safe plant operation. The aim of this thesis was to develop a computer program to calculate the maximum power for certain given heat source states.

The intention of the thesis was to use free software. PYTHON was considered a proper choice for the given task. However, the developed program is able to calculate the best performance as well as the heat transfer parameter of heat exchangers. The latter data provide a base to continue this work in order to evaluate the cost of such ORC plants. Power optimisation correlates with maximising the thermal efficiency due to the set up of the thermodynamic model which is explained in the related chapter. Parameter studies have been evaluated in a certain application range and should even support the user of the program in choosing the most suitable fluid. Finally the user obtains a first-look estimation about how much power in terms of electricity can be produced.

2 Software

This chapter covers a short introduction about the Software used to develop the program and write the paper.

2.1 REFPROP

REFPROP is a thermodynamic and transport properties database for some substances. It is provided by the National Institute of Standards and Technology (NIST) [7]. 105 pure fluids, 5 pseudo fluids (such as air) as well as mixtures with up to 20 components are included. In this thesis seven fluids, listed in Table 1, were selected for ORC investigations and their thermodynamic properties have been taken from REFPROP. REFPROP can be linked to other programs, for instance MATLAB, as long as an interface code already exists. For further information refer to REFPROP documentation available at [7].

2.2 PYTHON

First of all it was important to use a free ware programming language. The goal was to figure out the most suitable programming language that is able to solve given mathematical tasks properly. On the one hand, there is the Software Scilab [17]. This program is more or less a MATLAB clone and its syntax is even very similar. It is able to solve scientific or numerical challenges in a similar way as MATLAB does, but due to the fact that it is available for free, some restrictions exist.

On the other hand, PYTHON was examined whether it would satisfy the needs of ORC performance calculation. PYTHON is free to use because of its OSI-approved open source license, even for commercial products. Basically, it is an object orientated programming language, but allows applying procedural, scientific or numerical programming paradigms as well. PYTHON has a very clear and understandable syntax and is based on packages. These packages extend the skills of the basic PYTHON software and fulfil the needs of different programming communities. As mentioned before, PYTHON is able to solve mathematical assignments by numerical or scientific programming. Those specific programming implies the usage of so called ‘numpy’ and ‘scipy’ packages. Finally, PYTHON was considered to be the most suitable software for given tasks of thesis. The PYTHON user community is much bigger in contrast to Scilab. This is essential because more support is available in terms of program application problems. Incidentally Bruce Wernick has given his permission to use his written interface code for linking REFPROP with PYTHON. He provides his code at the FAQ of [7]. Therefore no additional ‘work’ had to be done before and the focus was only on ORC performance optimisation.

PYTHON is an interpreter language, which means that it checks the code immediately line for line. Furthermore PYTHON is applicable within different development environments. PYTHON can be downloaded on [18] as well as all related documentation about the program. General information for PYTHON programming is given by Beazly [19]. Apart from the official documentation many tutorials are available in the web, for instance on YouTube [20]. Information about packages and their implementation into the basic PYTHON software is also explained in the documentation. The standard download of PYTHON provides an integrated development environment (IDLE), also called PYTHON shell. Development of complex PYTHON programs needs powerful debugging tools but the standard IDLE does not supply efficient debugging functions. However, for those people who want to learn PYTHON deeply, other development environments are recommended. In order to develop the ORC optimisation program in this thesis, PYTHON was used within Eclipse. To link those two programs 'Pydev' can be used. For further information refer to PYTHON documentation. The download at [21] provides an advanced development as well as already preinstalled packages (numpy, scipy) within PYTHON. Therefore it is recommended to download the software at this webpage. Once PYTHON is installed, the user is able to program. It should be mentioned as well that PYTHON provides more powerful tools to create a Graphical User Interface (GUI) in contrast to Scilab.

PYTHON provides many different GUI toolkits in which proper graphical design helps computer users to pass some input data to the program. In the ORC PYTHON program the probably most powerful toolkit, Qt, has been used. Qt is known for GUI programming and originates from C++ programming. Nowadays, Qt is even applied in other programming languages, for instance PYTHON. The Qt Designer permits the design of windows, buttons, list boxes (and much more) by easy drag and drop movements with the mouse. Afterwards the PYTHON code is created automatically. Further recommended information about Qt programming in PYTHON is given in [22] and also in chapter 11.3.

In this thesis PYTHON version 2.6.5.5 was applied, although the more developed version 3 (or also called 3000) is already on the market. When discussing the latest version the PYTHON community arguments that it is not fully developed yet. Furthermore PYTHON 3 is not compatible with earlier versions. However, PYTHON 2.6.5.5 has been considered suitable enough for given problem.

2.3 Others

MS EXCEL, MS WORD and MS VISIO were used apart from PYTHON and REFPROP.

3 Flue gas

In this thesis, hot flue gas streams have been simulated as heat source. This chapter describes how the thermodynamic properties, for instance the enthalpy, are calculated and why the knowledge of the dew point of a (flue) gas mixture is essential for thermodynamic modelling. Usually, hot flue gas streams coming from industrial processes, content some water vapour in terms of humidity as well as sulphur with respect to SO_2 or SO_3. Each individual flue gas mixture has its own certain dew point that varies from 100 up to 140℃ commonly. Okkes [23], [24] proposed an equation to compute the acid dew point.

$$T_{dew} = 365.6905 + 11.9864 * \ln(p_{H_2O}) + 4.70336 * \ln(p_{SO_3}) + (0.446 * \ln(p_{SO_3}) + 5.2572)^{2.19} \quad [3.1]$$

In Equ. [3.1] the partial pressures in mmHg and the sulphuric acid dew point in K are given. In order to use more familiar pressure units, for instance kPa, the equation can be written as shown in Equ.[3.2].

$$T_{dew} = 365.6905 + 11.9864 * \ln(p_{H_2O} * 0.13332) + 4.70336 * \ln(p_{SO_3} * 0.13332) + (0.446 * \ln(p_{SO_3} * 0.13332) + 5.2572)^{2.19} \quad [3.2]$$

If flue gas is cooled below the dew point, some water (vapour) as well as sulphur is bonding and condensation takes place. Thus, the condensed acids are very corrosive to steel and almost all plastics as well as hydraulic cement composites. Therefore those mist of corrosive acid droplets is in particular highly detrimental to the stack and heat recovery equipments. As it is explained in chapter 4 the flue gas transfers heat to a thermal oil circuit. Such configuration of the plant allows operating the flue gas at atmospheric pressure [1] furthermore it ensures safe operation of the plant. In order to develop the optimisation program for ORC, the thermodynamic properties of flue gas mixture (at low pressure) have been calculated by using the law of ideal gas mixtures. Fig. 2 shows the input GUI for 15 common flue gas components. The molar heat capacity (kJ/kmolK) at a constant pressure and the molar entropy (kJ/kmolK) of certain substance are given by

$$c^0_{p,specie}(T) / \Re = a_1 * T^{-2} + a_2 * T^{-1} + a_3 + a_4 * T + a_5 * T^2 + a_6 * T^3 + a_7 * T^4 \quad [3.3]$$

and

$$S^0_{specie}(T) / \Re = -a_1 * \frac{T^{-2}}{2} - a_2 * T^{-1} + a_3 * \ln(T) + a_4 * T + a_5 * \frac{T^2}{2} + a_6 * \frac{T^3}{3} + a_7 * \frac{T^4}{4} + b \quad [3.4]$$

where a_1 to a_7 as well as b are constants, $\Re$ is the universal gas constant and T represents the temperature in K. Those equations are proposed in [25]. Additionally the constants for many different gases are expressed. The referenced paper describes a developed computer program in FORTRAN that is used for the calculation of thermodynamic properties. The developed FORTRAN program was reprogrammed in PYTHON but only for selected gas components.

However, above mentioned equations can also be written as

$$c_{p,specie_{integral}} = \frac{R}{T-T_0} * \left(\left(-a_1 * T^{-1} + a_2 * \ln(T) + a_3 * T + a_4 * \frac{T^2}{2} + a_5 * \frac{T^3}{3} + a_6 * \frac{T^4}{4} + a_7 * \frac{T^5}{5} \right) - \left(-a_1 * T_0^{-1} + a_2 * \ln(T_0) + a_3 * T_0 + a_4 * \frac{T_0^2}{2} + a_5 * \frac{T_0^3}{3} + a_6 * \frac{T_0^4}{4} + a_7 * \frac{T_0^5}{5} \right) \right) \quad [3.5]$$

and

$$S_{specie} = R * \left(-a_1 * \frac{T^{-2}}{2} - a_2 * T^{-1} + a_3 * \ln(T) + a_4 * T + a_5 * \frac{T^2}{2} + a_6 * \frac{T^3}{3} + a_7 * \frac{T^4}{4} \right) + b \quad [3.6]$$

Equ. [3.5] represents the integral specific heat capacity (kJ/kgK) with T_0 at 273.15 K and Equ. [3.6] delivers the specific entropy in kJ/kgK. The universal gas constant in kJ/kmolK was replaced with a specific gas constant (kJ/kgK) of a gaseous species. The equations [3.5] and [3.6] refer only to a certain substance and are the base for further gas mixture computations. Gas mixture equations derive from using the law of ideal gas mixture. Equations related to previous mentioned approach were taken from [26].

$$c_{p,mix_{integral}} = \sum \left(\xi_{specie} * c_{p,specie_{integral}} \right) \quad [3.7]$$

The integral specific heat capacity of flue gas mixture is shown in Equ. [3.7], whereas ξ_{specie} defines the weight fraction of a certain gas substance. Equ. [3.8] refers to absolute specific entropy (kJ/kgK) of the whole gas mixture.

$$S_{abs,mixture} = \sum \left(S_{specie} * \xi_{specie} \right) - R_{mix} * \ln\left(\frac{p}{p_0} \right) - S_{mix} \quad [3.8]$$

The S_{abs}, mixture indicates the absolute entropy expressed in kJ/kgK of the whole (ideal) gas mixture. R_{mix} is the specific gas constant of the mixture and S_{mix} reflects the deviations due to mixing different substances (see Equ. [3.9]) whereas x_{specie} is the mol or volume fraction of a gas component.

Flue gas

$$S_{mix} = -R_{mix} * \sum x_{specie} * \ln(x_{specie}) \quad [3.9]$$

Basically the integral specific heat capacity as well as the specific entropy of the flue gas mixture is applied to determine the heat input and the exergy destruction in the flue gas/thermal oil heat exchanger. More information can be found either in the referenced literature or in the PYTHON file, Flue_gas.py. The latter mentioned covers all equations for flue gas calculation. For each function included in this file, short explanations are available. The implementation of this file in the whole PYTHON program is explained in the upcoming chapters.

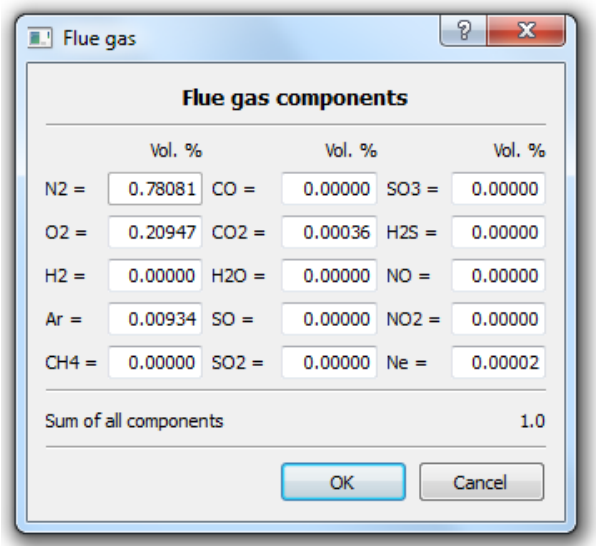

Fig. 2: Input GUI to pass flue gas components in volume fraction. The gas mixture substances can be passed as well to the program in weight fractions.

Nitrogen gas (N_2)

Molecular Oxygen (O_2)

Molecular Hydrogen (H_2)

Argon (Ar)

Methane (CH_4)

Carbon monoxide (CO)

Carbon dioxide (CO_2)

Water (vapour) (H_2O)

Sulphur oxide (SO)

Sulphur dioxide (SO_2)

Sulphur trioxide (SO_3)

Hydrogen sulphide (H_2S)

Nitrogen oxide (NO)

Nitrogen dioxide (NO_2)

Neon (Ne)

4 Thermodynamic Modelling

The developed PYTHON program is able to determine the optimum performance of ORC for two different plant configurations, either the very basic ORC or the configuration with internal heat exchanger (IHE). The thermodynamic model distinguishes depending on which configuration is chosen by the user of the program. However, in each case a thermal oil circuit is located in between of the hot flue gas and the ORC. The additional circuit has to extract the heat from flue gas streams and transfers it to the ORC working fluid. The operation of waste heat ORC plant in that specific configuration has some advantages. It was already mentioned in the previous chapter the advantage to allow the flue gas operating at atmospheric pressure within the flue gas/thermal oil heat exchanger. Thus, the consequences of this operation are desired advantages in construction as well as in safety aspects. Even high pressurised water is used in present waste heat recovery plants, but this fact was not considered in this thesis. The following reference has summarised the main issues of thermal oil in contrast to pressurised water [27]. Thermal oil has usually lower heat capacity than water. The heat capacity is even not constant, when temperature varies within certain ranges. In contrast to water where heat capacity remains (almost) at the same level over a wide temperature range. In order to set up the thermodynamic model, specific thermal oil, Mobiltherm 603, was used for the PYTHON program. Drescher [28] has proposed and even used a linear equation in his researches on ORC in biomass plants, shown in Equ.[4.1] The equation accords with the approach of an incompressible fluid, where the specific heat capacity depends only on temperature but not on pressure. The heat capacity is expressed by

$$c_{p,oil} = 0.0036 * T + 0.8184 \qquad [4.1]$$

where $c_{p,oil}$ is expressed in kJ/kgK. The equation was also validated in this essay and the following different temperatures were chosen in order to prove the validity of the equation.

Temperature [℃]	**$c_{p,oil}$ given by** [29] **[kJ/kgK]**	**$c_{p,oil}$ by Equ. [4.1] [kJ/kgK]**	**Rel. discrepancies [%]**
100	2.18	2.164	0.84
160	2.4	2.38	0.93
200	2.54	2.52	0.72
260	2.76	2.74	0.81
300	2.91	2.88	0.97

Table 2: Validation of proposed equation by Drescher [1]

As it is shown in Table 2, the relative discrepancies are lower than 1 % and therefore the equation is a proper approach. In order to avoid decomposition of the thermal oil, the maximum temperature of 285 ℃ (=558.15 K) has been assumed to be the upper limit [30]. Therefore, the thermal oil outlet temperature in the flue gas/thermal oil heat exchanger may not exceed this limit. Furthermore, the exergy destruction can be calculated in all thermal oil heat exchangers as follows. The thermal oil represents an incompressible fluid in the model, whereas Baehr [26] derived Equ. [4.2] for the computation of the entropy difference.

$$\triangle s = s(T_2) - s(T_1) = \int_{T_1}^{T_2} c_p(T) * \frac{dT}{T} \qquad [4.2]$$

If Equ. [4.1] is applied, the change in entropy due to different temperatures of the thermal oil can be expressed as

$$\triangle s = 0.0036 * (T_2 - T_1) + 0.8184 * \ln(T_2/T_1)\,. \qquad [4.3]$$

Equ. [4.3] is the base for calculations regarding to exergy destruction within thermal oil heat exchangers.

4.1 Basic Organic Rankine Cycle

The standard cycle has no internal heat exchanger (IHE) and is usually only more efficient in contrast to the advanced cycle when waste heat is available at very low grade. Fig. 3 shows the plant design for a standard configuration without IHE.

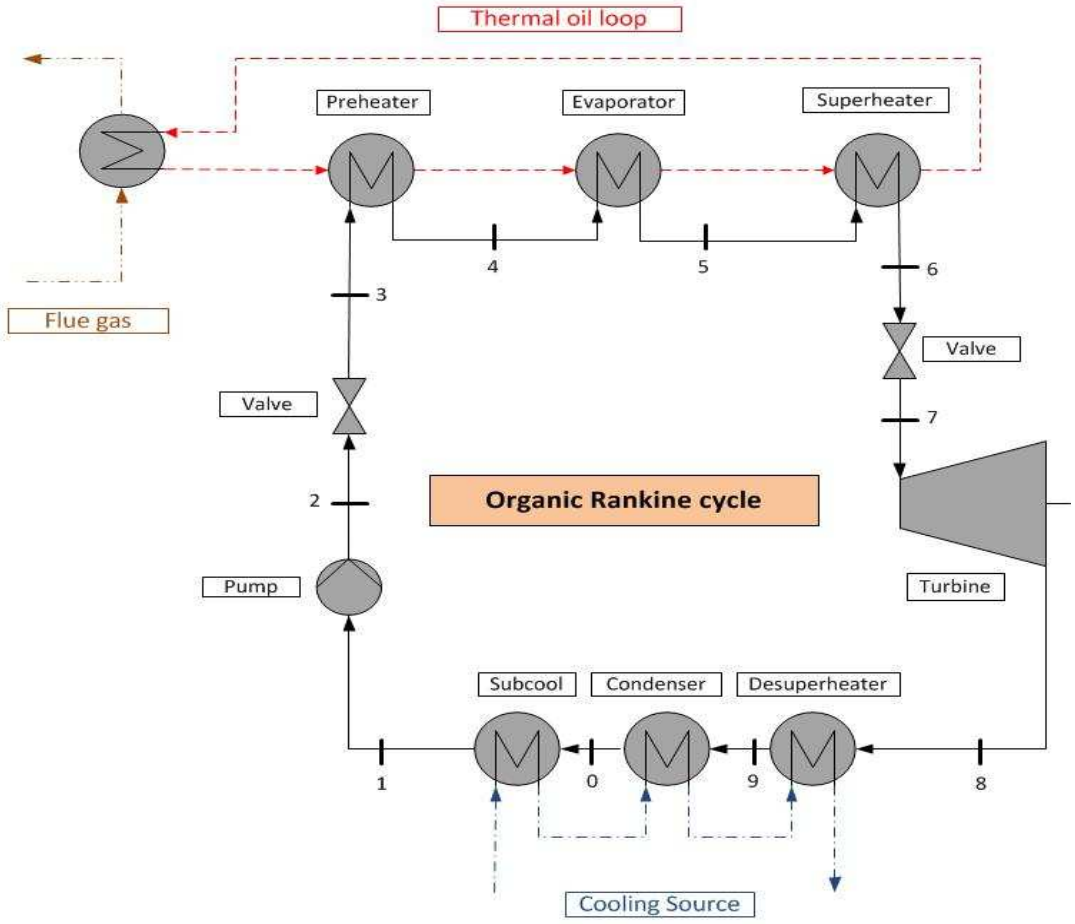

Fig. 3: Plant design of the basic ORC

As the ORC is similar to the basic steam power cycle the equations in terms of energy balances look identically. The heat source is provided by a hot flue gas stream where the heat is transferred to the (additional) thermal oil circuit. The ORC fluid is pressurised by the pump, afterwards evaporation takes place due to heat coming from thermal oil. Finally power is produced in the turbine due to expansion of the fluid. Fig. 3 does not illustrate the generator which is driven by the turbine. The circuit closes when condensation changes the aggregate state of the substance. The whole condensation is split into three distinct processes in the model. This approach accords to the more familiar modelling of the evaporation process. The separation takes the different heat transfer behaviour due to

different thermo-physical properties into account, for instance significant change of heat transfer coefficient (k-value), during condensation. The k-value depends on the aggregate phase (wet- or dry steam, liquid) of the working fluid and has considerable influence on heat exchanger areas in each section of condensation. Generally counter flow heat exchangers have been considered in all cases. Commonly there is only one component in a plant configuration, called the condenser, where whole condensation is realised. The oil inlet and outlet temperature expressions ($T_{oil,in}$ $T_{oil,out}$) always refer to flue gas/thermal oil heat exchanger. The same variables are used if balances relate to the evaporation process within the ORC. Additionally the Temperature-Entropy diagram shows the meaning of used variables. The following variables and equations comply with Fig. 3 and the T-s diagram shown in Fig. 4.

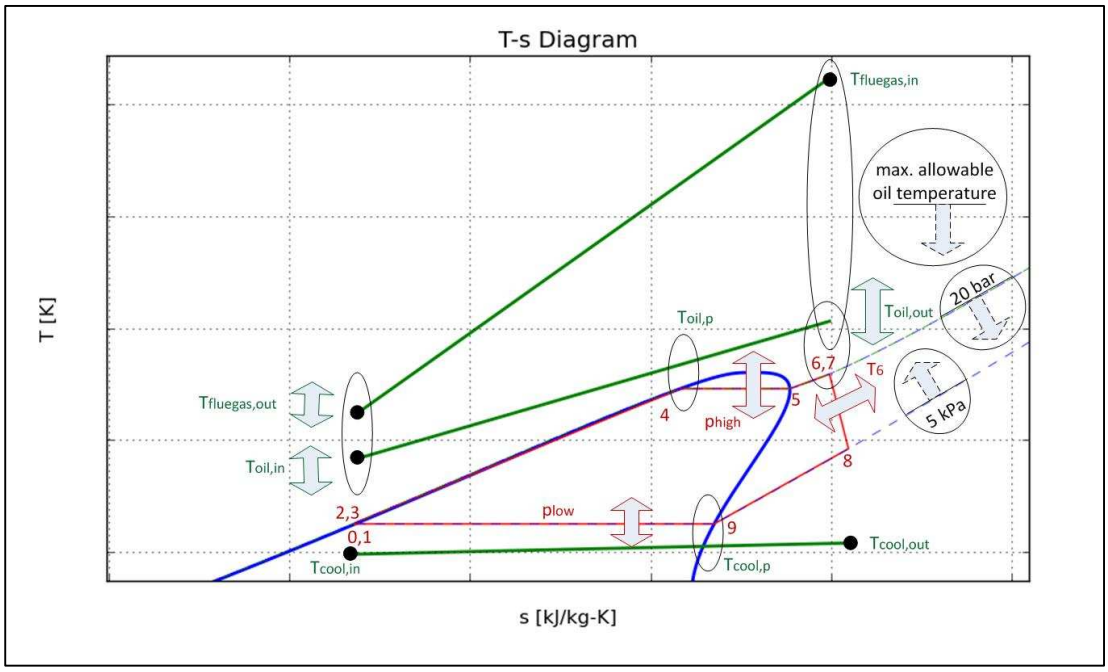

Fig. 4: Temperature-Entropy Diagram of basic ORC

The energy balances for flue gas stream and thermal oil are given by Equ. [4.4] and Equ. [4.5]. Q_{in} is expressed in kW in either case.

$$Q_{in} = \dot{m}_{fluegas} * \left(c_{p_{fluegas,in}} * T_{fluegas,in} - c_{p_{fluegas,out}} * T_{fluegas,out} \right) \quad [4.4]$$

$$Q_{in} = \dot{m}_{oil} * \left(0.0018 * \left(T_{oil,out}{}^{2} - T_{oil,in}{}^{2} \right) + 0.8184 * \left(T_{oil,out} - T_{oil,in} \right) \right) \quad [4.5]$$

The equations are valid for the second plant configuration, because the heat source is independent from plant design. Heat transfer to ORC is determined by Equ. [4.6].

$$Q_{in} = \dot{m}_{ORC} * \left(h_6 - h_3 \right) \quad [4.6]$$

Further cycle equations are listed below. For instance, the specific gross work output (kJ/kg) is defined by

$$w_t = (h_8 - h_7) * \eta_{m,t} * \eta_{e,t} \quad [4.7]$$

and the consumed specific work (kJ/kg) of the pump is

$$w_p = \frac{h_2 - h_1}{\eta_{p,m} * \eta_{p,e}} \quad [4.8]$$

where $\eta_{p,e}$ and $\eta_{p,m}$ are the mechanical and electrical efficiencies for the pump and the same applies to the turbine using the variables $\eta_{t,e}$ and $\eta_{t,m}$. The thermal efficiency is either expressed by

$$\eta_{th} = \frac{(-w_t) - w_p}{h_6 - h_3} \quad [4.9]$$

or

$$\eta_{th} = \frac{P}{Q_{in}} \quad [4.10]$$

whereas it is dimensionless. Equ. [4.10] shows for a defined heat input that power optimisation correlates with thermal efficiency optimisation. However, the reader should also be familiar with all other variables used in the PYTHON code. The heat sink is cooling water and the following energy balance describes the cooling behaviour.

$$\dot{m}_{cool} * c_{p_{cool}} * (T_{cool,in} - T_{cool,out}) = \dot{m}_{ORC} * (h_8 - h_1) \quad [4.11]$$

The heat capacity of cooling water is assumed to be constant over the whole cooling proces. Additionally the following balances are necessary to seek and find appropriate pressure levels in ORC.

$$moil * (0.0018 * (T_{oil,p}{}^2 - T_{oil,in}{}^2) + 0.8184 * (T_{oil,p} - T_{oil,in})) = m_{ORC} * (h_4 - h_3) \quad [4.12]$$

and

$$m_{cool} * c_{p_{cool}} * (T_{cool,p} - T_{cool,in}) = m_{ORC} * (h_9 - h_1) \quad [4.13]$$

Thermodynamic Modelling

In order to figure out the maximum power output, some restrictions have to be taken into account. Fig. 4 illustrates the chosen boundaries and the below listed restrictions have been assumed for modelling and are also marked within black ellipses or cycles in Fig. 4.

- Upper pressure limit of 20 bars
- Lower pressure limit of 5 kPa (considered due to selection of fluids)
- Pinch point in condenser
- Pinch point at evaporator/preheater to thermal oil
- Minimum allowable temperature difference at the cold side of the thermal oil/flue gas heat exchanger (defines the oil inlet temperature)
- Minimum allowable temperature difference at the hot side of the thermal oil/flue gas heat exchanger
- Minimum allowable temperature difference between the oil outlet temperature and temperature of state 6 (which was chosen to be equal to minimum allowable pinch point at evaporator/preheater to thermal oil)
- Maximum allowable thermal oil temperature (285℃).

Apart from above listed restrictions, the following assumptions are applied in the program:

- The program neglects pressure drops in all heat exchangers as illustrated in Fig. 5. In spite of this assumption a pressure drop simulation can be executed by using the throttles modelled in each plant configuration.
- Steady state in all components within the plant.
- The irreversibility in turbine and pump are simulated with isentropic efficiencies.

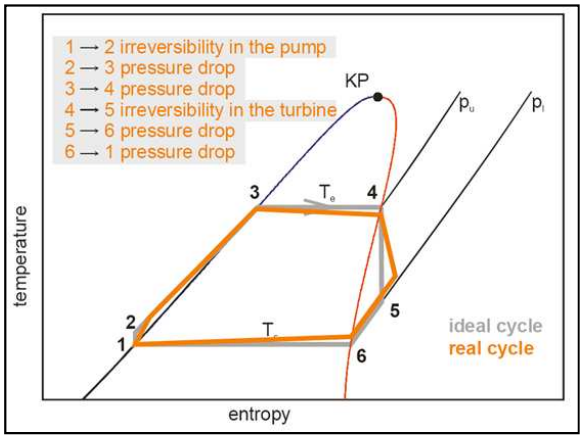

Fig. 5: Ideal cycle in contrast to real cycle [42]

- Adiabatic expansion in turbine as well as compression in pump.
- No heat losses in all heat exchangers except in the IHE

The flue gas and the thermal oil are figured as straight lines in the Temperature-Entropy diagram (Fig. 4). The cooling water is drawn as a straight line as well. Those straight lines do not represent the reality, but visualise the relations properly. As it is shown in Fig. 4, the black dots are fixed points given by the program user. Generally, the mass flow rate, the temperature as well as the components of the flue gas are given by the user. So far simple water cooling is assumed. Furthermore the inlet cooling temperature of cooling water, for instance river water, is supposed to be known. In many countries it is not permitted to exceed a certain cooling outlet temperature to protect the environment. Therefore the outlet cooling state is supposed to be given as well. Other cooling applications such as wet or dry cooling towers haven't been considered in this thesis. The double-arrows in the diagram indicate the degrees of freedom in the whole system.

4.1.1 Implementation into PYTHON file

The challenge of this thesis was to find a proper algorithm for the whole thermodynamic system. Since the thermodynamic equations of the basic ORC have already been mentioned, the implementation into a PYTHON file is explained in this chapter. The file Orc_optimisation.py only covers the optimisation algorithm for power output as well as the thermal efficiency for the standard ORC configuration. Furthermore OrcwithIHE_optimisation.py does the same in case of ORC with IHE. In addition the calculation of exergy destruction and kA values are included in the files. Equations for last mentioned parameters can be studied by the reader in the written PYTHON code. For more information on how the PYTHON files are linked and how they interact between each other is explained in the upcoming chapters.

Nevertheless the difficulty was to figure out the maximum performance. The impact of superheating is not absolutely clear yet and depends also on what kind of fluid has been chosen. Previous studies have mostly neglected the impact of superheating or used a fixed superheated temperature for their research. Basically they focused on the cycle itself and did not investigate the interaction of heat source and ORC. As the influence of superheating is not entirely known, the set up of optimisation algorithm should demonstrate the interaction of energy equations when superheating is applied step by step. Therefore some essential parameters are recorded during the optimisation procedure and diagrams (Parameter study 1-5 in output GUI) showing how the system behaves dependant on applied superheating.

Basically superheating is applied within a WHILE loop in the program. The program incrementally adds 1℃, starting from non superheat ing state. The loop terminates if either the oil temperature minus the highest process temperature in cycle is smaller than the given pinch point restriction at evaporator/preheater to the thermal oil or the oil outlet temperature

exceeds the maximum allowed oil temperature (285 °C). While the program gradually raises the superheating temperature the upper and lower pressure levels are set accurately to obtain minimum allowable pinch point temperatures given by the user. Those numerical approaches for suitable pressure levels are set by mathematical solvers provided by PYTHON.

As it was mentioned in Chapter 2.2, even PYTHON has some restrictions in comparison with MATLAB. As it is known (by the author) MATLAB offers a high variety of optimisation functions, either for unconstrained or constrained problems. The provided mathematical solvers are available in the so called 'Optimization Toolbox'. If more information about solvers in MATLAB is desired, please refer to the MATLAB documentation and [31]. PYTHON does not supply many distinct solvers. The Scipy package covers some solvers, but they are mostly unconstrained. Nevertheless, in order to calculate the maximum power the program uses one scalar function minimiser, called Brent method, as well as a general multidimensional root finding solver named fsolve. Information about provided solvers in PYTHON generally is given in scipy documentation [32].

Because of the limitations in solver opportunities, there are also some consequences for the developed ORC program in PYTHON. The upper as well as the lower pressure levels represent two independent variables. They are set to fulfil desired pinch points and in addition the upper pressure level may not exceed 20 bars (constrained solving). Since PYTHON does not provide a solver function for those specific tasks, the optimisation code (shown in Appendix 11.2) has been developed in order to obtain optimum ORC performance. In the first lines of the code, it was assumed the oil outlet temperature has the same temperature difference like flue gas inlet temperature compared to flue gas outlet temperature and oil inlet temperature. Thus, if the curves in temperature entropy diagram are considered as straight lines, they would be parallel, but in reality they are not straight, as already discussed before. As discussed also, the upper pressure level is set to 20 bars and the lower pressure level is supposed to be the vapour pressure at cooling water outlet temperature (it turned out, that this is a suitable approach). The pinch point at evaporator/preheater to thermal oil is evaluated by above mentioned assumptions. In the upcoming chapters, the term 'first guess calculation' refers to this approach.

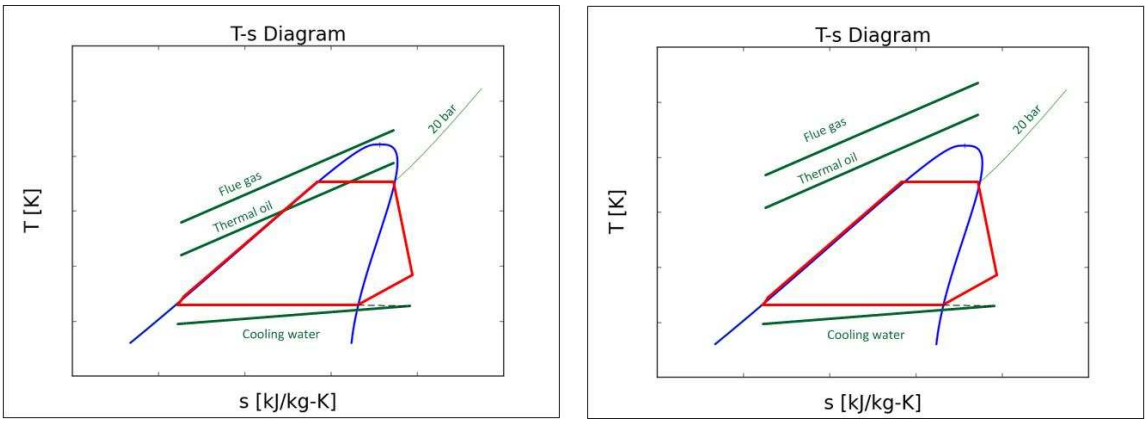

Fig. 6: The first guess calculation shows the relation between heat source (temperatures) and ORC. If flue gas/thermal oil temperature is relatively low (left diagram, first case), the upper pressure level in the cycle has to be reduced and fsolve is applied. Otherwise (right diagram, second case) the pressure is kept constant at 20 bars for optimisation and the single variable solver Brent is used.

If the evaluated pinch point of the first guess calculation is higher than the desired minimum (allowable) pinch point, the Brent solver of PYTHON applies by minimising the function

$$f = \text{absolut}\left(\Delta T_{cool,p} - \Delta T_{cool,p,seek}\right) \qquad [4.14]$$

where $\Delta T_{cool,p}$ means the pinch point in condenser caused by inappropriate, currently chosen pressure guesses done by the Brent solver, and $\Delta T_{cool,p,seek}$ is the minimum allowable pinch given by the user of the program. Minimising of Equ. [4.14] is based on the seeking process of the correct condenser pressure level, and in case of convergence the minimised function returns to zero. The Brent method is a single variable solver and seeks in our case the lower pressure level while the upper pressure level is kept constant at 20 bars. The search for the suitable pressure level has been done for each step of superheating temperature raise, caused by the WHILE loop (see Appendix 11.2.3). The most important parameters are recorded in vectors during optimisation until the WHILE loop is terminated. The oil outlet temperature is calculated in that case as well. The power output maximum is extracted from recorded vectors.

If the pinch point at the first guess calculation returns smaller values in comparison to the desired input pinches, another solver is used by PYTHON. The so called fsolve function seeks zeros of non linear equation systems and is a root finding solver. Two non linear equations, Equ. [4.15] and Equ. [4.16] are solved in that case and the proper lower as well as upper pressure level are returned by the solver.

$$\text{absolut}\left(\triangle T_{oil,ORC,p} - \triangle T_{oil,ORC,p,seek}\right) = 0 \qquad [4.15]$$

$$\text{absolut}\left(\triangle T_{cool,p} - \triangle T_{cool,p,seek}\right) = 0 \qquad [4.16]$$

The variables $\Delta T_{oil,ORC,p}$ and $\Delta T_{cool,p}$ are the presently calculated pinch points in the cycle caused by inaccurate pressure guesses from solver. $\Delta T_{oil,ORC,p,seek}$ as well as $\Delta T_{cool,p,seek}$ are the associated desired values given by the program user. The oil outlet temperature is fixed during processing the WHILE loop. The non linear equation solver needs some guess values in order to obtain convergence due to correct pressure solutions. In contrast to the Brent algorithm, no boundaries have to be set by the user and therefore the solver seeks the solution close to the guess input. The settings of required guess values were basically a disadvantage when developing a stable running ORC optimisation program for high variety of input flue gas temperatures. When analysing the parameter study (done in EXCEL Chapter 6), it turned out that in almost all cases convergence was found with chosen guess values proposed in PYTHON code (Appendix 11.2.3). In certain cases, the guess value had to be changed when the evaluation took place. This should be kept in mind when new evaluations (parameter studies) are prepared in future as well as if new fluids are added to the already existent program. If more information concerning solvers in PYTHON is required please refer to PYTHON documentation [18].

4.2 Organic Rankine Cycle with internal heat exchanger

Commonly ORC's with internal heat exchanger (IHE) are applied. The IHE is often called regenerator or recuperator. However, in this paper the letters IHE refer to the plant configuration as shown in Fig. 7.

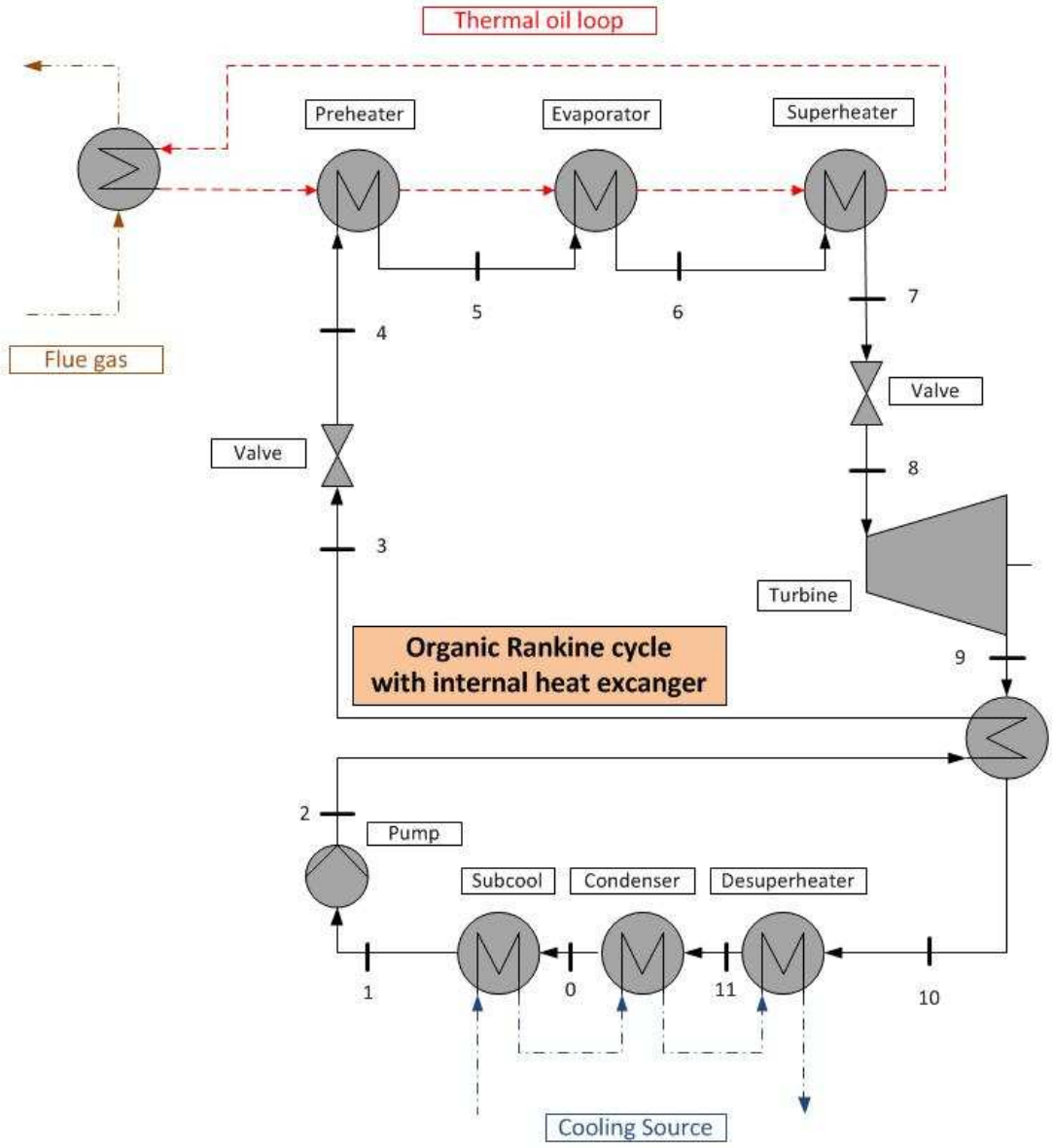

Fig. 7: Organic Rankine Cycle with internal heat exchanger

Basically the application of an ORC with IHE leads to better performance in comparison to traditional ORC on condition that these cycles work at same pressure levels. Usually the benefit shows up as some of the sensible heat after the turbine (superheated steam) can be used to preheat the working fluid. Following equations refer to ORC with IHE configuration. The heat input is given by Equ. [4.4]. Equ. [4.5] remains also equal like at basic ORC

configuration. These equations are defining the state of the heat source which implies that they are independent from cycle configuration. The transferred heat to the cycle is now referenced to other states which are shown in Equ. [4.17].

$$Q_{in} = m_{ORC} * (h_7 - h_4) \quad [4.17]$$

Below there are listed equations concerning the configuration of the second cycle. The output of work given in Equ. [4.18] is now referred to state 8 and state 9.

$$w_t = (h_9 - h_8) * \eta_{m,t} * \eta_{e,t} \quad [4.18]$$

The consumed work of the pump expressed in Equ. [4.8] has already been defined in Chapter 4.1. The thermal efficiency is either expressed by Equ. [4.9] or Equ. [4.19]. The latter equation refers to state 7 and 4 instead of state 6 and 3.

$$\eta_{th} = \frac{(-w_t) - w_p}{h_7 - h_4} \quad [4.19]$$

Equ. [4.20] describes cooling behaviour and Equ. [4.21] and Equ. [4.22] are both needed for pinch analysis. They also refer to the second plant configuration illustrated in Fig. 7.

$$\dot{m}_{cool} * c_{p_{cool}} * (T_{cool,in} - T_{cool,out}) = \dot{m}_{ORC} * (h_{10} - h_1) \quad [4.20]$$

$$m_{oil} * \left(0.0018 * \left(T_{oil,p}{}^2 - T_{oil,in}{}^2\right) + 0.8184 * \left(T_{oil,p} - T_{oil,in}\right)\right) = m_{ORC} * (h_5 - h_4) \quad [4.21]$$

$$m_{cool} * c_{p_{cool}} * (T_{cool,p} - T_{cool,in}) = m_{ORC} * (h_{10} - h_1) \quad [4.22]$$

The heat loss in the IHE is considered by Equ. [4.23]

$$\eta_{IHE} = \frac{h_3 - h_2}{h_9 - h_{10}} = 0.9 \quad [4.23]$$

An efficiency of 0.9 was considered as a proper approach for the simulation. The temperature of state 10 must be at least 10 ℃ high er than of state 2. In order to optimise power output with given equations, the same assumptions have been taken as mentioned in Chapter 4.1.

4.2.1 Implementation into PYTHON file OrcwithIHE_optimisation.py

The mathematical optimisation works very similar in comparison to traditional ORC configuration which is shown in Appendix 11.2.3. The specific configuration of ORC with IHE design together with the chosen model of fixed flue gas inlet as well as outlet temperature leads to another new restriction. Preheating of the fluid by IHE is limited because of a minimum allowable temperature difference at the cold side in preheater/thermal oil heat exchanger. There the temperature difference is assumed to be not less than 10 °C. However, the first guess calculation is calculated in a similar way but with equations mentioned in this chapter. Equ. [4.14], Equ. [4.15] and Equ. [4.16] are also used for optimisation of power output. It turned out that in the second case of the first guess calculation implying the application of solver function fsolve, almost all cases showed best performance when no superheating was applied (in either case ORC with or without IHE).

4.3 Validation of developed PYTHON program

While the ORC optimisation PYTHON program was created, Opitz [33] developed a similar program on the Engineering Equation Solver (EES). Some information about EES is published in [34]. EES also provides a great database of refrigerant substances as well as siloxane. Opitz has applied the same model for the basic ORC calculation, but users of this program have to set the degrees of superheating in advance. Due to the similarity of the EES and the developed PYTHON program the validation of basic ORC cycle was simple to execute. The programs have been compared for couple of different flue gas settings and they have shown almost similar results. The discrepancies were negligible small and probably caused by using different thermodynamic property databases. Opitz did not set up a model to optimise the ORC with IHE plant configuration, and thus validation was much more difficult. Previous studies, for instance [2] and [35], have calculated such plant design, but mostly without consideration of an additional thermal oil circuit. However, it is known from those studies that ORC with IHE should basically have a 1 to 5 % percentage higher thermal efficiency. For validation of ORC with IHE some assumed settings of the standard ORC program were calculated. Thereby flue gas outlet temperatures were chosen in that way that optimisation was always based on superheating at upper pressure limit of 20 bars. Afterwards the same settings were applied for ORC with IHE optimisation and then the results of different ORC designs were compared. The evaluation was in accordance with already experienced results from recent papers. The plant configuration with IHE shows considerable higher efficiencies, at least when the Brent solver of PYTHON was applied.

.

5 Graphical User Interface programming in PYTHON

This chapter contents a short introduction about GUI programming in PYTHON and in particular the application on the developed program. It presents the input as well as the output GUIs of the ORC program. Furthermore explanations about the file structure and how the PYTHON files are linked together are given in this chapter.

In chapter 2.2 it was mentioned that PYTHON supplies a big variety of GUI toolkits, whereat Qt is probably the most powerful. Therefore the designed GUIs for this ORC program have been developed with Qt version 4. This version permits to create a GUI either by written code or drag and drop design. In this regard Mark Summerfield's book [22] gives an excellent explanation on how to do GUI programming in either case. Designing a GUI with drag and drop movements is much more convenient and thus this method was used for this PYTHON program. The toolkit provides a so called Qt-Designer where GUI dialogs can be easily created without much effort. Qt-Designer can also be used to make signal-slot connections but only between built-in signals and slots. When a program developer completes a GUI draft, a PYTHON code has to be generated. PYTHON saves the design in this generated code. Afterwards the GUI mask has to be connected with some execution code lines, written by the developer, for instance a mathematical calculation. The linking is done in a developer environment, for instance Eclipse. Basically three files belong to one GUI.

1. One file where the GUI draft is stored for the Qt designer itself. In this case the file extension for the GUI draft is *.ui.
2. A file generated with the pyuic4 commandline program has the file structure ui_*.py. This file should not be modified once it was established
3. Finally a third file with common PYTHON file extension *.py imports the file of above mentioned ui_* file. The linking of certain user written code with the GUI is accomplished in this file.

In order to develop the optimisation program some files have been created. The goal of creating more than one file is to minimise the written code in the main program. The files are usually called modules or packages according to the PYTHON documentation. The split of a program code into several files has some advantages. For instance the file Flue_gas.py contents all equations belonging to the flue gas property calculation. In this file different functions are stored where each has its specific task. Short descriptions about what a function calculates generally are given in the so called docstring. A docstring is a string literal

that occurs as the first statement in a module, function, class or method definition. This derives from the PYTHON convention of user community. Furthermore Fig. 28 shows how the files are linked and what kinds of files are invoked by the program. The file Equations_of_States.py must be invoked by the main input GUI where it defines equation of states for thermodynamic properties of a certain fluid. If a fluid is added to the Program, a proper equation has to be chosen in order to run maximum process temperatures in the cycle of 280 ℃ or 553 K. Table 1 shows the chosen EoS for implemented fluids. Appendix 11.2.3 shows the PYTHON module Orc_optimisation.py where the thermodynamic optimisation of the cycle takes place. The optimisation algorithm of the latter file was already explained in the last chapter.

5.1 Input GUI

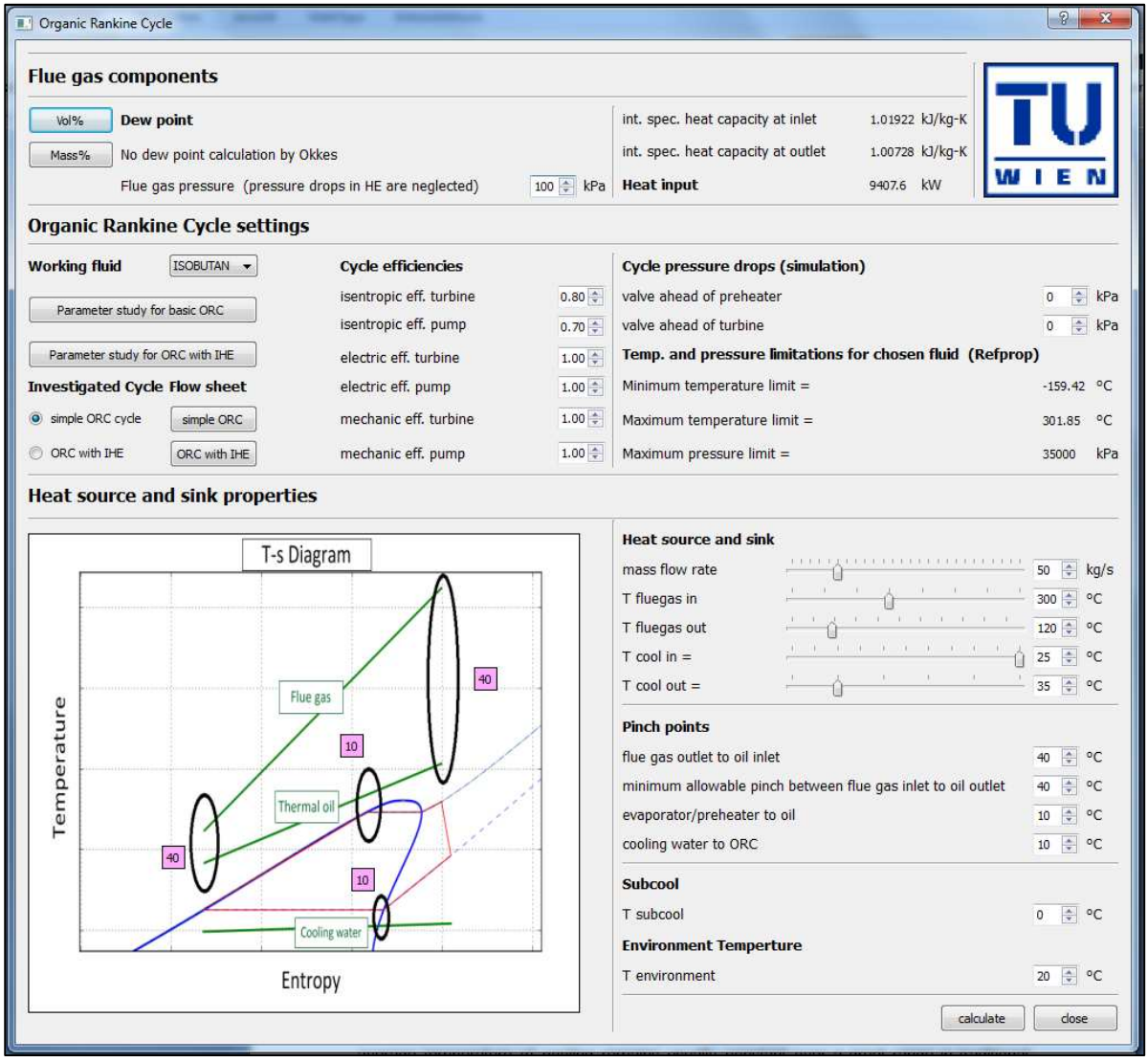

Fig. 8: Input GUI of the main program

On the upper left corner of the main GUI are push buttons to invoke the flue gas GUI shown in Fig. 2. When the user passes a certain flue gas composition and presses the “Ok” button, the flue gas GUI closes and the updated integral specific heat capacities as well as the heat input returns in the upper right corner within the main GUI. Furthermore the dew point temperature is computed and displayed. In Fig. 8 settings of dry air have been used and thus no dew point was calculated by the program. The ORC settings include efficiencies, pressure drop assumptions, and the choice of working fluid as well as the selection of plant configuration. The push button (‘Parameter study for basic ORC’ or ‘Parameter study ORC with IHE’) opens an EXCEL file where studies have been carried out. This is explained in detail in Chapter 6. Other push buttons only open figures of distinctive plant designs and have no further meaning. Basically the most important input data are the mass flow rate of flue gas, the flue gas inlet and the outlet temperature as well as the cooling temperatures. Finally the user must set the pinch points, the sub cooling temperature and the ambient temperature. Latter is used to calculate the exergy destruction. The push button “calculate” opens the output GUI with the data of the optimum performance.

5.2 Output GUI

Principally two output GUIs are available within this program, either for the basic ORC or the ORC with IHE configuration.

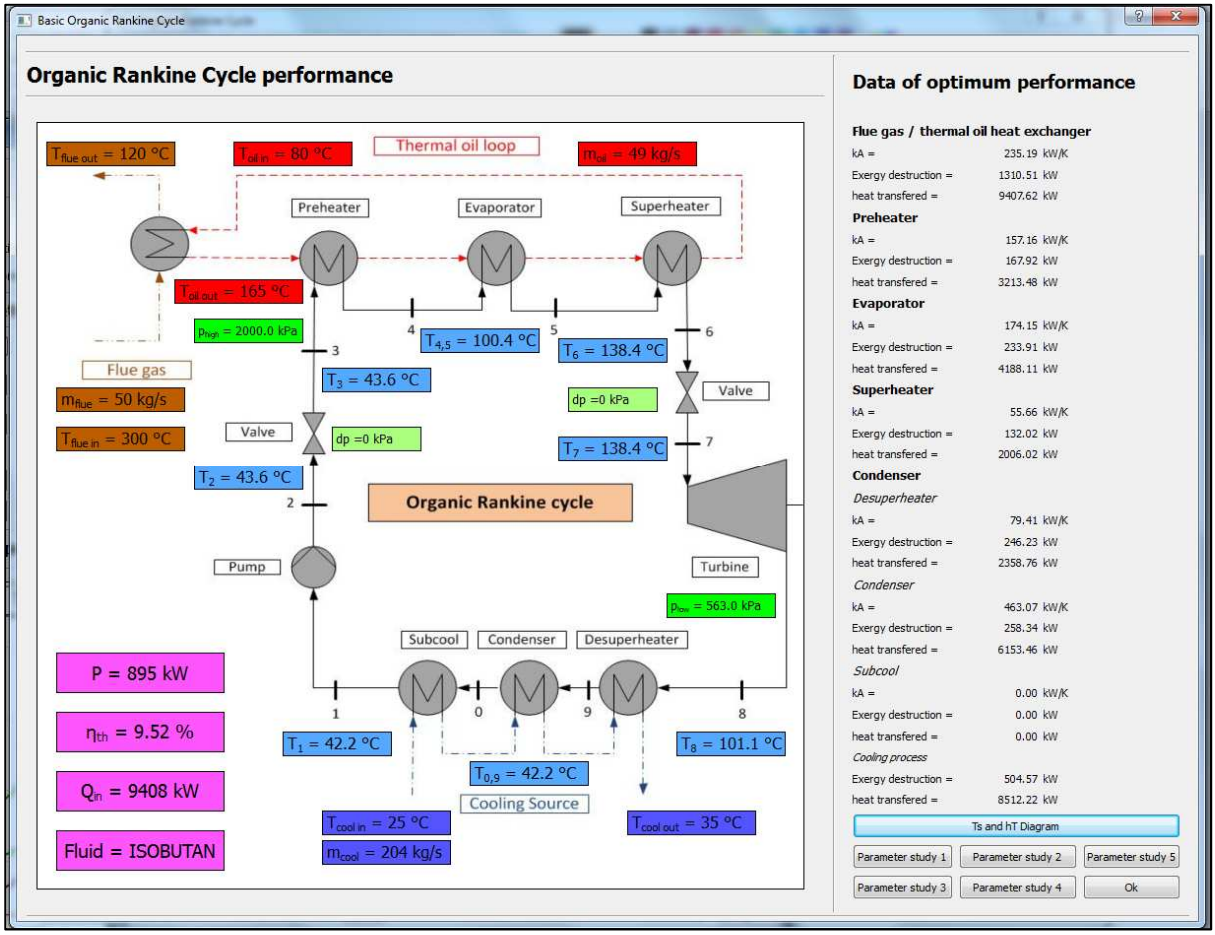

Fig. 9: Output GUI of optimum cycle performance

All important data of optimum cycle performance are displayed in the output GUI, for instance the temperatures, the mass flow rates of flue gas, the working fluid and the cooling water. One example on how such output GUI looks like is given in Fig. 9. Furthermore the pressure levels in the cycle and the power output as well as the thermal efficiency are declared. On the right side of the figure above the heat transfer coefficient, transferred heat and exergy destruction is shown for each heat exchanger component individually.

5.2.1 Parameter study figures of optimisation and T-s as well as h-T diagram

As it was mentioned in previous chapters, the program records parameters during optimisation in order to demonstrate in diagrams how the system behaves due to applied superheating. Most of the push buttons on the lower right corner of the output GUI deliver this recorded data in figures. The ‘T-s and h-T Diagram’ button opens the so called figures of optimum performance found by the optimisation algorithm. The ‘Parameter study 1’ shows a power output T_7, $T_{oil,out}$, $T_{evaporator}$ versus p_{high} diagram. This is informative when the first case of the ‘first guess calculation’ applies, since the already mentioned parameters depend on various p_{high} pressure levels. Otherwise the optimisation is based on a constant upper pressure level of 20 bars and the diagram is not demonstrative. However the second button shows the parameter p_{high}, p_{low}, power output and thermal efficiency depending on the cycle temperature T_7, which signifies the maximum process temperature in the cycle.

The mass flow rates of working fluid, cooling water and thermal oil are shown in ‘Parameter study 3’. The figure expresses in particular how much quantity of cooling water will be needed if such cooling temperatures are applied. This data might help the user in the selection of the cooling design of a specific potential location. If less river water than needed is available on site, other cooling opportunities, for instance a wet cooling tower, will be taken into account. The buttons 4 and 5 are useful to understand the optimisation itself done by the program. For instance ‘Parameter study 4’ shows how certain enthalpy differences behave and how they influence the thermal efficiency. ‘Parameter study 5’ displays some temperatures regarding the cooling process. In addition the average temperature of the whole heating process as well as the average temperature of the cooling process is put on view. This figure is essential to understand crucial distinctions of ORC in comparison to the traditional steam cycle. Therefore more detailed description is given below to support the user in analysis of this figure. Unfortunately it is not displayed how many degrees of superheating are applied during the optimisation in all diagrams, but the state of non superheating is always illustrated in dots. Therefore the diagrams demonstrate properly if superheating leads to significant improvement of cycle performance or not.

5.2.1.1 Evaluation of program results and diagrams

It was described before, what kind of settings the program user needs to pass to the input GUI. In this section of the essay the evaluation of the diagrams mentioned in Chapter 5.2.1 is explained more detailed. First of all the optimisation of the basic ORC will be figured and evaluated. Then thermodynamic behaviour will be explained in comparison with the traditional steam cycle. Furthermore the distinction to the more advanced plant design with internal heat exchanger will be described.

If the program calculates the optimum performance of settings shown in Fig. 8, but using ORC with IHE configuration, a power output of 1019 kW and a thermal efficiency of 10.83 % can be obtained. In contrast to the results shown in the output GUI in Fig. 9, the basic configuration leads to minor less power output and thermal efficiency. This behaviour was explained in Chapter 4.3 and accords to recent studies. Before the figures are evaluated some new variables are introduced. Equ. [6.1] defines the well known average temperature of heat input according to the T-s diagram of Fig. 4.

$$T_{m,in} = \frac{h_6 - h_3}{s_6 - s_3} \qquad [6.1]$$

When the ORC with IHE configuration is considered, state 7 must be set instead of state 6 and even state 3 must be replaced by state 4. When defining an average temperature of cooling in accordance to an average temperature of heating, this can be expressed by Equ. [6.2].

$$T_{m,out} = \frac{h_8 - h_1}{s_8 - s_1} \qquad [6.2]$$

In case of ORC with IHE the equation can be read as follows.

$$T_{m,out} = \frac{h_{10} - h_1}{s_{10} - s_1} \qquad [6.3]$$

The latter two equations are introduced to express the difference of ORC in comparison to the traditional steam cycle. Baehr [26] made a detailed analysis of the simple steam cycle in his book. He shows that fuel optimisation accords with maximising the thermal efficiency. The specific shape of water in the Temperature-Entropy diagram expresses great latent heat at low pressure levels. On the one hand the power optimisation is restricted due to turbine inlet temperatures because of limited heat resistance of materials. On the other hand there is limited expansion opportunity into the wet region. Baehr also mentioned that an increase of average temperature of heating leads to higher efficiencies. However the predefined average temperature of cooling usually will remain constant over a wide range in a traditional cycle if superheating is applied at a certain evaporation pressure level. This behaviour is opposite to ORC where the average temperature of cooling rises with additional applied superheating. Basically the specific, dry shape of organic fluids in the Temperature-Entropy diagram is responsible for the explained pattern of behaviour. Thus Fig. 10 demonstrates how key parameters react depending on various turbine inlet temperatures. At this point it should be noticed that in this case Isobutane was chosen for the evaluation and other fluids can show other results. Non superheating is expressed by the dots on the left side of the diagram.

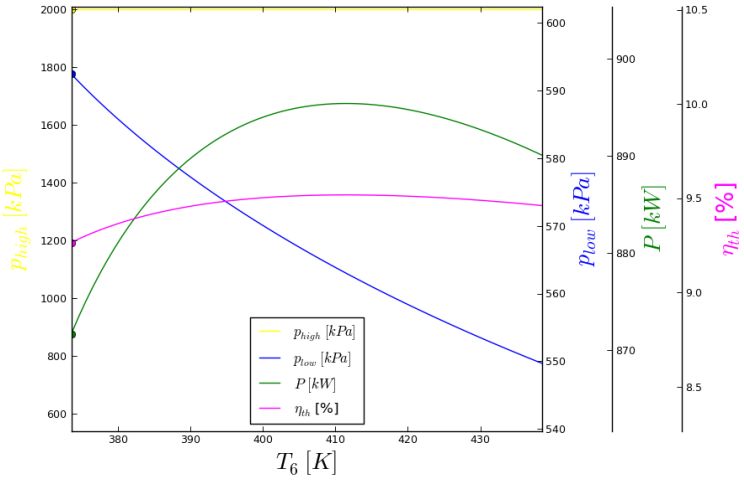

Fig. 10: Parameter study 2 for Isobutane: Different key parameters vs. turbine inlet temperature T_6

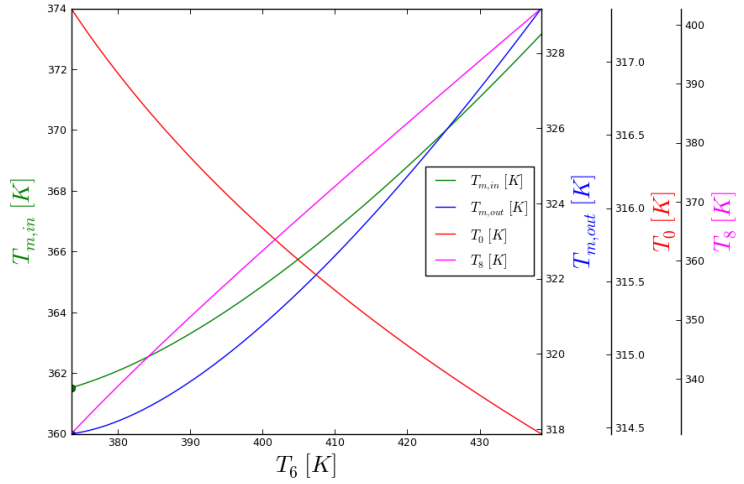

Fig. 11: Parameter study 5 for Isobutane: $T_{m,in}$ and $T_{m,out}$ as well as T_0 and T_8 vs. turbine inlet temperature T_6

It should be assessed that superheating leads to a maximum power output as well as thermal efficiency for predefined settings and Isobutane. Nevertheless in this specific case an additional component in the cycle would increase the installation costs and probably no superheating is more economically. This is not investigated in this thesis but further studies could analyse the economical issues. As it is shown in the figure, power maximum always correlates with thermal efficiency optimum according to Equ. [4.10] and the chosen model set up. As it is illustrated in Fig. 11 the rise of the average temperature of heating forces the average temperature of cooling to increase simultaneously. Aside from higher average temperature of heating the power output shows a peak at 38 ℃ of superheating. Fig. 10 also

shows that the condenser pressure level can be slightly reduced when superheating is applied. Thus this implies a small decrease of the condenser temperature T_0, as it is demonstrated in Fig. 11 as well. In spite of the lower condenser pressures at more advanced superheating the average temperature of cooling increases. The following conclusions can be drawn from the discussion above. The continuous increase of the temperature of state 8 is responsible for the rise of the average temperature of cooling in contrast to the steam cycle where the condenser temperature itself usually represents the average cooling temperature. Thus optimum performance behaviour appears at certain average temperatures. The complexity of superheating was analysed and a new variable was introduced to reveal that mainly the sensible heat in the cooling process distinguishes ORC from traditional cycle. However the enthalpy differences of heat input and cooling are crucial for calculation of the thermal efficiency and the power output. The following results have been extracted from the output vectors of the program in order to observe system performance in numbers.

T6 [K]	**Tsup. [K]**	**Tm,in [K]**	**Tm,out [K]**	**h6-h3 [kJ/kg]**	**h8-h1 [kJ/kg]**	**ηth [%]**	**Power [kW]**	**h6 [kJ/kg]**	**h8 [kJ/kg]**
373.51	0	361.51	317.87	366.36	332.42	9.265401	871.65	677.23	639.46
374.51	1	361.59	317.90	369.49	335.19	9.283829	873.38	680.17	642.05
375.51	2	361.66	317.94	372.59	337.93	9.30107	875.00	683.08	644.61
376.51	3	361.75	317.98	375.64	340.64	9.31720	876.52	685.96	647.14
377.51	4	361.83	318.04	378.66	343.32	9.33229	877.94	688.81	649.64
378.51	5	361.93	318.10	381.65	345.98	9.34644	879.27	691.63	652.13
	...								
410.51	37	366.82	322.71	469.42	424.74	9.51769	895.38	775.35	726.80
411.51	38	367.01	322.91	472.05	427.12	9.51779	895.39	777.88	729.08
412.51	39	367.22	323.11	474.67	429.50	9.51769	895.38	780.41	731.36
...	...								

Table 3: Evaluation of parameters for the given example

As above-mentioned the table refers to the given example. Basically superheating always increases the enthalpy differences of heat input as well as heat rejection. In the present example a substantial superheating of 38 °C shows the best performance and results in power improvement of more than 20 kW, in contrast to non superheating configuration. The cycle optimisation for Isobutane along two constant pressure levels is also demonstrated in the Appendix for a more clear understanding of the thermal efficiency peak. In all cases superheating does not lead to a power or even thermal efficiency improvement particularly for a standard ORC design. The thermo physical property of each fluid is responsible for its

specific behaviour. As already discussed above, more power output as well as thermal efficiency can be obtained by using an IHE. Fig. 12 and Fig. 13 show the optimisation in case of using an additional heat exchanger IHE.

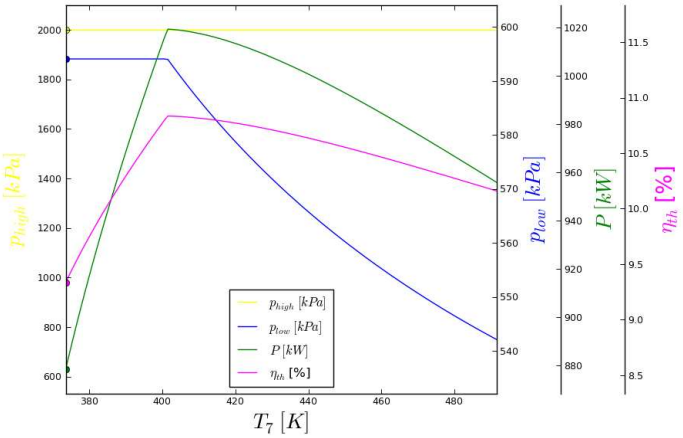

Fig. 12: Parameter study 2 for Isobutane: Different key parameters vs. turbine inlet temperature T_7

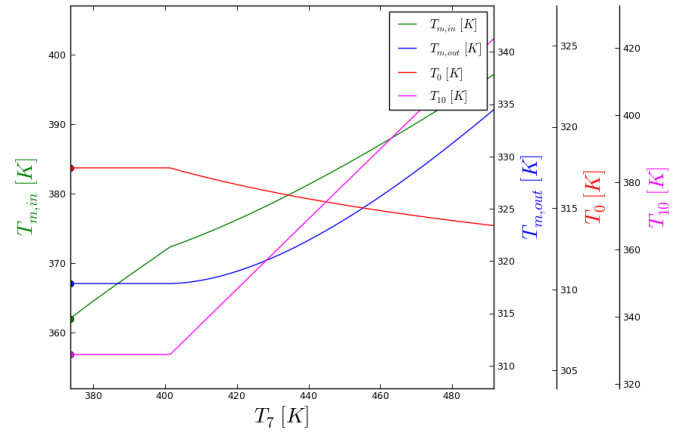

Fig. 13: Parameter study 5 for Isobutane: $T_{m,in}$ and $T_{m,out}$ as well as T_0 and T_{10} vs. turbine inlet temperature T_7

In contrast to the standard ORC configuration, applied superheating shows a significant increase of power output. This represents the strong slope of the power curve of the almost straight line in Fig. 12. Suddenly power and thermal efficiency reach a peak and further superheating does not lead to more outcomes. This fact is caused by the restriction of the limited temperature difference between the thermal oil inlet and the temperature of state 4. The temperature of 10℃ has been considered as proper assumption. Thus a limitation of maximum heat transfer within the IHE exists. If further superheating is applied, no more heat in the IHE can be shifted to support preheating the fluid after the pump. The consequence is

a rise of temperature of state 10 which is similar to the temperature increase of state 8 in the standard configuration before. This reduces the power in that case. The T-s and h-T diagram for the optimum performance is illustrated in following figure.

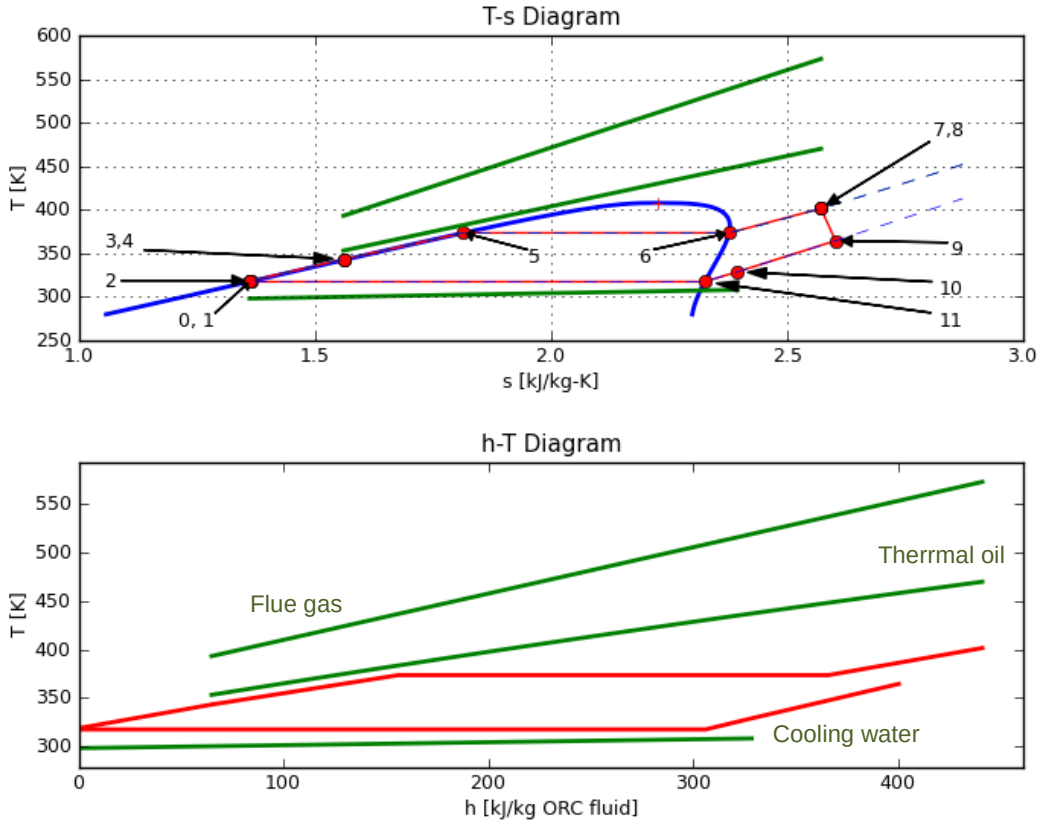

Fig. 14: T-s and h-T diagram for the given example with Isobutane

It should be noticed as well that in case of used IHE the pressure level in the condenser is kept constant until power peak is obtained in contrast to standard ORC where the condenser pressure declines even for small quantities of superheating.

6 Parameter studies for rough estimation of optimum performance

In the previous chapters the application of the developed PYTHON program was explained. In the PYTHON program the user has to set the flue gas outlet temperature whereat there is a limitation due to the dew point of the flue gas. This is one of the most essential parameters because of the following reasons. The upper pressure level in the cycle depends mainly on the chosen flue gas outlet temperature in case of the fluids with relatively high critical point. If small flue gas outlet temperature is chosen the pressure in the cycle will be forced to remain fairly low to match pinch point settings. Thereby only minor thermal efficiency can be obtained. In addition the temperature drop of the flue gas determines the heat input to the thermal oil as well as to the ORC as it is shown in Fig. 15. Although low flue gas outlet temperatures lead to higher heat input it does not have to be in accordance with maximum power output. Instead the optimum power output appears at a certain trade off between thermal efficiency and heat input. The temperature configuration in the whole system is responsible for the feasible high thermal efficiency where the heat input is most notably a function of the available mass flow rate of the heat source.

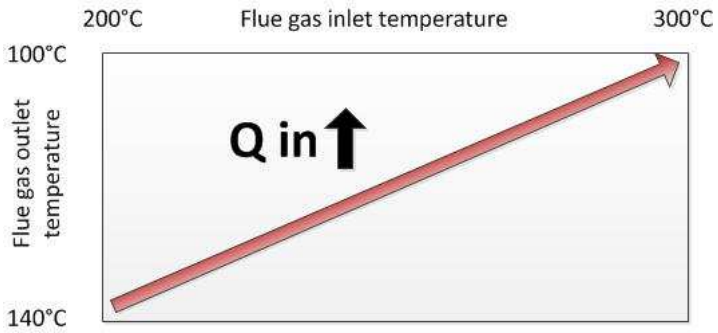

Fig. 15 shows how heat input depends on flue gas temperature configuration

Usually the program user does not know how to set the flue gas outlet temperature for maximum power output. Thus some parameter studies have been carried out for 6 working fluids. Octamethyltrisiloxane (MDM) was not considered for this study, because this substance is used for biomass applications and relatively low vapour pressure does not allow an operation with chosen cooling conditions in the parameter studies. The evaluation was made for flue gas inlet temperatures between 200 and 300 ℃ and flue gas outlet temperatures of 100 up to 150 ℃. In both cases the incremental step for evaluation was 10 ℃ with or without IHE. The flue gas composition of dry air has been chosen because for this study no dew point restriction was desired. Finally the study shall support the user of the program to figure out where the maximum performance is located with respect to the flue gas inlet and the outlet temperature configuration. In addition it is important to know on what

kind of fluid the user should focus for more detailed evaluation with other flue gas mass flow as well as the composition settings.

Parameter study-settings	
Flue gas data	
Flue gas composition =	dry air
m =	50kg/s
η,Iso,turbine =	80%-
η,iso,pump =	70%-
Pinch points settings	
Flue gas outlet/ Oil inlet =	40°C
Oil/Evaporator =	10°C
Flue gas inlet/ Oil outlet =	40°C
Condenser/ cooling water =	10°C
Cooling states	
T cool inlet =	25°C
T cool outlet =	35°C

Table 4 shows settings that have been chosen for the parameter studies. The flue gas composition of dry air has been taken from [26] and was already shown in Fig. 2.

As it was mentioned in Chapter 1 the investigated fluids are classified in low and high critical point fluids. The parameter study explanations refer to one selected fluid for either case. On the one hand Isopentane represents the behaviour of low critical point fluids and on the other hand Cyclopentane does the same for others. Therefore the interpretation and evaluations are done for these mentioned fluids and some patterns can be derived from the observed substances. The parameter studies of the remaining potential working fluids are even shown in Appendix 11.4. Furthermore the evaluations refer either to ORC with IHE or to the simple design. Finally some conclusions can be drawn when all parameter studies are compared to each other. The most suitable fluid for a certain chosen temperature configuration is the consequence of the evaluated studies. The comparison of fluids will be shown in Chapter 6.3.

6.1 Parameter study for Isopentane

6.1.1 Parameter study for basic ORC plant

	P [kW]	Tflue,in [°C]										
IPENTANE	Tflue,out [°C]	200	210	220	230	240	250	260	270	280	290	300
	100	219	303	418	566	742	936	1147	1280	1357	1434	1511
	110	354	443	549	672	812	969	1129	1206	1283	1360	1437
	120	391	478	577	690	815	955	1055	1132	1209	1286	1363
	130	386	472	567	672	788	904	981	1058	1134	1212	1289
	140	359	443	535	635	744	830	906	983	1060	1137	1214
	150	318	400	489	585	679	755	832	908	985	1062	1140

Table 5: Power output for distinct flue gas temperature configurations for Isopentane

	ηth [%]	Tflue,in [°C]										
IPENTANE	Tflue,out [°C]	200	210	220	230	240	250	260	270	280	290	300
	100	4.26	5.33	6.73	8.42	10.23	12.04	13.81	14.49	14.49	14.49	14.49
	110	7.63	8.58	9.65	10.82	12.06	13.34	14.49	14.49	14.49	14.49	14.49
	120	9.45	10.27	11.15	12.1	13.09	14.13	14.49	14.49	14.49	14.49	14.49
	130	10.67	11.39	12.15	12.95	13.79	14.49	14.49	14.49	14.49	14.49	14.49
	140	11.57	12.21	12.88	13.58	14.31	14.49	14.49	14.49	14.49	14.49	14.49
	150	12.27	12.84	13.44	14.06	14.49	14.49	14.49	14.49	14.49	14.49	14.49

Table 6: Thermal efficiency for distinct flue gas temperature configurations for Isopentane

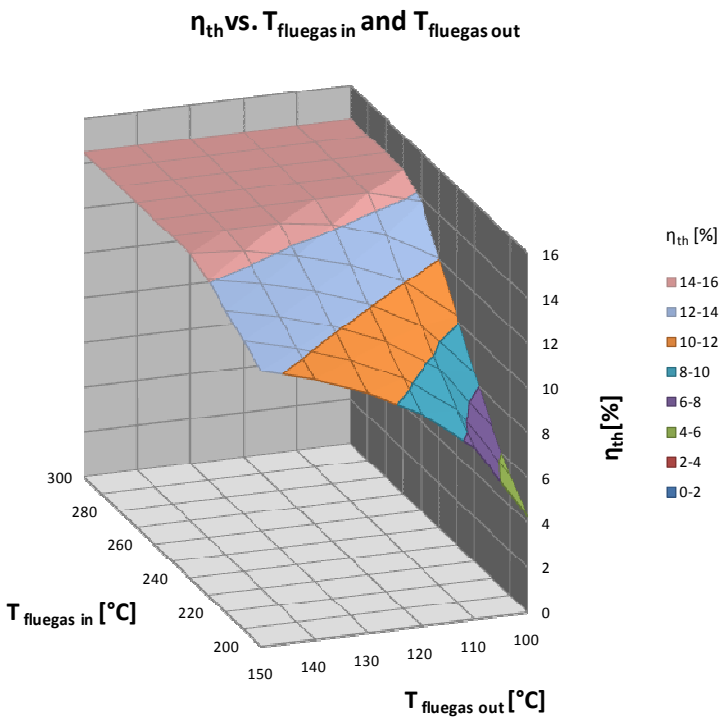

Fig. 16: Thermal efficiency vs. $T_{fluegas,in}$ and $T_{fluegas,out}$ for Isopentane

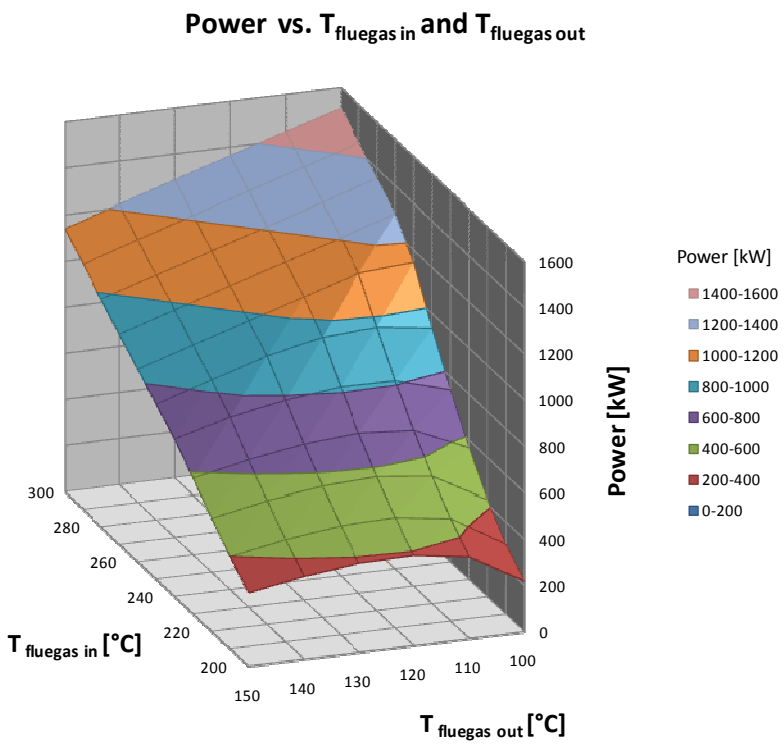

Fig. 17: Power output vs. $T_{fluegas,in}$ and $T_{fluegas,out}$ for Isopentane

Table 5 and Table 6 specify the calculation results in figures. Moreover Fig. 17 and Fig. 16 have been drawn from these data in the tables. The first figure shows that the thermal efficiency has an upper limit at 14.49 %. In the introduction it was mentioned that the temperature configuration of heat source and sink mainly affects the thermal efficiency. If the flue gas is available at relatively high temperatures, the second case of the first guess calculation will be used to optimise the power of fluids with reasonably small critical temperatures. This implies that an optimum of power is found along the isoline of 20 bars.

The upper limit of thermal efficiency is a consequence of thermo physical properties of a chosen working fluid. This limit could have been computed from cycle optimisation without consideration of the interaction of heat source and sink curves as well. The pinch analyses have to be taken into account in order to asses if optimisation is based on an upper pressure limit. In this regard it is essential to consider the interaction between flue gas, thermal oil and cooling water in order to obtain a meaningful application range of organic working fluids. It reveals the border where significantly smaller thermal efficiencies occur as consequence of the pinch analysis. The brake down of efficiency to lower values than 14.49 % is presented in Table 5 and is mainly affected by chosen flue gas outlet temperatures that are too small. These small temperatures are leading to low thermal oil inlet temperatures. In such case the pressure in the cycle cannot be raised to the upper limit of 20 bars to match the desired pinch points. Thereby the optimisation takes place with the function fsolve that reflects the

first case in the first guess calculation. At this point it should be mentioned that 100 ℃ has been chosen as lowest investigated flue gas outlet temperature in this studies, because commonly dew point temperatures are higher.

However if dew point temperatures are lower, the cooling of flue gas streams will be limited due to a minimum temperature difference that is permitted between thermal oil inlet and the temperature of working fluid after it has been pressurised in the pump. It should be kept in mind that there is more power output potential in comparison to evaluations shown in this chapter when the dew point temperatures are lower than 100℃. Since the user is interested in maximum power output, a second surface plot must be drawn. Fig. 17 shows the power output for arbitrary chosen mass flow rates and pinch settings which are listed in Table 4. The power does not only depend on the thermal efficiency, it is also a function of heat input. Therefore the power output figure is evaluated in this thesis and thus the user must do the same for other given flue gas inlet temperature and the mass flow rate. The power output diagram is only shown to explain the complexity in using different working fluids and to derive how power output behaves in the whole system. If the grid line is observed along 300 ℃ flue gas inlet temperature, a power increase can be noticed. This arises from Equ. [4.10] where within an investigated temperature range the thermal efficiency is constant and the heat input grows with lower flue gas outlet temperatures. If the temperature line from 250 ℃ inlet at a constant outlet temperature of 100 ℃ is followed a rise can be notified. Thus this behaviour is also obtained due to more available heat of the flue gas streams. The figure also signals a significant drop of power at flue gas inlet temperatures at around 240 up to 250 ℃. This shows the complex result of interaction between thermal efficiency and heat input whereat the power drop is caused by considerable low upper pressure levels in cycle. In some cases there appears a higher power output in spite of a smaller heat input. This is illustrated along the isoline of 200 ℃ flue gas inlet temperature. In such case the choice of another more suitable working fluid with a smaller critical point leads usually to more power output.

6.1.2 Parameter study for ORC with IHE plant

	P [kW]	Tflue,in [°C]										
IPENTANE	Tflue,out [°C]	200	210	220	230	240	250	260	270	280	290	300
	110	333	408	496	600	723	870	1093	1292	1375	1457	1540
	120	377	457	550	657	781	926	1101	1271	1357	1444	1531
	130	385	469	565	672	795	938	1111	1231	1330	1420	1510
	140	369	455	551	659	780	919	1047	1164	1283	1383	1477
	150	334	421	518	624	743	866	985	1103	1217	1333	1434

Table 7: Power output for distinct flue gas temperature configurations for Isopentane

	ηth [%]	Tflue,in [°C]										
IPENTANE	Tflue,out [°C]	200	210	220	230	240	250	260	270	280	290	300
	110	7.18	7.9	8.72	9.65	10.73	11.87	14.02	15.53	15.53	15.53	15.53
	120	9.11	9.83	10.63	11.53	12.55	13.71	15.12	16.27	16.27	16.27	16.27
	130	10.63	11.33	12.1	12.96	13.92	15.02	16.41	16.86	16.98	16.98	16.98
	140	11.87	12.54	13.28	14.09	15	16.04	16.74	17.15	17.53	17.63	17.63
	150	12.9	13.54	14.24	15	15.85	16.62	17.15	17.59	17.89	18.18	18.23

Table 8: Thermal efficiency for distinct flue gas temperature configurations for Isopentane

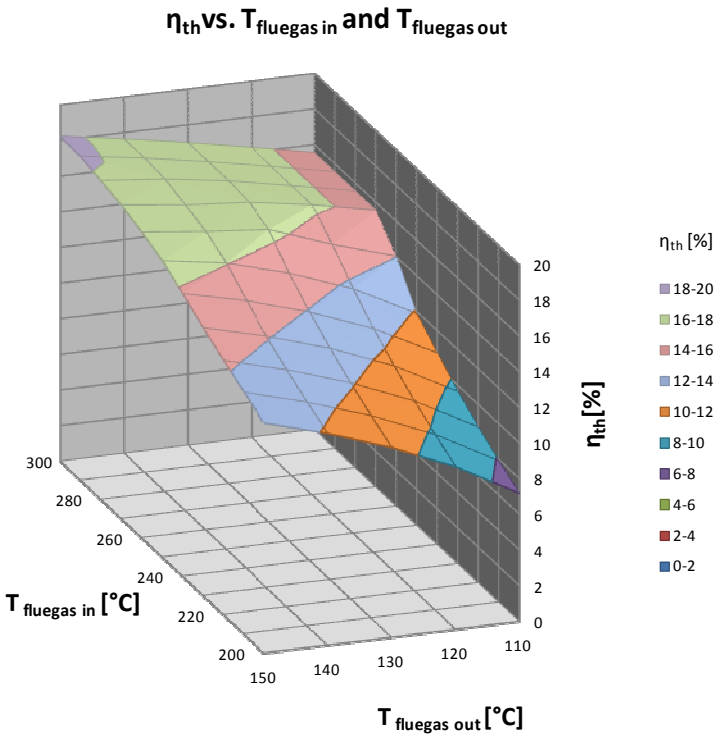

Fig. 18: Thermal efficiency vs. $T_{fluegas,in}$ and $T_{fluegas,out}$ for Isopentane

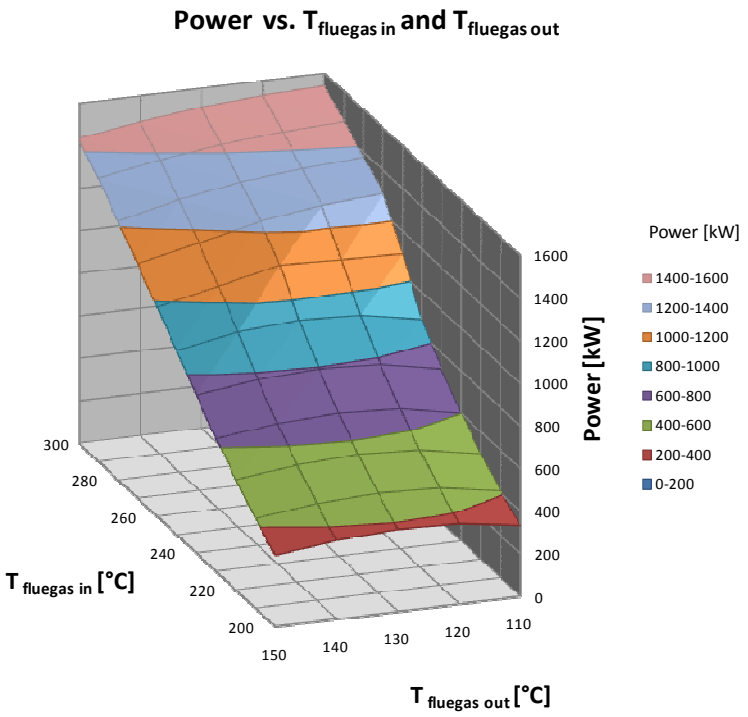

Fig. 19: Power output vs. $T_{fluegas,in}$ and $T_{fluegas,out}$ for Isopentane

The evaluation for the advanced plant design has been carried out for a smaller application range. The studies do not content flue gas outlet temperatures of 100 °C. The restriction of a minimum temperature difference that is permitted between thermal oil inlet and preheater inlet usually leads to a limited benefit in thermal efficiency in contrast to standard ORC, when flue gas cools down to such low temperatures. Only small quantities of heat can be transferred to preheat the working fluid by regeneration.

Nevertheless the user can solve such temperature configurations given that the program is able to process. If Fig. 16 is compared to Fig. 18 it will attract some attention. In the previous chapter a certain upper limit of thermal efficiency for standard ORC configuration was explained. The efficiency of the advanced plant design does not have the same tendency. It is illustrated in Fig. 18, for instance along the 300 °C flue gas inlet temperature curve that a rise of flue gas outlet temperature slightly improves the thermal efficiency. This behaviour arises from the minimum permitted temperature difference boundary that was mentioned before. A difference of 10 °C has been chosen in th e model set up as suitable approach. A higher flue gas outlet temperature implies also a higher thermal oil inlet temperature. Thus better performance can be found as more heat transfer in the IHE can take place. If temperature increase of flue gas outlet continues the efficiency will be enhanced whereas there is less heat available for energy conversion. It should be also mentioned that considerable improved efficiencies are obtained at higher available heat source temperatures. The behaviour is a consequence of optimisation along the upper pressure

limit of 20 bars (second case of first guess calculation). If no high flue gas inlet temperature is present, the efficiency will be lower in ORC with IHE in comparison with the standard ORC. It was experienced from parameter studies that the upper pressure level in the cycle is smaller for the ORC with an additional heat exchanger application when the same settings have been used for evaluation at low flue gas temperatures (second case of first guess calculation). In the optimisation the most significant influence on the average temperature of the heat input is caused by the evaporator pressure which implies a high impact on the thermal efficiency. However an optimum of power derives from appropriate trade off between the thermal efficiency and heat input.

6.2 Parameter study for Cyclopentane

6.2.1 Parameter study for basic ORC plant

CYCLOPENTANE	P [kW]	Tflue,in [°C]										
	Tflue,out [°C]	200	210	220	230	240	250	260	270	280	290	300
	100	146	171	200	245	312	404	533	710	940	1214	1516
	110	276	333	401	481	578	693	831	994	1181	1393	1628
	120	343	413	492	582	685	802	936	1087	1256	1442	1647
	130	365	440	524	618	722	839	968	1110	1267	1438	1618
	140	356	435	522	617	721	835	960	1096	1244	1404	1530
	150	325	407	495	591	694	806	928	1058	1199	1336	1439

Table 9: Power output for distinct flue gas temperature configurations for Cyclopentane

CYCLOPENTANE	ηth [%]	Tflue,in [°C]										
	Tflue,out [°C]	200	210	220	230	240	250	260	270	280	290	300
	100	2.83	3.01	3.23	3.65	4.31	5.2	6.42	8.04	10.04	12.27	14.53
	110	5.94	6.45	7.05	7.75	8.57	9.54	10.66	11.94	13.34	14.84	16.41
	120	8.31	8.87	9.5	10.2	11	11.88	12.85	13.96	15.05	16.25	17.51
	130	10.07	10.63	11.24	11.91	12.64	13.44	14.3	15.21	16.18	17.2	18.19
	140	11.45	11.98	12.57	13.19	13.86	14.58	15.35	16.15	17	17.89	18.26
	150	12.56	13.07	13.62	14.2	14.82	15.47	16.16	16.88	17.63	18.22	18.29

Table 10: Thermal efficiency for distinct flue gas temperature configurations for Cyclopentane

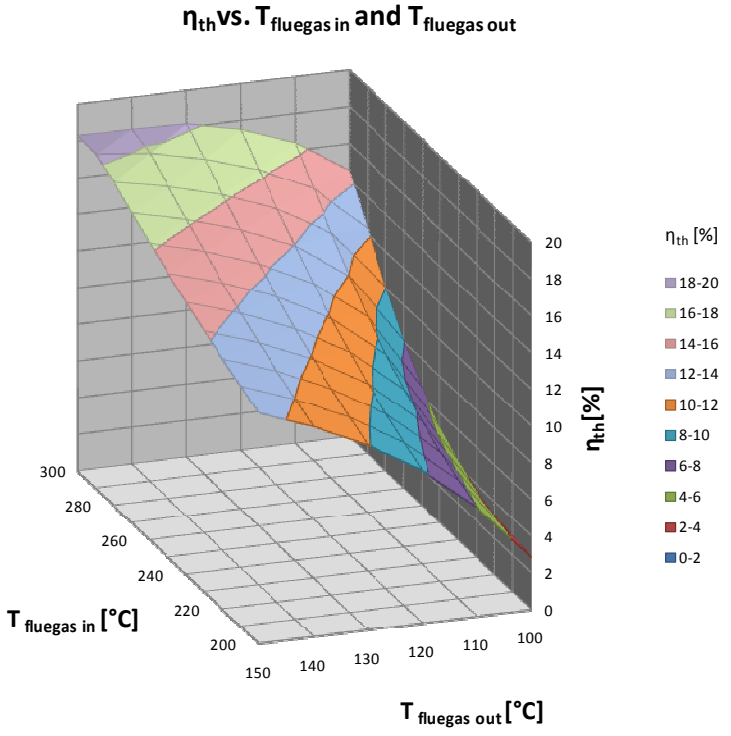

Fig. 20: Thermal efficiency vs. $T_{fluegas,in}$ and $T_{fluegas,out}$ for Cyclopentane

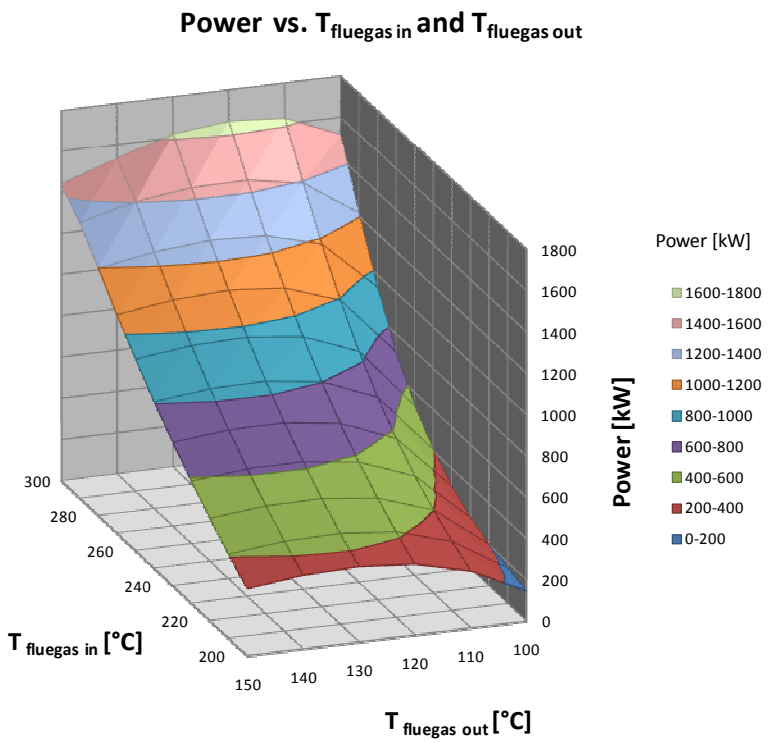

Fig. 21: Power output vs. $T_{fluegas,in}$ and $T_{fluegas,out}$ for Cyclopentane

Fig. 20 and Fig. 21 demonstrate the performance for Cyclopentane for the chosen settings listed in Table 4. Cyclopentane has a relatively high critical point (100 ℃ higher critical temperature than Isobutane). Thus the system behaves differently in terms of thermal efficiency and power output. Indeed Fig. 21 does not show an upper limit for thermal efficiency in contrast to Isopentane which is illustrated in Fig. 16. Nevertheless the thermal efficiency is restricted in either case, but the optimum of thermal efficiency for Cyclopentane does not appear at those chosen temperature ranges. It is shown clearly along one flue gas inlet temperature isoline that an increase of one incremental step of flue gas outlet temperature raises the thermal efficiency. Therefore the maximum can be found when further temperature configurations are carried out at a higher flue gas outlet temperature or even at higher flue gas inlet temperatures. However in this thesis only a temperature range up to 300 ℃ of the flue gas inlet and 150 ℃ of th e flue gas outlet temperature have been investigated. At this point it should be mentioned that substantial efficiencies over 18 % can be obtained at sufficient available flue gas temperatures which are significant higher in comparison to researched low critical point substances. In the upcoming chapters all investigated fluids are compared and the most suitable fluid for a specific application temperature range is shown. Thus the user is immediately able to observe what kind of fluid should be investigated for a given problem more detailed from the figures shown in this chapter as well as in the Appendix.

6.2.2 Parameter study for ORC with IHE plant

	P [kW]	Tflue,in [°C]										
CYCLOPENT.	Tflue,out [°C]	200	210	220	230	240	250	260	270	280	290	300
	110	NA	NA	NA	NA	577	678	796	933	1091	1274	1487
	120	NA	411	487	573	669	777	900	1038	1195	1373	1578
	130	363	437	519	610	711	822	947	1085	1240	1414	1612
	140	356	435	521	615	719	832	957	1094	1247	1416	1608
	150	323	412	500	596	701	816	940	1076	1226	1391	1560

Table 11: Power output for distinct flue gas temperature configurations for Cyclopentane

	ηth [%]	Tflue,in [°C]										
CYCLOPENT.	Tflue,out [°C]	200	210	220	230	240	250	260	270	280	290	300
	110	NA	NA	NA	NA	8.56	9.34	10.22	11.21	12.32	13.57	14.99
	120	NA	8.84	9.41	10.04	10.74	11.51	12.35	13.29	14.32	15.47	16.77
	130	10.03	10.56	11.14	11.76	12.44	13.18	13.99	14.87	15.84	16.91	18.12
	140	11.47	11.99	12.55	13.16	13.82	14.53	15.3	16.13	17.04	18.05	19.19
	150	12.47	13.24	13.75	14.34	14.97	15.65	16.38	17.17	18.02	18.97	19.83

Table 12: Thermal efficiency for distinct flue gas temperature configurations for Cyclopentane

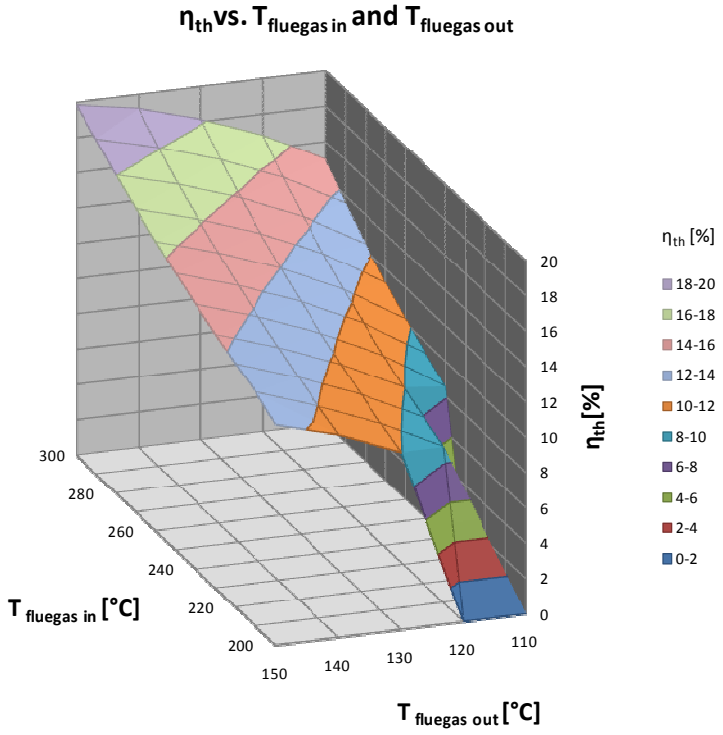

Fig. 22: Thermal efficiency vs. $T_{fluegas,in}$ and $T_{fluegas,out}$ for Cyclopentane

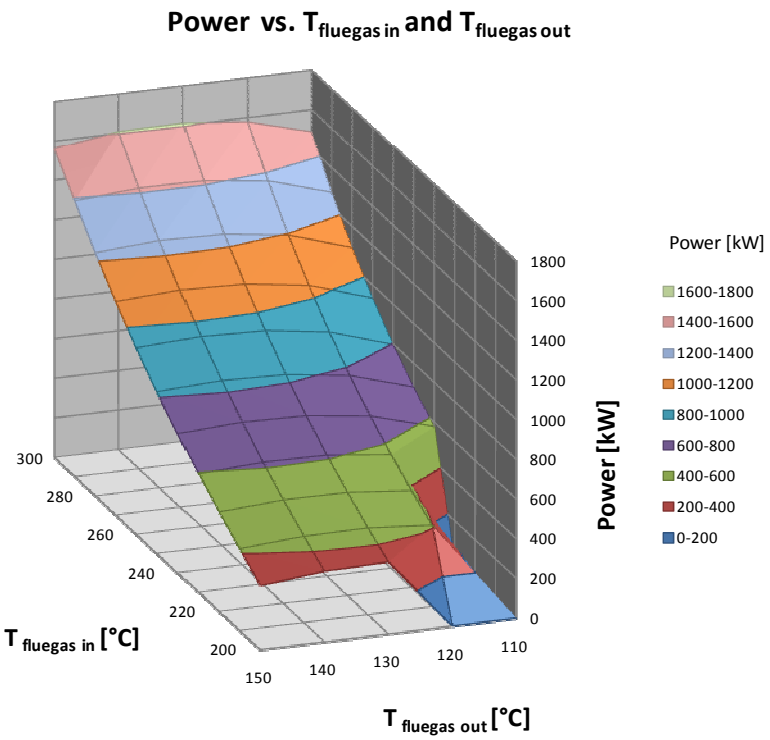

Fig. 23: Power output vs. $T_{fluegas,in}$ and $T_{fluegas,out}$ for Cyclopentane

Fig. 22 represents the performance of the thermal efficiency for ORC with IHE and Cyclopentane. Thereby no solutions have been found for relatively low temperature configurations. The temperature of state 10 has to be at least 10 ℃ higher than the temperature of state 2 because of the restriction within the IHE. When the flue gas inlet and outlet temperatures are quiet small then the 10 ℃- difference cannot be satisfied. Thus the limitation forces the program to terminate the process of optimisation. The investigated temperature range always leads to the first case of the first guess calculation. The explanations given in Chapter 6.1.2 also apply for high critical point fluids. Power output has the maximum at relatively high flue gas outlet temperatures. As it is shown in Table 40 the maxima can even occur at higher flue gas outlet temperatures.

6.3 Comparison and application range of fluids

Global: all fluids	ηth [%]	Tflue,in [°C]									
	Tflue,out [°C]	200	210	220	230	240	250	260	270	280	290	300
	100	6.12	8.51	9.41	9.5	10.23	12.04	13.81	15.04	15.31	15.31	15.31
	110	9.14	9.45	9.65	10.82	12.06	13.34	14.49	15.31	15.31	15.31	16.41
	120	9.5	10.27	11.15	12.1	13.09	14.13	15.05	15.31	15.31	16.25	17.51
	130	10.67	11.39	12.15	12.95	13.79	14.62	15.31	15.31	16.18	17.2	18.19
	140	11.61	12.24	12.91	13.61	14.34	15.1	15.35	16.15	17	17.89	18.26
	150	12.56	13.07	13.62	14.2	14.82	15.47	16.16	16.88	17.63	18.22	18.55

Table 13: Thermal efficiency performance for basic ORC plant design

Global: all fluids	Performance	Tflue,in [°C]									
	Tflue,out [°C]	200	210	220	230	240	250	260	270	280	290	300
	100	ISOBUTAN	ISOBUTAN	ISOBUTAN	ISOBUTAN	IPENTANE	IPENTANE	IPENTANE	PENTANE	PENTANE	PENTANE	PENTANE
	110	ISOBUTAN	ISOBUTAN	IPENTANE	IPENTANE	IPENTANE	IPENTANE	IPENTANE	PENTANE	PENTANE	PENTANE	CYCLOPENTANE
	120	ISOBUTAN	IPENTANE	IPENTANE	IPENTANE	IPENTANE	IPENTANE	PENTANE	PENTANE	PENTANE	CYCLOPENTANE	CYCLOPENTANE
	130	IPENTANE	IPENTANE	IPENTANE	IPENTANE	IPENTANE	PENTANE	PENTANE	PENTANE	CYCLOPENTANE	CYCLOPENTANE	CYCLOPENTANE
	140	PENTANE	PENTANE	PENTANE	PENTANE	PENTANE	PENTANE	CYCLOPENTANE	CYCLOPENTANE	CYCLOPENTANE	CYCLOPENTANE	CYCLOPENTANE
	150	CYCLOPENTANE	CYCLOPENTANE	CYCLOPENTANE	CYCLOPENTANE	CYCLOPENTANE	CYCLOPENTANE	CYCLOPENTANE	CYCLOPENTANE	CYCLOPENTANE	CYCLOPENTANE	CYCLOHEXANE

Table 14: Power output performance for basic ORC plant design

In order to draw some conclusions of evaluations shown in the previous chapters, a comparison was made for the selected fluids. As it is shown in Table 13 and Table 14, one fluid shows better performance than others in distinct temperature ranges. At low available temperatures Isobutane and Isopentane are better than fluids with a higher critical point. Cyclopentane and Cyclohexane are more suitable in the case of higher available temperatures in contrast to fluids with a relatively low critical point. As it was already mentioned the power output is not only a function of thermal efficiency. The heat input depends on the flue gas outlet temperature and therefore influences the power output as well. Thus tables displayed above shall give the program user a rough guess, what kind of fluid should be applied for given temperatures. It allows the user to preselect a certain fluid more detailed for further studies when new evaluations are carried out. For instance the reduction of the incremental step of 10 ℃ in temperature tables leads to more accurate information about optimum performance and usually also to higher desired power output.

Parameter studies for rough estimation of optimum performance

Global: all fluids	ηth [%]	Tflue,in [°C]										
	Tflue,out [°C]	200	210	220	230	240	250	260	270	280	290	300
	110	9.03	9.66	9.95	10.24	10.73	11.87	14.02	15.53	16.34	16.34	16.34
	120	9.84	10.17	10.63	11.53	12.55	13.71	15.12	16.27	17.09	17.09	17.09
	130	10.63	11.33	12.1	12.96	13.92	15.02	16.41	17.32	17.81	17.84	18.12
	140	11.87	12.54	13.28	14.09	15	16.04	16.96	17.68	18.19	18.53	19.19
	150	12.92	13.54	14.24	15	15.85	16.66	17.54	18.07	18.53	18.97	19.83

Table 15: Thermal efficiency performance for ORC with IHE plant design

Global: all fluids	Performance	Tflue,in [°C]										
	Tflue,out [°C]	200	210	220	230	240	250	260	270	280	290	300
	110	ISOBUTAN	ISOBUTAN	ISOBUTAN	ISOBUTAN	IPENTANE	IPENTANE	IPENTANE	IPENTANE	PENTANE	PENTANE	PENTANE
	120	ISOBUTAN	ISOBUTAN	IPENTANE	IPENTANE	IPENTANE	IPENTANE	IPENTANE	IPENTANE	PENTANE	PENTANE	PENTANE
	130	IPENTANE	IPENTANE	IPENTANE	IPENTANE	IPENTANE	IPENTANE	IPENTANE	PENTANE	PENTANE	PENTANE	CYCLOPENTANE
	140	IPENTANE	IPENTANE	IPENTANE	IPENTANE	IPENTANE	IPENTANE	PENTANE	PENTANE	PENTANE	PENTANE	CYCLOPENTANE
	150	PENTANE	IPENTANE	IPENTANE	IPENTANE	IPENTANE	PENTANE	PENTANE	PENTANE	PENTANE	CYCLOPENTANE	CYCLOPENTANE

Table 16: Power output performance for ORC with IHE plant design

The ORC with IHE application leads to distinct fluids in different flue gas temperature configurations. In both cases (standard ORC or ORC with IHE) the high critical point temperature substances show enhanced performance for greater available flue gas temperatures in contrast to low critical point fluids. The opposite applies for rather moderate heat source temperatures. Thus the following conclusions can be drawn. Table 13 and Table 15 show up the advantages and disadvantages of each plant design in terms of their thermal efficiency. The restriction of a limited upper pressure level in each cycle leads to a distinct system behaviour in either case. If the first case of the first guess calculation applies in optimisation, the standard plant without heat regeneration will have improved performance. There the upper pressure level is higher than in the advanced plant design which leads to a higher average temperature of heat input and even to better performance in terms of power generation. If the optimisation is based on the second case of the first guess calculation the power maximum is found on the 20 bar of isoline. In the case that the optimisation process of different cycles takes place at the same upper pressure level, for instance at 20 bars, there will always be higher thermal efficiencies in the advanced plant design. Obviously the advanced plant design does not lead to best performance in all cases. Therefore it should be mentioned that it always depends on the temperature configuration which causes the available enthalpy at the turbine inlet state.

7 Case study for an industrial plant

One example where industrial processes cause much waste heat in terms of flue gas is a steel manufacturing company. In such industrial plants, the potential of waste heat recovery is enormous. It is usually economical feasible and strongly recommended. Therefore this chapter explains how much electricity can be produced when an ORC plant would be applied to convert the heat of flue gas streams coming from such manufacturing processes. Realistic data of flue gas streams have been assumed and are listed in the following tables.

	$T_{fluegas, in}$ [°C]	density [kg/Nm³]	quantity of wet gas [Nm³/a]	operating hours [h/a]	mass flow rate [kg/s]	dew point [°C]
Industrial furnace 1	220	1.40013829	626523532	7801	31	95
Industrial furnace 2	300	1.28915700	1057513754	8239	46	109
Industrial furnace 3	280	1.2416744	365542806	7339	17	113

Table 17: Mass flow rate and dew point of flue gas streams

Table 17 shows the mass flow rate of the different flue gas stream coming from different industrial furnaces. Typical dew point temperatures with respect to each mentioned industrial furnace are listed as well. In reality higher flue gas outlet temperatures than the given dew point must be applied in the recovery equipment. This higher outlet temperature derives from fluid dynamics as it is known that smaller temperature occurs at walls of equipment components in comparison to the core stream some distance away. This can be observed for instance in a chimney. However the flue gas composition is also given by such characteristic industrial plant, figured in Table 18.

weight %	N_2	O_2	Ar	CO_2	H_2O	SO_2	sum
Industrial furnace 1	0.61981	0.05119	0.00721	0.30004	0.02170	0.00005	1.0
Industrial furnace 2	0.70100	0.08122	0.01096	0.14246	0.06435	0.00001	1.0
Industrial furnace 3	0.73068	0.11887	0.01220	0.05510	0.08309	0.00006	1.0

Table 18: Assumed flue gas composition of industrial furnaces

In the calculations two different cooling scenarios have been investigated. On the one hand it was assumed that the river water of a river can be used to reject the heat from ORC, whereby the river has yearly an average temperature of 10℃. Thus this temperature was used to get a figure how much the ORC would be able to produce in average. It was assumed that the water is not permitted to heat up more than 10 ℃. On the other hand appropriate water temperatures have been supposed to simulate a wet cooling tower on site.

Thereby the knowledge of wet bulb temperature is essential. The wet bulb temperature is around 20 ℃ in summer in middle Europe / Austria. The emphasis was based on that season, since in many cases ORC plants are only operated in summer while the waste heat is used for district heating purpose in winter. An approach of 5 ℃ has been taken into account. Therefore the cooling water temperatures of 25 ℃ and 35 ℃ have been supposed for calculations with respect to inlet and outlet.

7.1 Wet cooling tower scenario

In the wet cooling tower scenario the most suitable fluid for ORC calculation can be easily found because the parameter studies have been carried out with the same cooling conditions. In Table 13 and Table 15 the most suitable fluids for a certain flue gas inlet and outlet temperature configuration are listed. The industrial furnace 1 flue gas temperature is 220 ℃ and can be cooled down to 105℃ lowest. In e ach EXCEL file that figures the parameter studies a table sheet called INPUT can be found. These table sheets are shown in Table 19 and Table 20 for a basic as well as an advanced plant design.

$T_{flue,out}$[°C]	Q [kW]	ηth [%]	P [kW]	Fluid
100	4007.9	9.41	377	ISOBUTANE
110	3679.4	9.65	355	IPENTANE
120	3349.9	11.15	374	IPENTANE
130	3019.4	12.15	367	IPENTANE
140	2687.9	12.91	347	PENTANE
150	2355.5	13.62	321	CYCLOPENT.

Table 19: Industrial furnace 1: INPUT table sheet of basic ORC and cooling by tower

$T_{flue,out}$[°C]	Q [kW]	ηth [%]	P [kW]	Fluid
110	3679.4	9.95	366	ISOBUTANE
120	3349.9	10.63	356	IPENTANE
130	3019.4	12.1	365	IPENTANE
140	2687.9	13.28	357	IPENTANE
150	2355.5	14.24	335	IPENTANE

Table 20: Industrial furnace 1: INPUT table sheet of ORC with IHE and cooling by tower

The heat inputs have been calculated by using the developed PYTHON program with a given flue gas composition and a mass flow rate. As it is shown, the industrial furnace 1 provides heat energy to produce electricity of more than 350 kW in either case. The additional heat exchanger IHE does not automatically lead to more output. As it is shown different fluids deliver best performance for different temperature configurations. Further more accurate studies can be evaluated with Isopentane for a basic ORC plant at temperature ranges between 110 and 130 ° but this w as not examined in this thesis. The rough estimation was considered to be acceptable.

Case study for an industrial plant

The following tables show performance of other components.

$T_{flue,out}$[°C]	Q [kW]	ηth [%]	P [kW]	Fluid
100	10305.2	15.31	1578	PENTANE
110	9802.3	16.41	1609	CYCLOPENT.
120	9298.3	17.51	1628	CYCLOPENT.
130	8793.1	18.19	1599	CYCLOPENT.
140	8286.6	18.26	1513	CYCLOPENT.
150	7778.9	18.55	1443	CYCLOHEX.

Table 21: Industrial furnace 2: INPUT table sheet of basic ORC and cooling by tower

$T_{flue,out}$[°C]	Q [kW]	ηth [%]	P [kW]	Fluid
110	9802.3	16.34	1602	PENTANE
120	9298.3	17.09	1589	PENTANE
130	8793.1	18.12	1593	CYCLOPENT.
140	8286.6	19.19	1590	CYCLOPENT.
150	7778.9	19.83	1543	CYCLOPENT.

Table 22: Industrial furnace 2: INPUT table sheet of ORC with IHE and cooling by tower

In the industrial furnace 2 considerable more power can be produced. This fact derives from higher available temperatures as well as a greater quantity of flue gas. It should be noticed that the highest efficiency of 19.83 % can be obtained in ORC with IHE using Cyclopentane as a working fluid. Due to less heat input the power maximum is at other flue gas temperature configurations. It should be also notified that no cooling of flue gas lower than 119℃ would be tolerated in that case and 123 ℃ in case of industrial furnace 3. Those temperatures are typical dew points for such flue gas streams.

$T_{flue,out}$[°C]	Q [kW]	ηth [%]	P [kW]	Fluid
100	3452	15.31	529	PENTANE
110	3263.9	16.41	536	CYCLOPENT.
120	3075.5	17.51	539	CYCLOPENT.
130	2886.7	18.19	525	CYCLOPENT.
140	2697.5	18.26	493	CYCLOPENT.
150	2507.9	18.55	465	CYCLOHEX.

Table 23: Industrial furnace 3: INPUT table sheet of ORC with IHE and cooling by tower

$T_{flue,out}$[°C]	Q [kW]	ηth [%]	P [kW]	Fluid
110	3263.9	16.34	533	PENTANE
120	3075.5	17.09	526	PENTANE
130	2886.7	18.12	523	CYCLOPENT.
140	2697.5	19.19	518	CYCLOPENT.
150	2507.9	19.83	497	CYCLOPENT.

Table 24: Industrial furnace 3: INPUT table sheet of basic ORC and cooling by tower

In all cases the settings for efficiencies shown in Fig. 8 have been applied. In reality minor less power can be obtained as for this study no electric and mechanic efficiencies have been taken into account. However all data express a rough estimation how much power can be produced in terms of electricity.

7.2 Cooling by river water scenario

$T_{flue,out}$[°C]	Q [kW]	ηth [%]	P [kW]	Fluid
100	4007.9	12.1	485	IPENTANE
110	3679.4	13.29	489	IPENTANE
120	3349.9	14.13	473	IPENTANE
130	3019.4	14.8	447	PENTANE
140	2687.9	15.47	416	CYCLOPENT.
150	2355.5	16.29	384	CYCLOPENT.

Table 25: Industrial furnace 1: heat 220_280_300_cool 10-20 table sheet. Basic ORC and cooling by river water

$T_{flue,out}$[°C]	Q [kW]	ηth [%]	P [kW]	Fluid
110	3679.4	13.08	481	ISOBUTANE
120	3349.9	14.26	478	IPENTANE
130	3019.4	15.36	464	IPENTANE
140	2687.9	16.27	437	IPENTANE
150	2355.5	17.06	402	IPENTANE

Table 26: Industrial furnace 2: heat 220_280_300_cool 10-20 table sheet. ORC with IHE and cooling by river water

If Table 25 and Table 26 are compared with Table 19 and Table 20 some conclusions can be drawn. It can be observed that considerable higher power output as well as thermal efficiencies is obtained due to the different cooling of either standard ORC or ORC with IHE: Basically this improved system behaviour arrange because the lower cycle pressure can be reduced when lower cooling temperatures are applied as it is shown in the example with the river water. Thus not only the heat source temperatures significantly influence the performance but even the cooling is essential for powerful ORC operation. In addition the following tables accomplish case study evaluations where the dew point restriction applies also for the second cooling application.

$T_{flue,out}$[°C]	Q [kW]	ηth [%]	P [kW]	Fluid
100	10305.2	18.75	1932	CYCLOPENT.
110	9802.3	19.63	1924	CYCLOPENT.
120	9298.3	20.22	1880	CYCLOPENT.
130	8793.1	20.31	1786	CYCLOPENT.
140	8286.6	20.46	1695	CYCLOHEX.
150	7778.9	20.78	1616	CYCLOHEX.

Table 27: Industrial furnace 2: heat 220_280_300_cool 10-20 table sheet. Basic ORC and cooling by river water

$T_{flue,out}$[°C]	Q [kW]	ηth [%]	P [kW]	Fluid
110	9802.3	19.45	1907	PENTANE
120	9298.3	20.4	1897	CYCLOPENT.
130	8793.1	21.33	1876	CYCLOPENT.
140	8286.6	21.93	1817	CYCLOPENT.
150	7778.9	22.4	1742	CYCLOPENT.

Table 28: Industrial furnace 2: heat 220_280_300_cool 10-20 table sheet. ORC with IHE and cooling by river water

$T_{flue,out}$[°C]	Q [kW]	ηth [%]	P [kW]	Fluid
100	3452	17.22	594	PENTANE
110	3263.9	17.29	564	CYCLOPENT.
120	3075.5	18.26	562	CYCLOPENT.
130	2886.7	18.99	548	CYCLOPENT.
140	2697.5	19.56	528	CYCLOPENT.
150	2507.9	20.02	502	CYCLOPENT.

Table 29: Industrial furnace 3: heat 220_280_300_cool 10-20 table sheet. Basic ORC and cooling by river water

$T_{flue,out}$[°C]	Q [kW]	ηth [%]	P [kW]	Fluid
110	3263.9	19.45	635	PENTANE
120	3075.5	20.12	619	PENTANE
130	2886.7	20.45	590	PENTANE
140	2697.5	20.82	562	PENTANE
150	2507.9	21.22	532	PENTANE

Table 30: Industrial furnace 3: heat 220_280_300_cool 10-20 table sheet. ORC with IHE and cooling by river water

8 Conclusion

The evaluation of the applied model settings reveals the difference of a standard ORC and an ORC with IHE application. Therefore some conclusions can be drawn provided that the data of the parameter studies are observed carefully. Basically only evaluations of available flue gas temperatures between 200 and 300 °C have been under investigation. It was shown that the thermo physical behaviour of each fluid has the highest influence on the system performance, especially on how the critical point of the chosen fluid relates to a given flue gas temperature configuration. The model has been set up to find out the maximum power for a certain heat input.

Thus some unexpected but conceivable outcomes have been discovered. The standard ORC configuration shows better performance when relatively low enthalpy difference is available in order to produce power through the turbine, whereas the ORC with IHE is more powerful when optimisation takes place along a constant upper pressure isobar. The first case implies that considerable cooling of the flue gas does not permit to shift enough heat from the turbine exhaust to preheat the working fluid in the ORC with IHE plant design. It is derived from the restriction of a minimum temperature difference allowed between thermal oil inlet and preheater inlet temperature. If the flue gas outlet temperatures are sizeable higher, less heat can be extracted from the heat source but higher thermal efficiencies can be obtained by the ORC with IHE plant configuration. Apparently the parameter studies demonstrate how the system behaves depending on a chosen temperature configuration and a certain plant design. The temperature configuration of heat source defines the obtainable thermal efficiencies in the cycle regardless how much heat is supplied with respect to mass flow rate or flue gas composition. The parameter studies also illustrate that power optimum is a complex function of obtainable thermal efficiency and heat input. It can be summarised that the consideration of interaction between heat source, ORC and heat sink is essential to understand system performance quite clearly in either plant design, with or without IHE. The pinch analysis reveals the application range for each plant configuration.

The model set up shows the impact of superheating on the performance. Superheating leads in certain cases to slightly better performance in terms of efficiency and power output for a given amount of heat input. This was outlined in this thesis in particular for Isobutane. However the minor benefit for an applied superheating does not often account for the extra money that has to be spent for the installation of an additional heat exchanger component in terms of a superheater. The program records and visualises all data calculated during the optimisation process and therefore the user will be able to assess if superheating is beneficial for the problem given. It has been demonstrated that fluids with a relatively high

critical point are more suitable for higher flue gas temperatures in contrast to low critical point fluids. The reverse conclusion applies for rather low heat source temperatures.

9 Future work

This thesis can act as a base for further studies concerning the costs of such ORC plants. In order to obtain some figures, the developed PYTHON program provides some data about heat transfer properties in applied heat exchangers, in particular the k*A values. The overall heat transfer coefficient k and the heat exchanger area A are crucial for the heat exchanger design. Therefore they play a dominant role in every cost evaluation of heat exchangers within an ORC. The proper estimation of the heat transfer coefficient is the base to obtain the costs depending on the heat exchanger areas. Some guesses as well as experiences for these values can be found in [16], [36], [37], [38] and [39]. Apart from heat exchanger installation costs the turbine as well as the pump costs have to be determined. The pump has minor contribution on whole plant costs, but the turbine represents a major component. DiPippo [16] suggests a model on how to estimate the turbine size depending on sonic velocity. Rowshanzadeh [39] also suggests an equation to compute the turbine size based on volumetric flow and isentropic enthalpy difference. The turbine size is a proper indicator for component installation costs, since turbines can contribute up to 60 % of total installation cost of an ORC plant. The type of the turbine on the market is either a simple scroll expander or an axial turbine. Based on the preferred power range and ORC speed, the degree of superheat or the quality of the inlet fluid of turbine, lubrication as well as the sealing type, expander or axial turbine of ORC can be selected. This is demonstrated in Fig. 24.

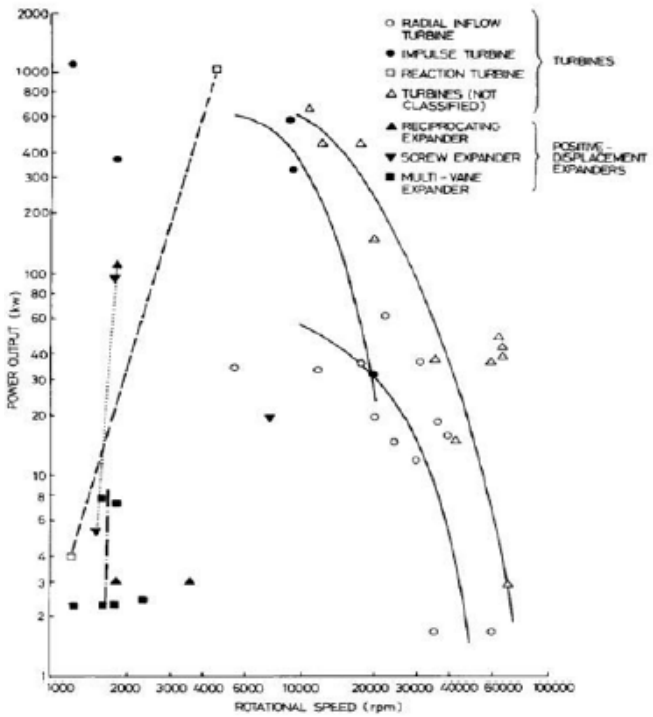

Fig. 24: Turbine and expander selection based on power range, [40].

10 References

[1] Drescher, U., Brüggemann, D. Fluid selection for Organic Rankine Cycle in biomass power and heat plants. Applied Thermal Engineering. 2007, 27, pp. 223-228.

[2] Anh Lai, N., Wendland, M. , Fischer, J. Working fluids for high-temperature organic Rankine cycles. Energy. 2011, 36, pp. 199-211.

[3] Roy, J. P., Mishra, M.K, Misra, A. Parametric optimization and performance analysis of a waste heat recovery system using Organic Rankine Cycle. Energy. 2010, 35, pp. 5049-5062.

[4] Borsukiewicz-Gozdur, A. Influence of heat recuperation in ORC power plant on efficiency of waste heat utilization. archives of thermodynamics. 2010, Vol. 31, 4, pp. 111-123.

[5] Wei, D., Lu, X. , Lu, Z., Gu, J. Performance analysis and optimization of organic Rankine cycle for waste heat recovery. [ed.] Elsevier. Energy Conversion & Management. 2007, 48, pp. 1113-1119.

[6] Declaye, Sébastien. Design ,optimization and modeling of an organic Rankine cycle for waste heat recovery. Université de Liège. 2009. Thesis.

[7] Lemmon, E.W., Huber, M.L., McLinden, M.O. NIST Standard Reference Database 23: Reference Fluid Thermodynamic and Transport Properties-REFPROP, Version 9.0, National Institute of Standards and Technology, Standard Reference Data Program. 2010.

[8] Polt, A., Platzer, B., and Maurer, G. Fluid Thermodynamic Properties for Light Petroleum Systems. 1973.

[9] Buecker, D. and Wagner, W. Reference Equations of State for the Thermodynamic Properties of Fluid Phase n-Butane and Isobutane. 2006.

[10] Colonna, P., Nannan, N. R., and Guardone, A. Multiparameter Equations of State for selected Siloxanes. Fluid Phase Equilibria. 2011, 244, pp. 193-211.

[11] Lemmon, E. W. and Span, R. Short Fundamental Equations of State for 20 Industrial Fluids. Journal of Chemical Engineering Data. 2006, 51, pp. 785-850.

[12] Penoncello, S. G., Goodwin, A. R. H., and Jacobsen, R. T. A Thermodynamic Property Formulation for Cyclohexane. International Journal of Thermophysics. 1995, Vol. 16, 2, pp. 519-531.

[13] Gedanitz, H., Davila, M. J., Lemmon, E. W. unpublished equation. 2008.

[14] Span, R. and Wagner, W. Equations of State for Technical Applications. II. Results for Nonpolar Fluids. International Journal of Thermophysics. 2003, Vol. 24, 1, pp. 41-109.

[15] Wagner, W. and Pruss, A. The IAPWS Formulation 1995 for the Thermodynamic Properties of Ordinary Water Substance for General and Scientific Use. [ed.] American Inst ute of Physics. 2002, pp. 1-149.
[16] Di Pippo, Ronald. Geothermal Power Plants - Principles, Applications, Case studies and Environmental Impact. 2nd Edition. s.l. : Butterworth-Heinemann, 2007.
[17] http://www.scilab.org. [Online]
[18] Python Software Foundation. http://www.python.org. [Online]
[19] Beazly, M. D. Python - Essential Reference. 3rd Edition. s.l. : Sams Publishing, 2006.
[20] http://www.youtube.com. [Online]
[21] http://www.pythonxy.com. [Online]
[22] Summerfield, Mark. Rapid GUI Programming with Python and Qt. s.l. : Pearson Education, Inc., 2008.
[23] Bahman ZareNezhad ⇑, Ali Aminian. Accurate prediction of the dew points of acidic combustion gases by using an artificial neural network model. Energy Conversion and Management. 2011, 52, pp. 911-916.
[24] Okkes, A. G. Get Acid dew point of flue gas. Hydrocarbon Process. 1987.
[25] McBride, B. J., Zehe, M. J., Gordon, S. NASA Glenn Coefficients for Calculating Thermodynamic Properties of Individual Species. [ed.] Glenn Research Center. 2002.
[26] Baehr, H.D. Thermodynamik. 13th Edition. s.l. : Springer, 2006.
[27] Classen Apparatebau Wiesloch GmbH. http://www.apparatebau-wiesloch.com. Wärmeübertragung mit organischen Wärmeträgern: Thermalölanlagen. [Online]
[28] Drescher, U. Optimierungspotenzial des Organic Rankine Cycle für biomassegefeuerte und geothermische Wärmequellen. 1st Edition. s.l. : Logos Verlag Berlin GmbH, 2008.
[29] Wagner Technik Service. http://www.wts-online.de. Stoffdaten von Wärmeträgerölen. [Online]
[30] Mobil. http://www.mobil.com. /Mexico-English/Lubes/PDS/GLXXENINDMOMobiltherm_603.aspx. [Online]
[31] MathWorks. http://www.mathworks.com. /products/optimization/. [Online]
[32] Python Software Foundation. http://docs.scipy.org. /doc/scipy/reference/optimize.html. [Online]
[33] Opitz, E. Auslegung von ORC- und Dampfkraftprozessen zur Abwärmenutzung. Vienna University of Technology. 2011. Thesis.
[34] http://highered.mcgraw-hill.com. /sites/0072383321/student_view0/ees_software.html. [Online]

[35] Saleh, B., Koglbauer, G., Wendland, M., Fischer, J. Working fluids for low-temperature organic Rankine cycles. Energy. 2007, 32, pp. 1210-1221.

[36] Lukawski, M. Design and Optimization of Standardized Organic Rankine Cycle Power Plant for European Conditions. RES - The School for Renewable Energy Sources. 2009. Thesis.

[37] Caixia, S. Feasibility Study of Geothermal Utilization of Yangbajain Field in Tibet Autonomous Region, P. R. China. University of Iceland. Thesis.

[38] McMahan, A. Design and Optimization of Organic Rankine Cycle Solar-Thermal Power Plants. University of Wisconsin-Madison. 2006. Thesis.

[39] Rowshanzadeh, R. Performance and cost evaluation of Organic Rankine Cycle at different technologies. KTH Sweden. Thesis.

[40] Badr., O., O'Callghan, P., Hussein, M., Probert, S. D. Multi-vane expanders as prime movers for low-grade energy organic Rankine-cycle engines. Applied Energy. 1984, 16, pp. 129-146.

[41] Adoratec. http://www.adoratec.com. /produktnav.html. [Online]

[42] Köhler, S., Ziegler, F. http://engine.brgm.fr/. web-offlines/conference-Electricity_generation_from_Enhanced_Geothermal_Systems_-_Strasbourg,_France,_Workshop5/other_contributions/31-kohler.html. [Online] 2006.

11Appendix

11.1 ORC unit supplier

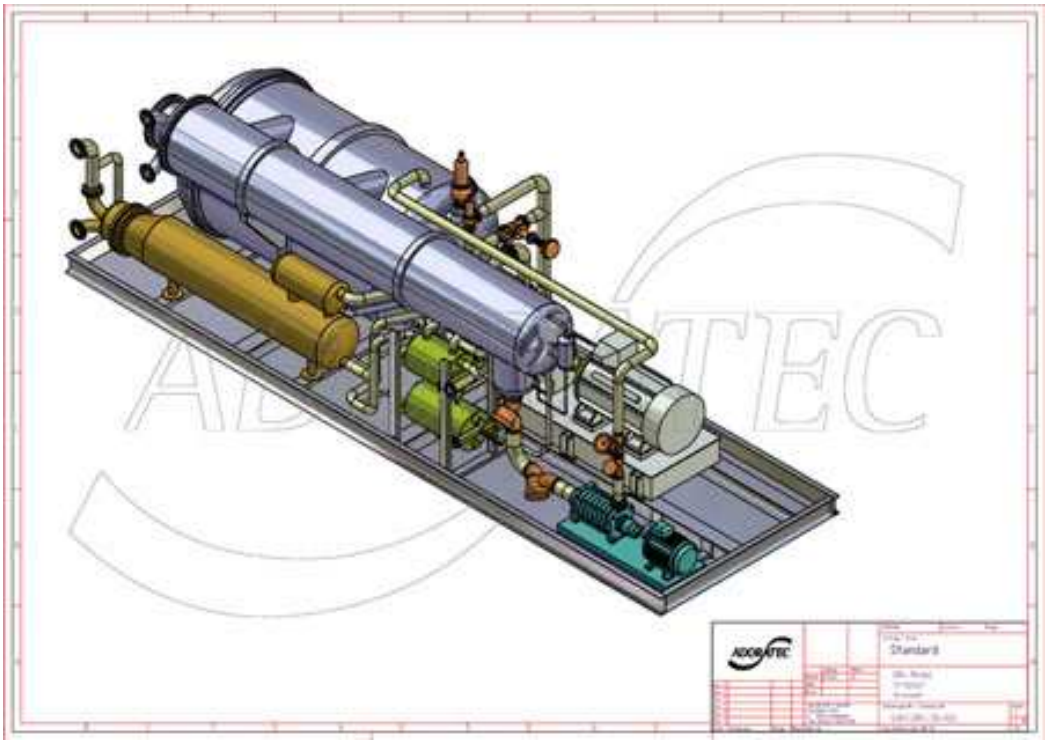

Fig. 25: ORC unit of supplier Adoratec, source [41].

Many suppliers offer a great variety of ORC modules, see Table 31

Company	**Application**	**Site**
GMK	Geothermal heat, waste heat recovery and biomass plants	Germany
ADORATEC GmbH	Waste heat recovery and biomass plants	Germany
Conpower Technik	Waste heat recovery plants	Germany
Maxxtec AG	Waste heat recovery, biomass plants	Germany
Turboden	Geothermal heat, waste heat recovery, biomass plants	Italy
Ormat	Geothermal heat, waste heat recovery plants	Israel
Tri-O-Gen B.V.	Waste heat recovery plants	Netherlands
Infinity Turbine	Geothermal heat , waste heat recovery plants	USA

Table 31: ORC supplier

11.2 Optimisation algorithm

11.2.1 Nomenclature

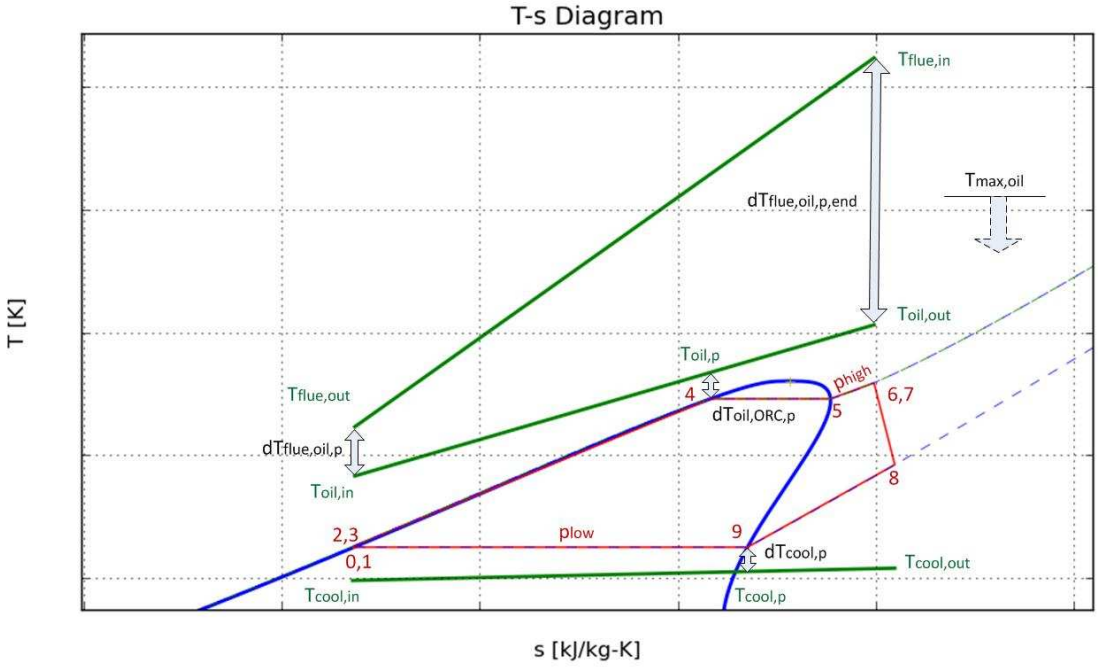

Fig. 26: Nomenclature of used abstracts and variables in the PYTHON code

Variable	Meaning	Unit
T_oil_in, out	Oil temperatures	K
T_flue_in, out	Flue gas temperatures	K
T_SI_state	Temperature of certain state	K
T_cool_in,out	Cooling water temperatures	K
T_max_oil	Max. allowable oil temperature	K
dT_flue_oil_p	Temperature difference at cold side of the flue gas/thermal oil heat exchanger	K
T_superheat	Temperature difference between T_SI_6 (or in case of an IHE configuration, T_SI_7) and T_high_ev	K
T_subcool_cond	Temperature difference due to sub cooling	K
T_high_ev	Temperature where evaporation takes place	K
dT_flue_oil_p_end	Temperature difference at the hot side of flue gas/thermal oil heat exchanger	K
dT_oil_ORC_p	Pinch at evaporator/preheater to thermal oil	K
dT_oil_ORC_p_seek	Desired pinch at evaporator/preheater to thermal oil, given by program user	K

dT_cool_p	Pinch in condenser	K
dT_cool_p-seek	Desired pinch in condenser, given by the program user	K
T_oil_p	Temperature of thermal oil at pinch in evaporator	K
T_cool_p	Temperature of cooling water at pinch in condenser	K
P_high	Upper pressure level	kPa
P_low	Lower pressure level	kPa
p_min	Min. allowable pressure level	kPa
p_limit_he_start	Max. allowable pressure level	kPa
cp_cool	Heat capacity of cooling water	kJ/kg-K
dp_state1_state2	Pressure drop from state 1 to state 2 given by the program user	kPa
h_SI_state	Enthalpy of a certain state	kJ/kg
s_si_state	Entropy of a certain state	kJ/kg
m_ORC	Mass flow rate of ORC fluid	kg/s
m_cool	Mass flow rate of cooling water	kg/s
m_oil	Mass flow rate of thermal oil	kg/s
m_flue	Mass flow rate of flue gas	kg/s
Q_in/Q_input	Available heat from flue gas	kW
eta_e_t,p	Electrical efficiency of turbine or pump	[-]
eta_m_t,p	Mechanical efficiency of turbine or pump	[-]
eta_th	Thermal efficiency	[-]
P_cycle	Power output	kW
wt	Specific work of turbine in ORC	kJ/kg
wp	Specific work of pump in ORC	kJ/kg
wnet	Net work of cycle	kJ/kg
ORC_superheated	Function to calculate states in ORC, is not shown in following code snippet	

Table 32: Nomenclature of variables used in the PYTHON code

The additional *extensions* *_*start* refer to the first guess calculation and are the basis of what kind of solver is used. In addition the *extensions* *_*vec*, for instance P_cycle_vec, indicate a vector. In these vectors all data are stored, for instance the power, as the while loop is executed and superheating is applied. The first entry regards to non superheating, the last entry represents the highest superheating configuration. The highest applied superheating temperature depends on the moment the loop is terminated. Some of the variables shown in Table 32 are even illustrated in Fig. 26.

11.2.2 Flow chart of optimisation algorithm

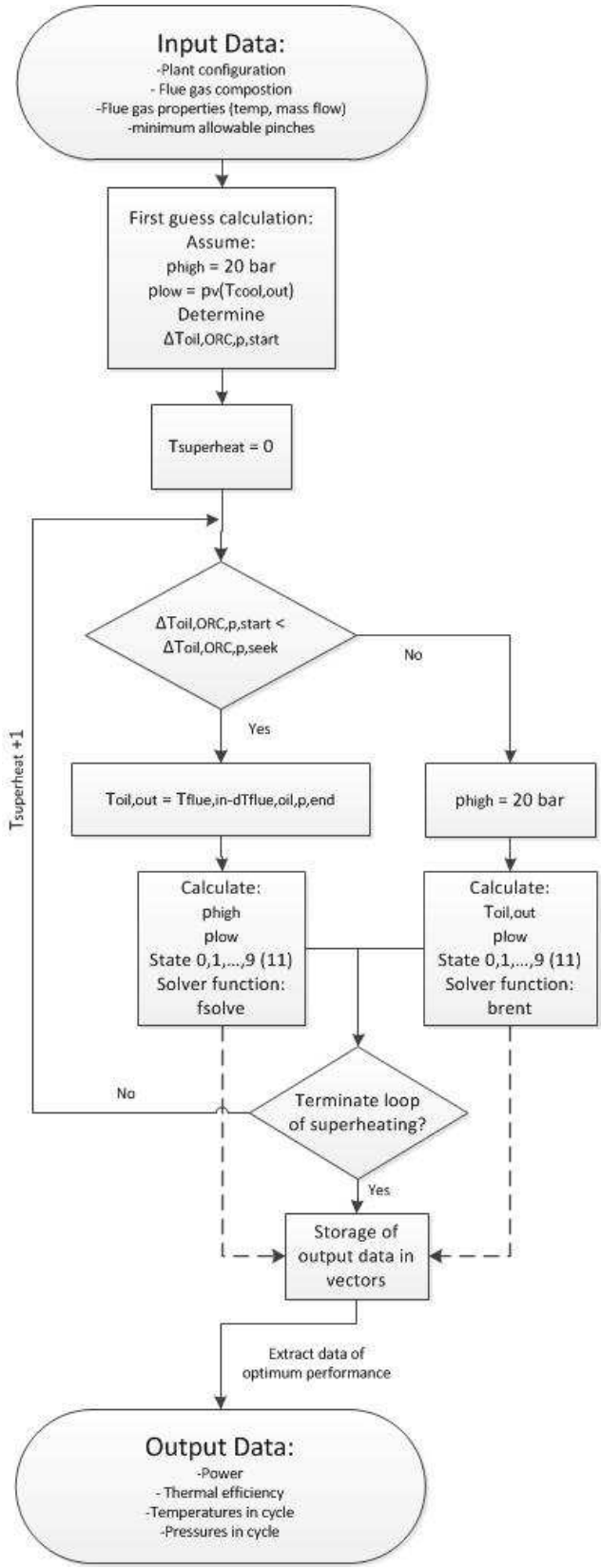

Fig. 27: The flow chart refers to the code snippet shown in chapter 11.2.3. It is applied in either file, Orc_optimisation.py and OrcwithIHE_optimisation.py

11.2.3 Code-snippet from PYTHON file Orc_optimisation.py

```
def Flue_watercooled_superheated(Fluid, eta_e_t, … , r_NO2, r_Ne):
    "optimises the thermodynamic cycle by using other functions like
    ORC_superheated"
    T_oil_in = T_flue_out - dT_flue_oil_p
    cp_cool = add_function.cp_liquid(T_cool_in, Fluid, 'WATER')
    T_max_oil = 558.15 #[K]
    p_min = 5 #[kPa]
    p_limit_he_start = 2000 #[kPa]
    #Initialize some vectors
    P_cycle_vec = np.array([])
    …
    p_low = REFPROP.TQFLSH(T_cool_out + dT_cool_p_seek ,0,1)[1]
    p_high_start = p_limit_he_start
    if (T_flue_in - dT_flue_oil_p_end) < T_max_oil:
        T_oil_out_start = T_flue_in - dT_flue_oil_p_end
    else:
        T_oil_out_start = T_max_oil
    T_high_ev_start = REFPROP.PQFLSH(p_high_start,0,1)[1]
    Q_input_start = m_flue *(cpi_flue_in * T_flue_in - cpi_flue_out
    *T_flue_out)
    m_oil_start = Q_input_start/(0.0018*(T_oil_out_start**2-
    T_oil_in**2)+0.8184*(T_oil_out_start-T_oil_in))
    h_SI_start = ORC_superheated(T_high_ev_start, p_high_start,
    p_low, eta_e_t, eta_e_p, eta_m_t, eta_m_p, eta_s_p, eta_s_t,
    dp_2_3, dp_6_7, T_subcool_cond)[0]
    m_ORC_start  = Q_input_start/(h_SI_start[6]-h_SI_start[3])
    coeff = [m_oil_start *0.0018, 0.8184*m_oil_start, - (m_oil_start
    * 0.0018 * T_oil_in**2) - m_oil_start * 0.8184 * T_oil_in -
    m_ORC_start * (h_SI_start[4]-h_SI_start[3])]
    T_oil_p_start = np.roots(coeff)[1]
    dT_oil_ORC_p_start = T_oil_p_start - T_high_ev_start
    #calculation of pinch point at evaporator/preheater) at max
    allowable pressure and max allowable oil outlet temperature.
    T_superheat = 0
    p_high_start_vec = np.array([])
    p_low_start_vec = np.array([])
```

```
z = (T_high_ev_start - T_cool_out)/3.0 #it turned out this ia a
proper guess value for almost all cases experienced in parameter
study
if T_oil_in < T_cool_out + z:
    guess_value_start_p_high = REFPROP.TQFLSH(T_oil_in ,0,1)[1]
else:
    guess_value_start_p_high =
    REFPROP.TQFLSH((T_oil_in+T_high_ev_start)/2.0 ,0,1)[1]
    p_high_start_vec =
    np.append(p_high_start_vec,guess_value_start_p_high)
    p_low_start_vec = np.append(p_low_start_vec,
    REFPROP.TQFLSH(T_cool_out + dT_cool_p_seek ,0,1)[1]-1)
while (True):
#while loop is applied to predefine superheating configuration
    if dT_oil_ORC_p_start >= dT_oil_ORC_p_seek and p_high_start >
    p_low:
            p_high = p_high_start

            def y1(p_low):
                "y1 = f(p_low)"
                global p_high
                …
                p_high = p_high_start
                Q_input = m_flue *(cpi_flue_in * T_flue_in -
                cpi_flue_out* T_flue_out)
                T_high_ev = T_high_ev_start
                dT_oil_ORC_p = dT_oil_ORC_p_seek
                T_oil_p = T_high_ev + dT_oil_ORC_p
                T_SI_6 = T_superheat + T_high_ev
                h_SI, s_SI, T_SI, w_t, w_p, w_net, eta_th =
                ORC_superheated(T_SI_6, p_high, p_low, eta_e_t,
                eta_e_p, eta_m_t, eta_m_p, eta_s_p, eta_s_t,
                dp_2_3, dp_6_7, T_subcool_cond)
                m_ORC  = Q_input/(h_SI[6]-h_SI[3])
                m_oil = m_ORC*(h_SI[4]-h_SI[3])/
                (0.0018*(T_oil_p**2-T_oil_in**2)+0.8184*(T_oil_p-
                T_oil_in))
```

```
            coeff = [m_oil*0.0018, 0.8184*m_oil, - (m_oil *
            0.0018 * T_oil_in**2) - m_oil * 0.8184 * T_oil_in
            - Q_input]
            T_oil_out = np.roots(coeff)[1]
            dT_oil_superheat = T_oil_out-T_SI[6]
            #cooling states
            m_cool = m_ORC * (h_SI[8]-
            h_SI[1])/(cp_cool*(T_cool_out - T_cool_in))
            T_cool_p = m_ORC/(m_cool*cp_cool) *(h_SI[9] -
            h_SI[1]) + T_cool_in
            dT_cool_p = T_SI[9] - T_cool_p
            return abs(dT_cool_p-dT_cool_p_seek)
            #optimization by Brent: Given a function of one-
            variable and a possible bracketing interval,
            return the minimum of the function isolated to a
            fractional precision of tol.
            #The Brent method uses Brent's algorithm for
            locating a minimum.
        lower_bound = p_min
        upper_bound = REFPROP.TQFLSH(T_cool_out +
        dT_cool_p_seek ,0,1)[1]
        guess_value = REFPROP.TQFLSH(T_cool_out +
        dT_cool_p_seek ,0,1)[1]-1
        p_low = brent(y1, brack
        =(lower_bound,guess_value,upper_bound), tol=0.000001)
else:
        def y2(x):
            "y2 = f(p_low, p_high)"
            global p_high
            …
            p_high = x[0]
            p_low = x[1]
            Q_input = m_flue *(cpi_flue_in * T_flue_in -
            cpi_flue_out* T_flue_out)
            T_high_ev = REFPROP.PQFLSH(p_high,0,1)[1]
            T_oil_out = T_oil_out_start
            m_oil = Q_input/(0.0018*(T_oil_out**2-
            T_oil_in**2)+0.8184*(T_oil_out-T_oil_in))
            T_SI_6 = T_superheat + T_high_ev
```

```
                h_SI, s_SI, T_SI, w_t, w_p, w_net, eta_th =
                ORC_superheated(T_SI_6, p_high, p_low, eta_e_t,
                eta_e_p, eta_m_t, eta_m_p, eta_s_p, eta_s_t,
                dp_2_3, dp_6_7, T_subcool_cond)
                m_ORC  = Q_input/(h_SI[6]-h_SI[3])
                coeff = [m_oil*0.0018, 0.8184*m_oil, - (m_oil *
                0.0018 * T_oil_in**2) - m_oil * 0.8184 * T_oil_in
                - m_ORC * (h_SI[4]-h_SI[3])]
                T_oil_p = np.roots(coeff)[1]
                dT_oil_ORC_p = T_oil_p - T_high_ev #calculation of
                pinch point at evaporator (preheater)
                #cooling states
                m_cool = m_ORC * (h_SI[8]-
                h_SI[1])/(cp_cool*(T_cool_out - T_cool_in))
                T_cool_p = m_ORC/(m_cool*cp_cool) *(h_SI[9] -
                h_SI[1]) + T_cool_in
                dT_cool_p = T_SI[9] - T_cool_p
                return abs(dT_oil_ORC_p - dT_oil_ORC_p_seek), \
                       abs(dT_cool_p-dT_cool_p_seek)
        guess_value_p_low = p_low_start_vec[0]
        guess_value_p_high = p_high_start_vec[0]
        p_high, p_low = fsolve(y2, x0=[guess_value_p_high,
        guess_value_p_low
        p_high_start_vec[0] = p_high
        p_low_start_vec[0] = p_low
 #calculation of kA values and exergy destruction
P_cycle = m_ORC *(abs(w_t)-w_p)
P_cycle_vec = np.append(P_cycle_vec, P_cycle)
if T_oil_out == T_oil_out_start and T_SI[6] < (T_oil_out-
dT_oil_ORC_p_seek) and T_oil_out <= T_oil_out_start and
p_high > p_low:
       T_superheat = T_superheat + 1
elif p_high == p_high_start and T_SI[6] < (T_oil_out-
dT_oil_ORC_p_seek) and T_oil_out <= T_oil_out_start
       T_superheat = T_superheat + 1
else:
       P_cycle_vec = np.delete(P_cycle_vec,-1)
       …
break
```

11.3 GUI programming in PYTHON

11.3.1 File structure and linking of GUIs

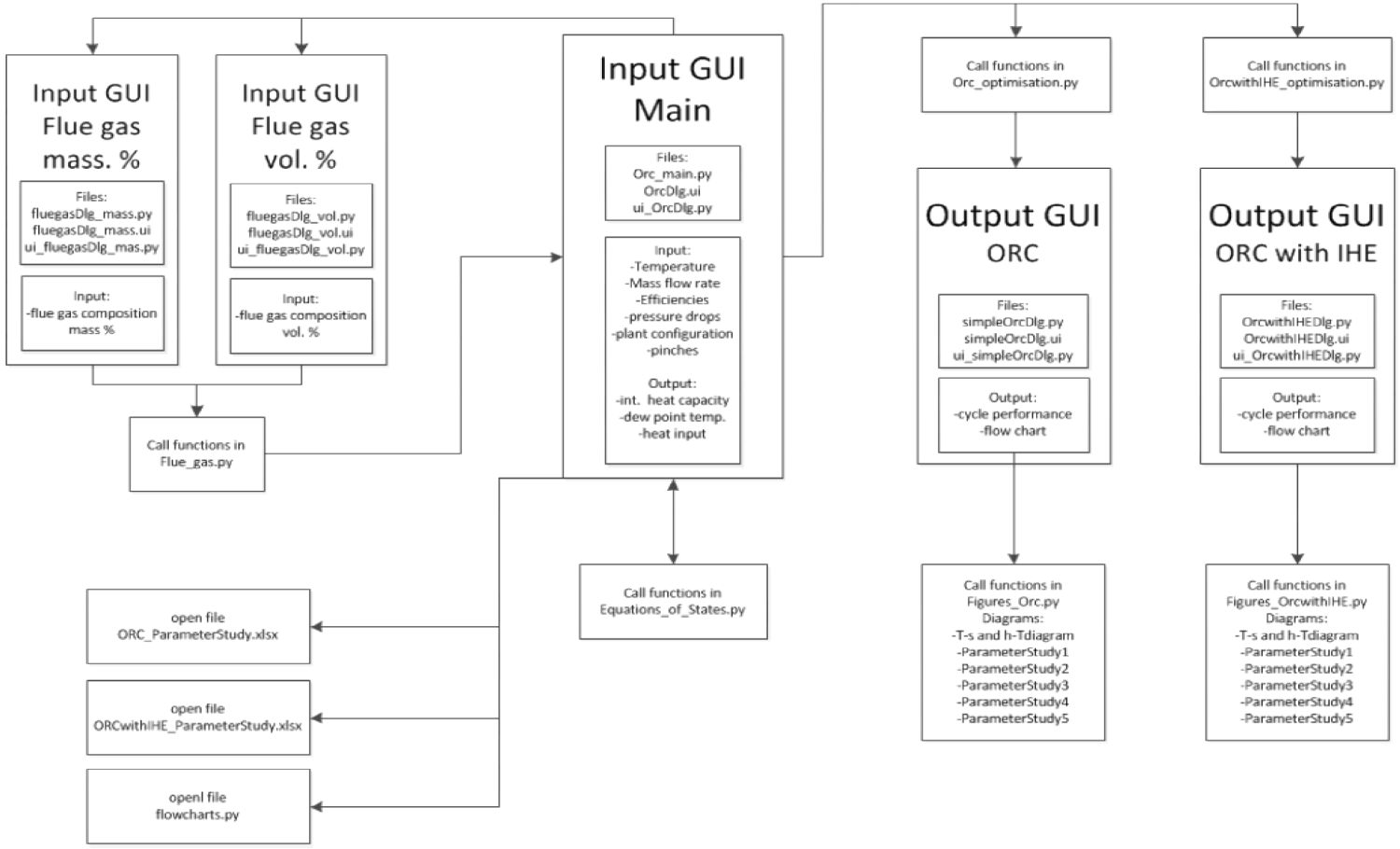

Fig. 28: File structure of the main program. Figure shows how the GUIs interact with each other and what files are invoked

11.3.2 Optimisation along two different constant pressure levels for Isobutane without consideration of pinch restrictions

The optimisation at constant pressure levels should show how the thermo physical properties impact the thermal efficiency. The pinch point restrictions have not been considered in this study. Therefore the interaction of a cycle with the heat source and sink is out of focus. The study has been carried out for the following pressure levels:

- p_{low} = 0.56299254 MPa
- p_{high} = 2 MPa

The isentropic efficiencies have been set to 1 for the turbine as well as the pump. Isobutane has been used as working fluid. The results are presented in Table 33 and Fig. 29. The nomenclature of variables with respect to the states used in Table 33 refers to Fig. 30.

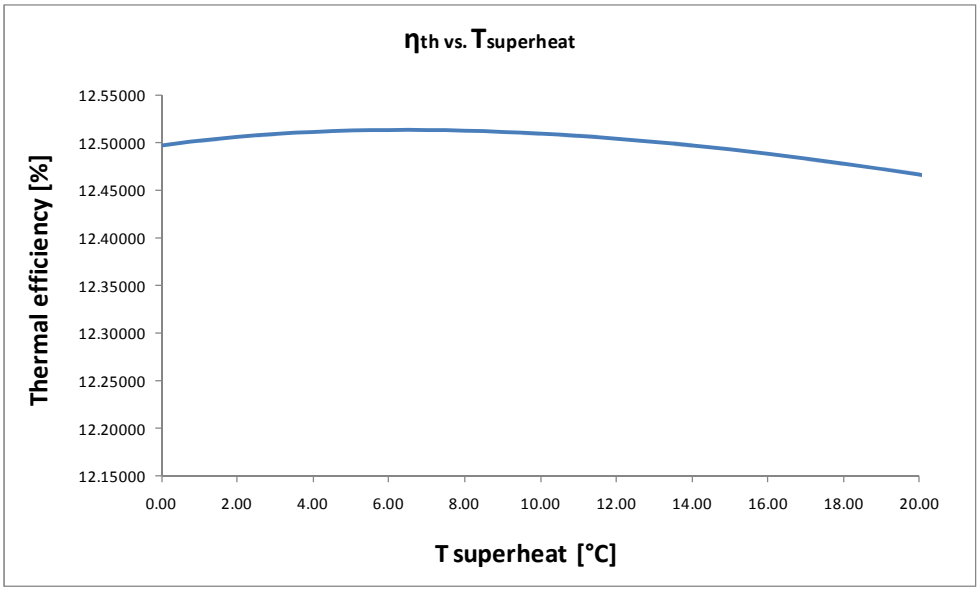

Fig. 29: Thermal efficiency vs. applied superheating temperature

The study shows that the peak in thermal efficiency originates from thermodynamic properties of Isobutane. For Isobutane the Equation of State correlations of [9] have been implemented into the PYTHON program. The improvement due to superheating mainly depends on enthalpy differences that define specific heat input and specific heat rejection. The interaction of enthalpy differences and how they influence the efficiency is extremely sensitive. It was shown for Isobutane that superheating leads to a slight enhanced cycle efficiency. If such small benefit in efficiency is obtained by applied superheating the flue gas quantity is crucial in terms of economics and the final decision of plant design. Nevertheless superheating mostly does not lead to better performance when other substances are used.

Appendix

T_6 [K]	$T_{sup.}$ [K]	h_1 [kJ/kg]	h_2 [kJ/kg]	h_3 [kJ/kg]	h_4 [kJ/kg]	h_5 [kJ/kg]	h_6 [kJ/kg]	h_7 [kJ/kg]	h_5-h_2 [kJ/kg]	h_6-h_1 [kJ/kg]	η_{th} [%]	wt [kJ/kg]
373.51	0	301.96	304.67	467.08	677.23	677.23	627.96	610.73	372.56	326.00	12.49777	49.28
374.51	1	301.96	304.67	467.08	677.23	680.18	630.52	610.73	375.50	328.56	12.50278	49.66
375.51	2	301.96	304.67	467.08	677.23	683.09	633.05	610.73	378.41	331.09	12.50676	50.04
376.51	3	301.96	304.67	467.08	677.23	685.97	635.55	610.73	381.29	333.59	12.50980	50.41
377.51	4	301.96	304.67	467.08	677.23	688.81	638.04	610.73	384.14	336.08	12.51198	50.78
378.51	5	301.96	304.67	467.08	677.23	691.63	640.50	610.73	386.96	338.54	12.51336	51.14
379.51	6	301.96	304.67	467.08	677.23	694.43	642.94	610.73	389.76	340.98	12.51400	51.49
380.51	7	301.96	304.67	467.08	677.23	697.21	645.37	610.73	392.53	343.41	12.51395	51.84
381.51	8	301.96	304.67	467.08	677.23	699.96	647.78	610.73	395.29	345.82	12.51326	52.18
382.51	9	301.96	304.67	467.08	677.23	702.70	650.18	610.73	398.02	348.22	12.51197	52.51
383.51	10	301.96	304.67	467.08	677.23	705.41	652.57	610.73	400.74	350.61	12.51012	52.85
384.51	11	301.96	304.67	467.08	677.23	708.11	654.94	610.73	403.44	352.98	12.50774	53.18
385.51	12	301.96	304.67	467.08	677.23	710.80	657.30	610.73	406.13	355.34	12.50486	53.50
386.51	13	301.96	304.67	467.08	677.23	713.48	659.66	610.73	408.80	357.70	12.50152	53.82
387.51	14	301.96	304.67	467.08	677.23	716.14	662.00	610.73	411.46	360.04	12.49773	54.14
388.51	15	301.96	304.67	467.08	677.23	718.79	664.34	610.73	414.11	362.38	12.49353	54.45
389.51	16	301.96	304.67	467.08	677.23	721.43	666.66	610.73	416.75	364.70	12.48894	54.76
390.51	17	301.96	304.67	467.08	677.23	724.05	668.98	610.73	419.38	367.03	12.48397	55.07
391.51	18	301.96	304.67	467.08	677.23	726.67	671.30	610.73	422.00	369.34	12.47864	55.37
392.51	19	301.96	304.67	467.08	677.23	729.28	673.61	610.73	424.61	371.65	12.47298	55.68
393.51	20	301.96	304.67	467.08	677.23	731.89	675.91	610.73	427.21	373.95	12.46700	55.97

Table 33: Parameters of the optimisation study along two distinct pressure levels

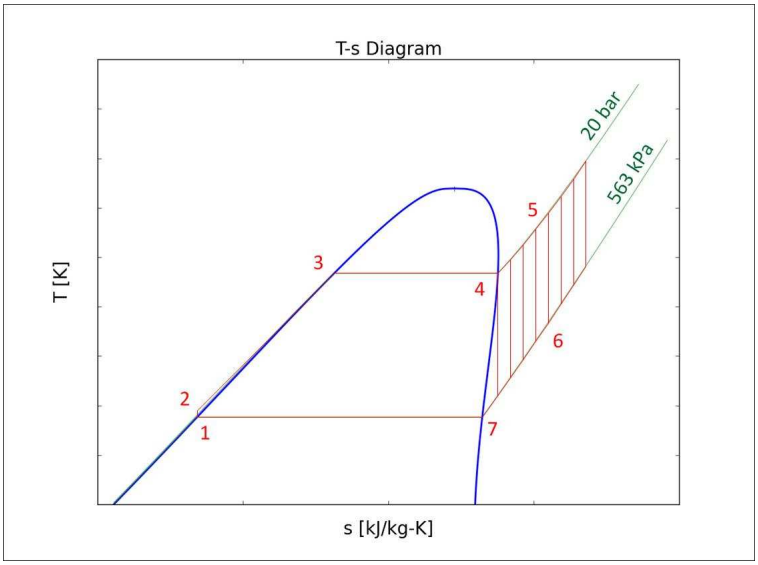

Fig. 30: Thermal efficiency optimisation along two constant pressure levels

It should also be mentioned that continuous increase of superheating causes even more spec. work output. This is shown in the figures in the last column in Table 33. Lukawski [36] has explained this behaviour in his thesis. In this work it was mentioned that there is only slight divergence of the entropy isolines in the gas phase in the p-h diagram of ORC working fluids in contrast to water. The spec. work output would increase more significantly if the same study would be carried out for water due to considerable more deviations of the isolines. However there is not only the work output that plays a role in thermal efficiency optimisation. While the work output increases due to the divergence of entropy isolines in case that additional superheating is applied, the specific heat input even rises. Therefore a certain trade off these parameters leads to optimum performance for working fluids used in ORC plants.

11.4 Parameter studies

11.4.1 Parameter studies of low critical point fluids

11.4.1.1 Isobutane

11.4.1.1.1 Basic ORC plant

ISOBUTANE	P [kW]	Tflue,in [°C]										
	Tflue,out [°C]	200	210	220	230	240	250	260	270	280	290	300
	100	315	483	583	639	690	740	790	841	891	942	993
	110	424	488	541	591	641	692	742	792	843	893	944
	120	393	443	493	543	593	643	693	743	794	845	895
	130	345	394	444	494	544	594	644	695	745	796	847
	140	294	343	392	442	492	541	591	641	692	742	792
	150	NA	NA	NA	NA	NA	NA	NA	NA	NA	NA	NA

Table 34: Power output for distinct flue gas temperature configurations for Isobutane

ISOBUTANE	ηth [%]	Tflue,in [°C]										
	Tflue,out [°C]	200	210	220	230	240	250	260	270	280	290	300
	100	6.12	8.51	9.41	9.5	9.52	9.52	9.52	9.52	9.52	9.52	9.52
	110	9.14	9.45	9.52	9.52	9.52	9.52	9.52	9.52	9.52	9.52	9.52
	120	9.5	9.52	9.52	9.52	9.52	9.52	9.52	9.52	9.52	9.52	9.52
	130	9.52	9.52	9.52	9.52	9.52	9.52	9.52	9.52	9.52	9.52	9.52
	140	9.45	9.45	9.45	9.45	9.45	9.45	9.45	9.45	9.45	9.45	9.45
	150	NA	NA	NA	NA	NA	NA	NA	NA	NA	NA	NA

Table 35: Thermal efficiency for distinct flue gas temperature configurations for Isobutane

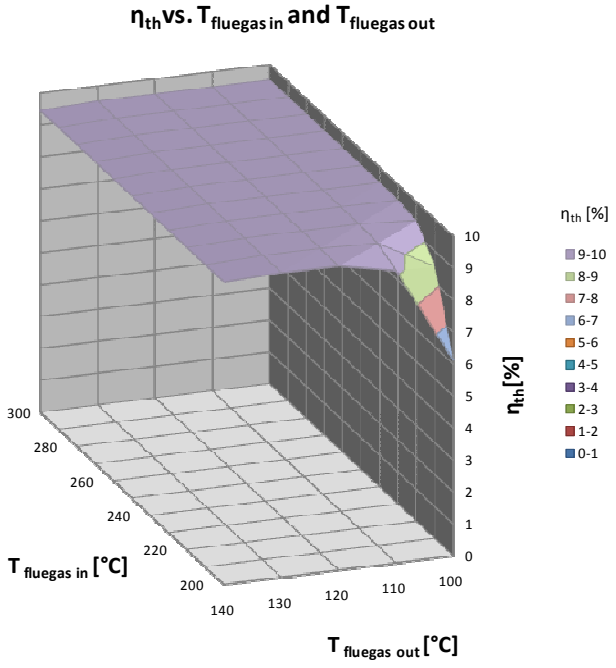

Fig. 31: Thermal efficiency vs. $T_{fluegas,in}$ and $T_{fluegas,out}$ for Isobutane

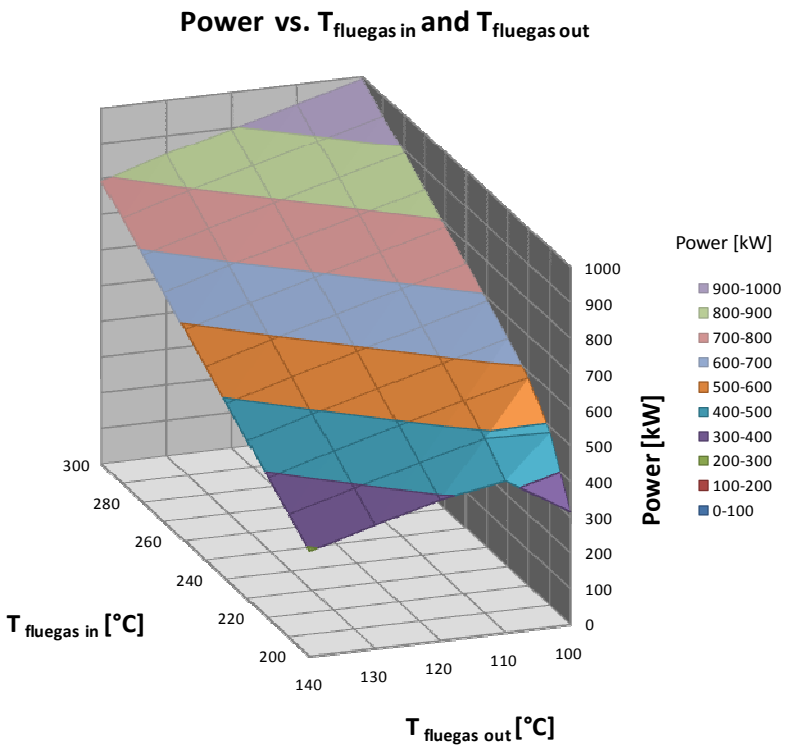

Fig. 32: Power output vs. $T_{fluegas,in}$ and $T_{fluegas,out}$ for Isobutane

11.4.1.1.2 ORC with IHE plant

	P [kW]	Tflue,in [°C]										
ISOBUTANE	Tflue,out [°C]	200	210	220	230	240	250	260	270	280	290	300
	110	419	499	566	636	692	747	801	855	910	965	1019
	120	407	473	542	610	675	732	789	846	904	961	1019
	130	381	447	514	580	648	711	771	832	892	953	1014
	140	354	419	484	550	616	682	746	809	873	936	1000
	150	NA	NA	NA	NA	NA	NA	NA	NA	NA	NA	NA

Table 36: Power output for distinct flue gas temperature configurations for Isobutane

	ηth [%]	Tflue,in [°C]										
ISOBUTANE	Tflue,out [°C]	200	210	220	230	240	250	260	270	280	290	300
	110	9.03	9.66	9.95	10.24	10.28	10.28	10.28	10.28	10.28	10.28	10.28
	120	9.84	10.17	10.47	10.7	10.83	10.83	10.83	10.83	10.83	10.83	10.83
	130	10.52	10.8	11.01	11.18	11.34	11.4	11.4	11.4	11.4	11.4	11.4
	140	11.38	11.54	11.66	11.77	11.84	11.91	11.93	11.93	11.93	11.93	11.93
	150	NA	NA	NA	NA	NA	NA	NA	NA	NA	NA	NA

Table 37: Thermal efficiency for distinct flue gas temperature configurations for Isobutane

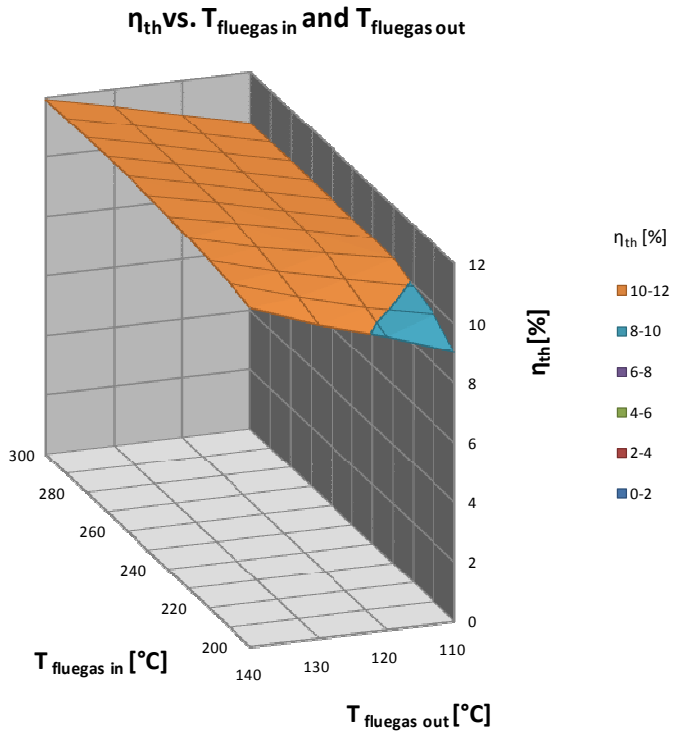

Fig. 33: Thermal efficiency vs. $T_{fluegas,in}$ and $T_{fluegas,out}$ for Isobutane

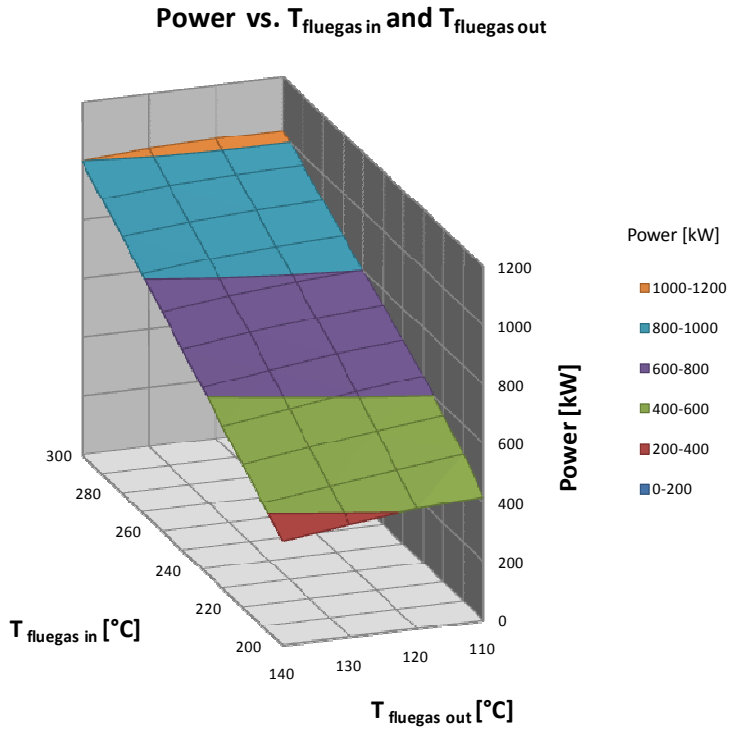

Fig. 34: Power output vs. $T_{fluegas,in}$ and $T_{fluegas,out}$ for Isobutane

11.4.1.2 Pentane

11.4.1.2.1 Basic ORC plant

	P [kW]	Tflue,in [°C]										
PENTANE	Tflue,out [°C]	200	210	220	230	240	250	260	270	280	290	300
	100	203	277	380	519	691	886	1097	1329	1434	1515	1597
	110	344	430	532	652	790	946	1117	1274	1355	1437	1518
	120	386	472	570	681	805	943	1096	1196	1277	1358	1440
	130	385	470	565	670	785	912	1036	1117	1198	1280	1362
	140	360	444	536	636	745	865	957	1039	1120	1201	1283
	150	320	402	492	588	693	798	879	960	1041	1122	1204

Table 38: Power output for distinct flue gas temperature configurations for Pentane

	ηth [%]	Tflue,in [°C]										
PENTANE	Tflue,out [°C]	200	210	220	230	240	250	260	270	280	290	300
	100	3.94	4.87	6.13	7.72	9.53	11.39	13.21	15.04	15.31	15.31	15.31
	110	7.42	8.32	9.35	10.49	11.73	13.01	14.34	15.31	15.31	15.31	15.31
	120	9.34	10.13	11	11.94	12.93	13.96	15.05	15.31	15.31	15.31	15.31
	130	10.64	11.35	12.1	12.9	13.74	14.62	15.31	15.31	15.31	15.31	15.31
	140	11.61	12.24	12.91	13.61	14.34	15.1	15.31	15.31	15.31	15.31	15.31
	150	12.36	12.93	13.52	14.15	14.79	15.31	15.31	15.31	15.31	15.31	15.31

Table 39: Thermal efficiency for distinct flue gas temperature configurations for Pentane

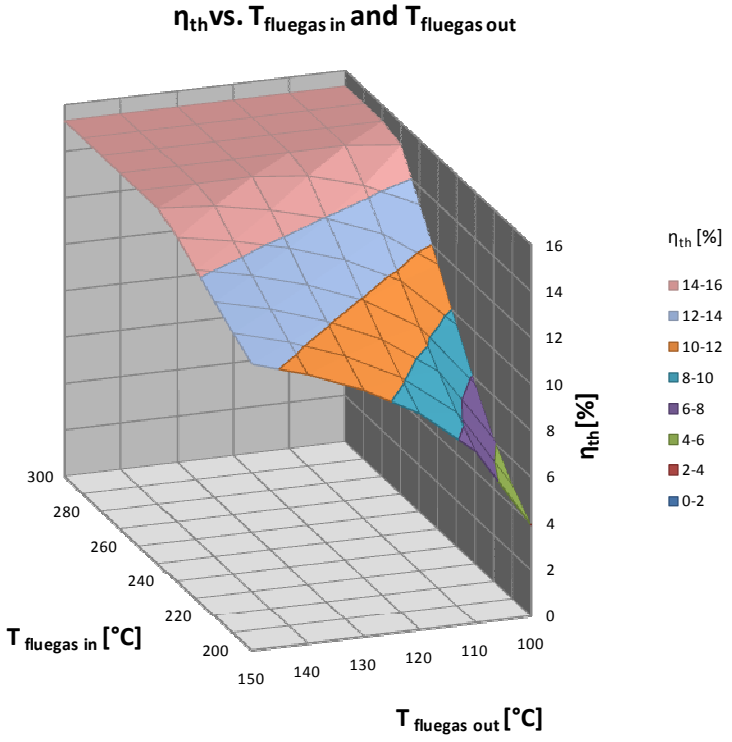

Fig. 35: Thermal efficiency vs. $T_{fluegas,in}$ and $T_{fluegas,out}$ for Pentane

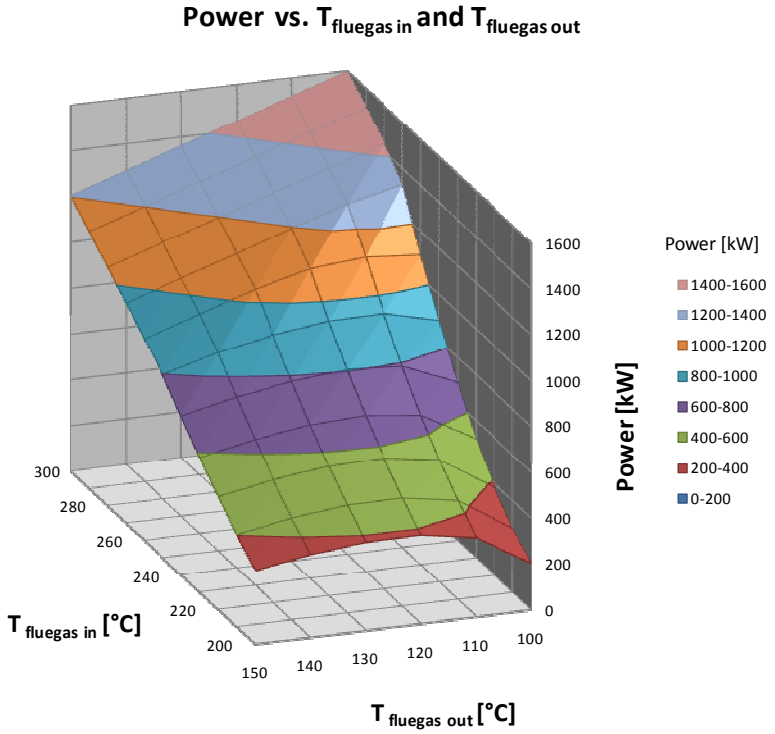

Fig. 36: Power output vs. $T_{fluegas,in}$ and $T_{fluegas,out}$ for Pentane

11.4.1.2.2 ORC with IHE plant

	P [kW]	Tflue,in [°C]										
PENTANE	Tflue,out [°C]	200	210	220	230	240	250	260	270	280	290	300
	110	327	399	484	584	702	842	1017	1285	1447	1534	1621
	120	373	452	542	646	766	906	1070	1271	1426	1517	1608
	130	383	466	560	665	785	922	1081	1264	1395	1492	1587
	140	368	453	548	654	773	906	1061	1199	1330	1454	1553
	150	335	421	517	622	738	868	1007	1133	1260	1386	1507

Table 40: Power output for distinct flue gas temperature configurations for Pentane

	ηth [%]	Tflue,in [°C]										
PENTANE	Tflue,out [°C]	200	210	220	230	240	250	260	270	280	290	300
	110	7.04	7.72	8.5	9.39	10.41	11.59	13.05	15.44	16.34	16.34	16.34
	120	9.01	9.7	10.47	11.34	12.31	13.41	14.69	16.27	17.09	17.09	17.09
	130	10.58	11.25	12	12.82	13.74	14.77	15.97	17.32	17.81	17.84	17.84
	140	11.85	12.5	13.21	14	14.86	15.83	16.96	17.68	18.19	18.53	18.53
	150	12.92	13.53	14.21	14.95	15.75	16.66	17.54	18.07	18.53	18.9	19.16

Table 41: Thermal efficiency for distinct flue gas temperature configurations for Pentane

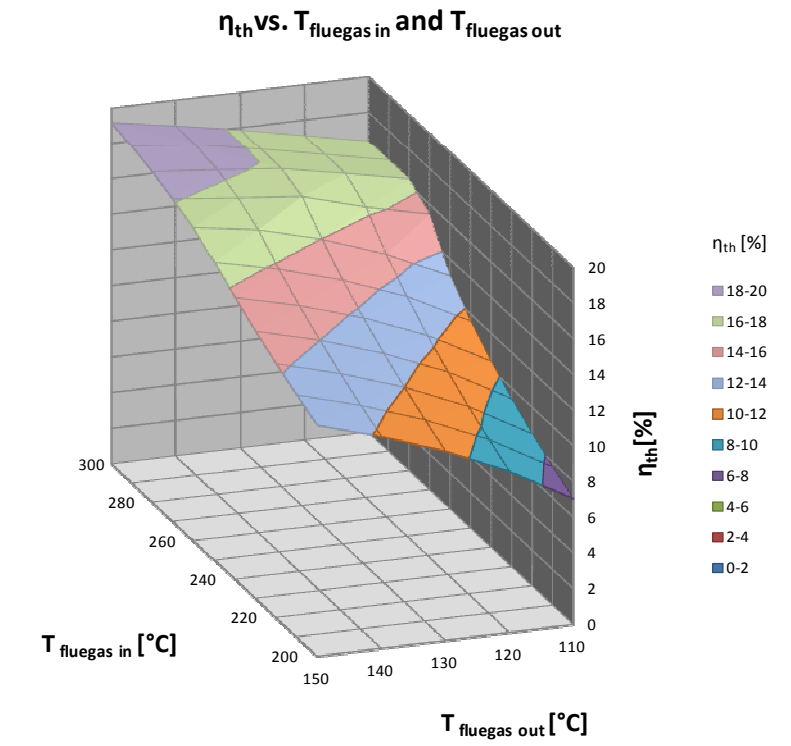

Fig. 37: Thermal efficiency vs. $T_{fluegas,in}$ and $T_{fluegas,out}$ for Pentane

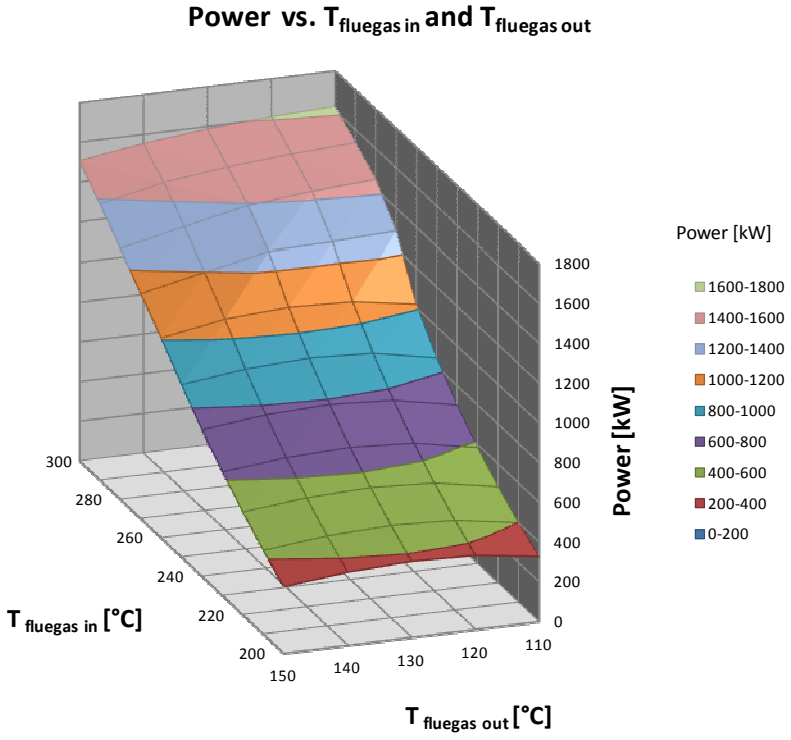

Fig. 38: Power output vs. $T_{fluegas,in}$ and $T_{fluegas,out}$ for Pentane

11.4.2 Parameter studies of high critical point fluids

11.4.2.1 Toluene

11.4.2.1.1 Basic ORC plant

	P [kW]	Tflue,in [°C]										
TOLUENE	Tflue,out [°C]	200	210	220	230	240	250	260	270	280	290	300
	100	139	163	189	218	257	319	401	511	658	847	1076
	110	261	311	369	437	516	609	718	845	992	1160	1348
	120	331	394	466	546	636	737	851	978	1120	1277	1447
	130	357	428	506	592	687	792	907	1033	1170	1318	1478
	140	352	428	511	601	698	804	919	1043	1176	1319	1472
	150	325	405	491	583	682	788	902	1024	1155	1293	1440

Table 42: Power output for distinct flue gas temperature configurations for Toluene

	ηth [%]	Tflue,in [°C]										
TOLUENE	Tflue,out [°C]	200	210	220	230	240	250	260	270	280	290	300
	100	2.7	2.87	3.05	3.23	3.54	4.1	4.83	5.78	7.02	8.55	10.32
	110	5.61	6.02	6.49	7.03	7.66	8.38	9.21	10.15	11.2	12.36	13.59
	120	8.01	8.48	8.99	9.57	10.21	10.91	11.68	12.52	13.43	14.38	15.38
	130	9.85	10.33	10.85	11.42	12.03	12.69	13.39	14.15	14.94	15.77	16.62
	140	11.33	11.8	12.31	12.85	13.43	14.04	14.69	15.37	16.08	16.81	17.56
	150	12.56	13.01	13.5	14.01	14.55	15.12	15.72	16.34	16.98	17.64	18.31

Table 43: Thermal efficiency for distinct flue gas temperature configurations for Toluene

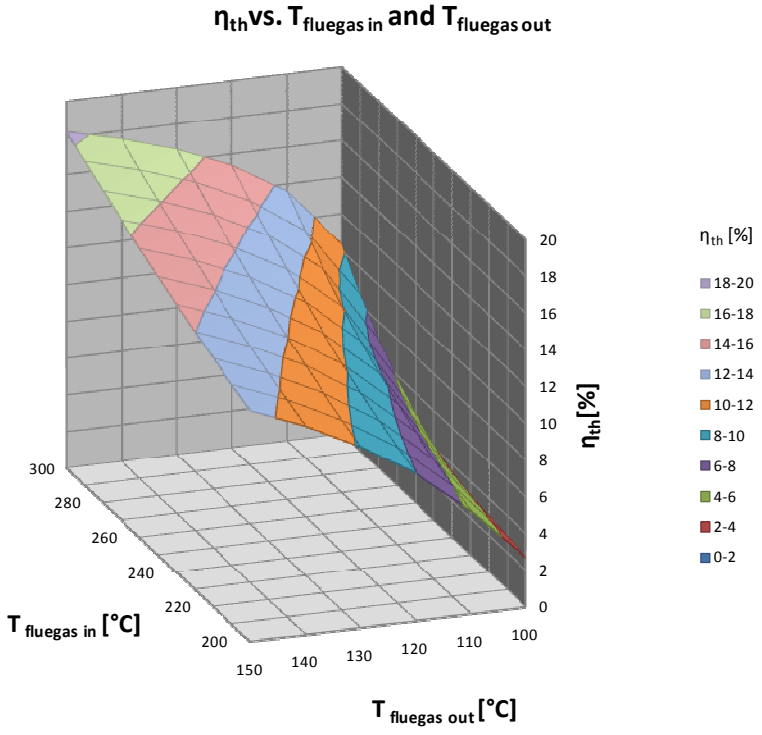

Fig. 39: Thermal efficiency vs. $T_{fluegas,in}$ and $T_{fluegas,out}$ for Toluene

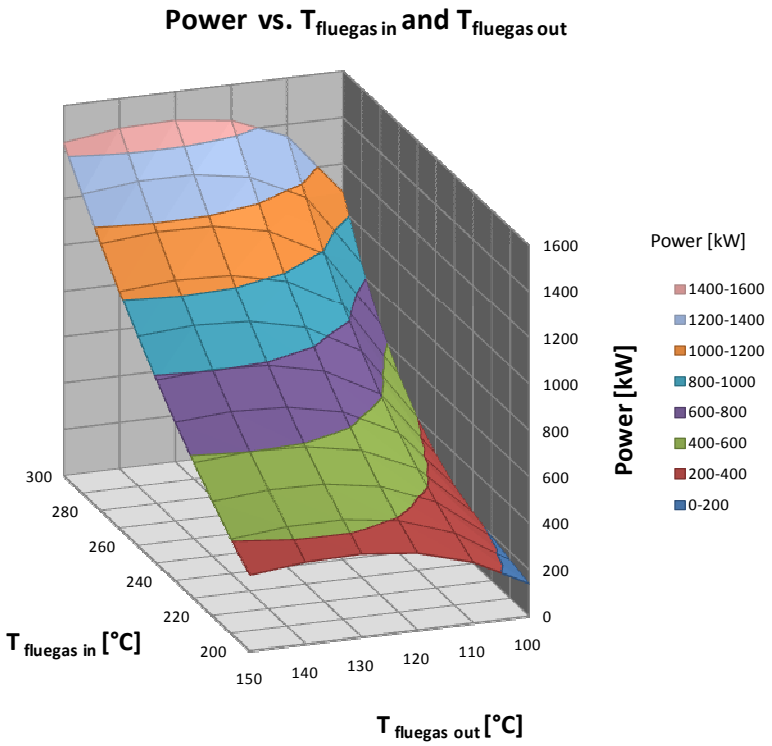

Fig. 40: Power output vs. $T_{fluegas,in}$ and $T_{fluegas,out}$ for Toluene

11.4.2.1.2 ORC with IHE plant

	P [kW]	Tflue,in [°C]										
TOLUENE	Tflue,out [°C]	200	210	220	230	240	250	260	270	280	290	300
	110	NA	NA	NA	NA	NA	608	704	812	934	1072	1226
	120	NA	394	463	539	623	717	820	935	1061	1201	1354
	130	355	425	501	584	675	774	882	1000	1129	1270	1423
	140	352	428	509	597	692	795	907	1028	1158	1299	1451
	150	331	409	494	586	684	790	904	1027	1158	1299	1450

Table 44: Power output for distinct flue gas temperature configurations for Toluene

	ηth [%]	Tflue,in [°C]										
TOLUENE	Tflue,out [°C]	200	210	220	230	240	250	260	270	280	290	300
	110	NA	NA	NA	NA	NA	8.37	9.03	9.76	10.55	11.42	12.36
	120	NA	8.46	8.94	9.45	10.01	10.61	11.26	11.96	12.72	13.53	14.4
	130	9.81	10.26	10.74	11.26	11.81	12.4	13.03	13.7	14.42	15.19	15.99
	140	11.33	11.78	12.26	12.77	13.31	13.89	14.5	15.15	15.83	16.55	17.31
	150	12.77	13.13	13.58	14.08	14.61	15.17	15.75	16.37	17.03	17.71	18.43

Table 45: Thermal efficiency for distinct flue gas temperature configurations for Toluene

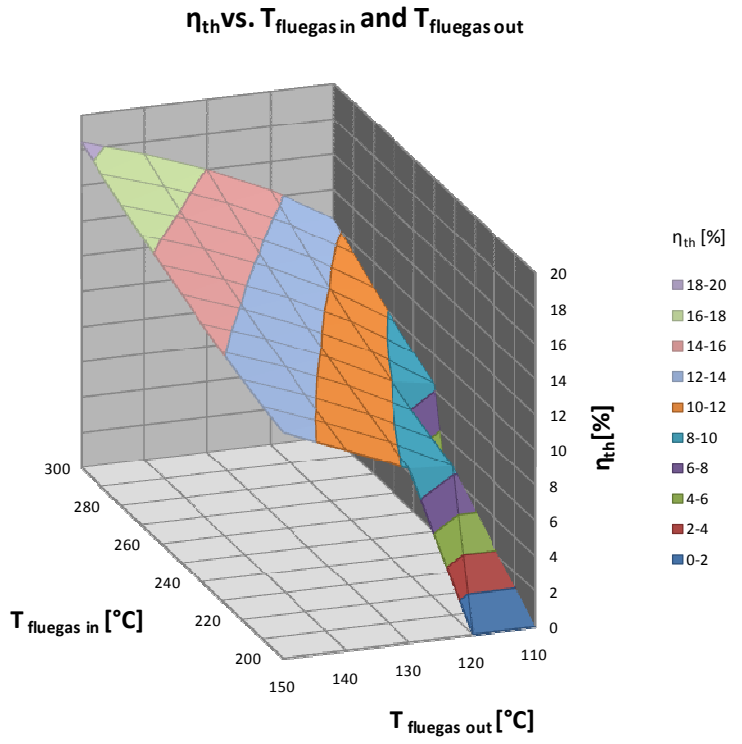

Fig. 41: Thermal efficiency vs. $T_{fluegas,in}$ and $T_{fluegas,out}$ for Toluene

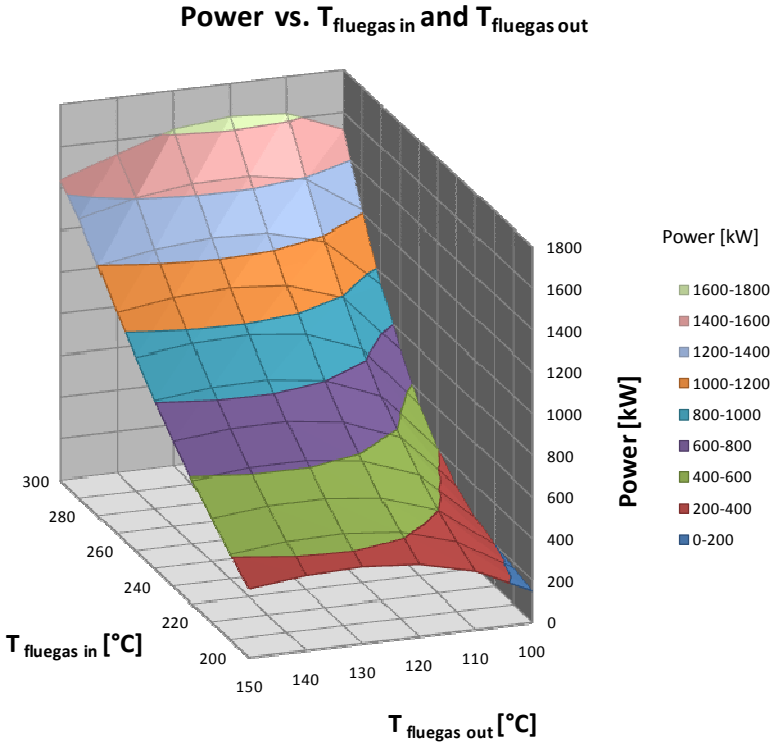

Fig. 42: Power output vs. $T_{fluegas,in}$ and $T_{fluegas,out}$ for Toluene

11.4.2.2 Cyclohexane

11.4.2.2.1 Basic ORC plant

CYCLOHEXANE	P [kW]	Tflue,in [°C]										
	Tflue,out [°C]	200	210	220	230	240	250	260	270	280	290	300
	100	147	174	214	274	354	466	616	808	1033	1277	1526
	110	286	347	419	505	607	727	866	1025	1202	1392	1591
	120	350	422	503	595	699	817	948	1093	1250	1418	1595
	130	368	445	530	624	728	843	968	1104	1249	1404	1567
	140	357	437	523	618	721	833	954	1083	1221	1367	1520
	150	325	407	495	589	691	801	918	1043	1175	1314	1459

Table 46: Power output for distinct flue gas temperature configurations for Cyclohexane

CYCLOHEXANE	ηth [%]	Tflue,in [°C]										
	Tflue,out [°C]	200	210	220	230	240	250	260	270	280	290	300
	100	2.85	3.06	3.46	4.07	4.89	5.99	7.42	9.15	11.03	12.9	14.63
	110	6.15	6.71	7.36	8.12	9	10	11.12	12.32	13.57	14.83	16.04
	120	8.48	9.06	9.71	10.44	11.23	12.1	13.02	13.99	14.99	15.98	16.95
	130	10.18	10.75	11.36	12.03	12.74	13.5	14.3	15.12	15.96	16.79	17.62
	140	11.5	12.04	12.61	13.22	13.87	14.55	15.25	15.97	16.69	17.42	18.13
	150	12.56	13.07	13.6	14.17	14.75	15.36	15.99	16.63	17.27	17.91	18.55

Table 47: Thermal efficiency for distinct flue gas temperature configurations for Cyclohexane

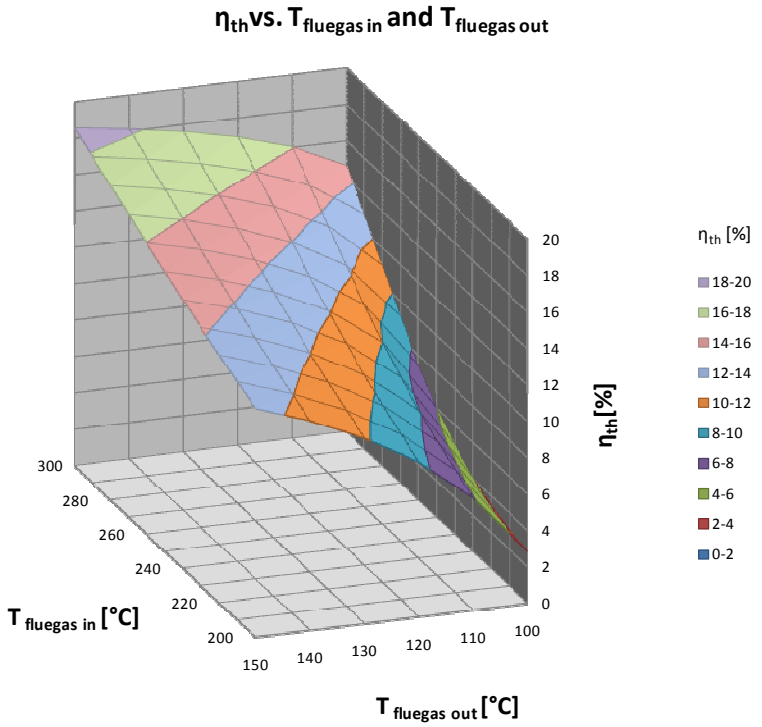

Fig. 43: Thermal efficiency vs. $T_{fluegas,in}$ and $T_{fluegas,out}$ for Cyclohexane

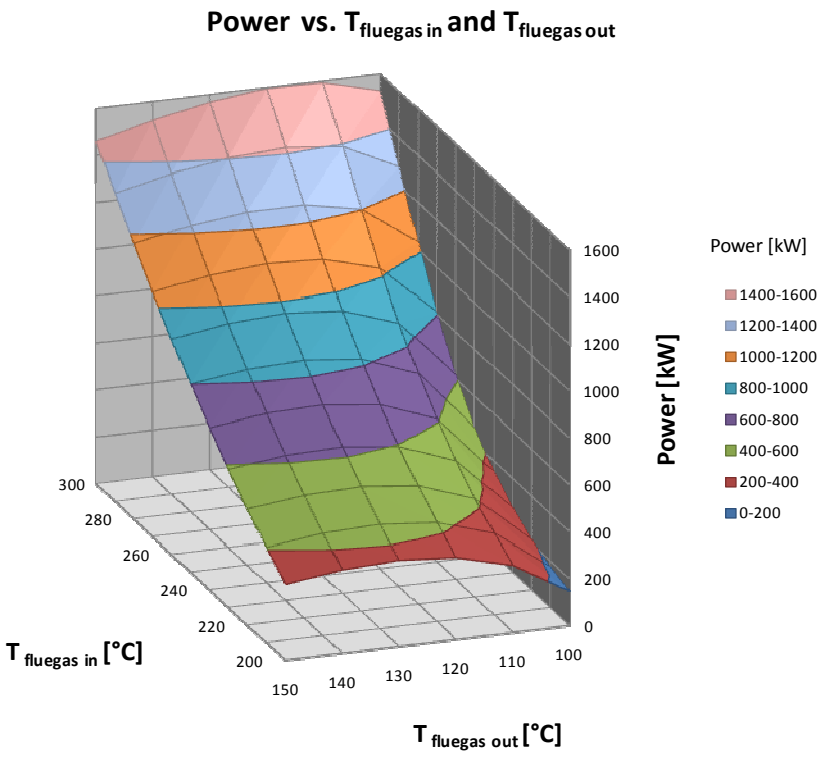

Fig. 44: Power output vs. $T_{fluegas,in}$ and $T_{fluegas,out}$ for Cyclohexane

11.4.2.2.2 ORC with IHE plant

	P [kW]	Tflue,in [°C]										
CYCLOHEX	Tflue,out [°C]	200	210	220	230	240	250	260	270	280	290	300
	110	NA	344	409	484	569	666	778	905	1050	1215	1400
	120	344	411	485	569	662	766	883	1013	1158	1320	1499
	130	364	438	519	608	707	815	934	1065	1210	1368	1543
	140	358	437	523	616	717	828	949	1080	1224	1380	1550
	150	332	414	503	599	703	816	937	1068	1211	1364	1531

Table 48: Power output for distinct flue gas temperature configurations for Cyclohexane

	ηth [%]	Tflue,in [°C]										
CYCLOHEX	Tflue,out [°C]	200	210	220	230	240	250	260	270	280	290	300
	110	NA	6.66	7.19	7.78	8.44	9.17	9.98	10.88	11.86	12.94	14.11
	120	8.32	8.82	9.37	9.98	10.63	11.35	12.12	12.97	13.88	14.87	15.93
	130	10.07	10.58	11.13	11.72	12.36	13.06	13.8	14.16	15.45	16.37	17.34
	140	11.54	12.05	12.59	13.17	13.8	14.46	15.17	15.92	16.73	17.58	18.49
	150	12.83	13.31	13.85	14.41	15.01	15.65	16.32	17.04	17.8	18.61	19.46

Table 49: Thermal efficiency for distinct flue gas temperature configurations for Cyclohexane

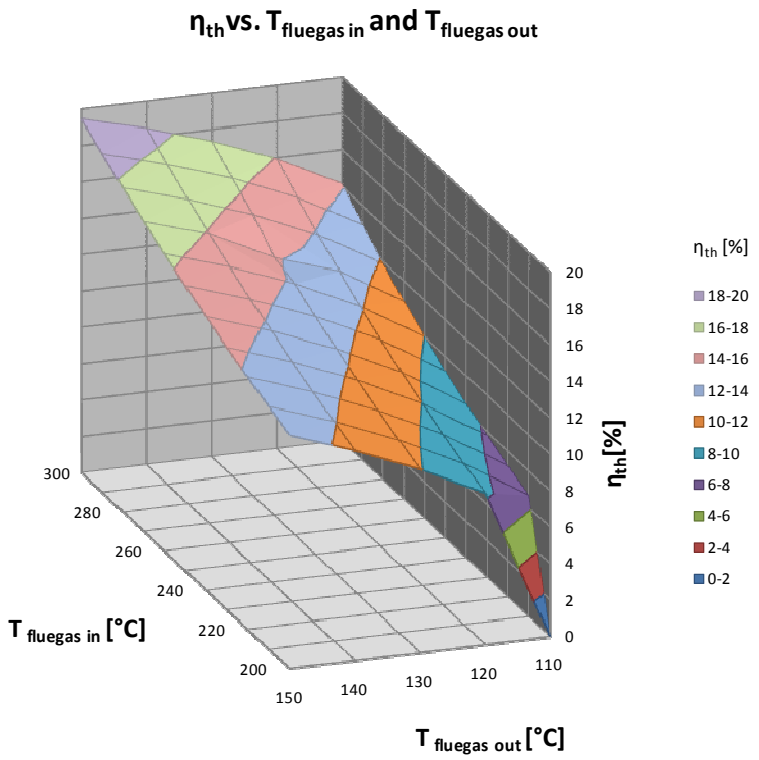

Fig. 45. Thermal efficiency vs. $T_{fluegas,in}$ and $T_{fluegas,out}$ for Cyclohexane

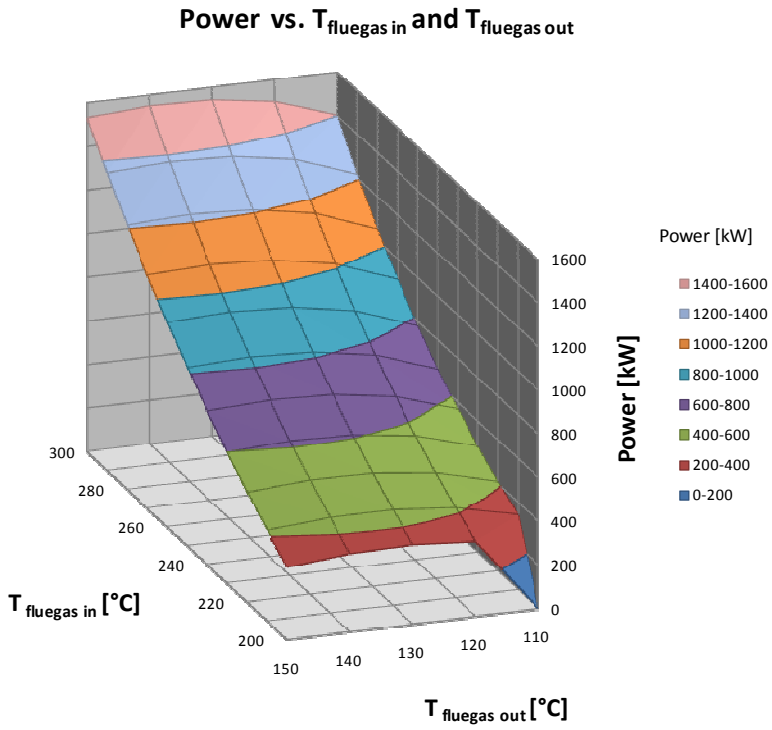

Fig. 46: Power output vs. $T_{fluegas,in}$ and $T_{fluegas,out}$ for Cyclohexane

11.5 Parameter study for case study

11.5.1 Parameter study for basic ORC

	ηth [%]	Tflue,in [°C]																
ALL FLUIDS	Tflue,out [°C]	220	280	300	220	280	300	220	280	300	220	280	300	220	280	300	220	280	300
	100	11.85	11.85	11.85	12.1	16.42	16.42	11.84	17.22	17.22	NA	NA	NA	9.79	16.08	18.35	9.43	15.93	18.75
	110	11.85	11.85	11.85	13.29	16.42	16.42	13.16	17.22	17.22	NA	NA	NA	11.87	17.21	19.08	11.62	17.29	19.63
	120	11.85	11.85	11.85	14.13	16.42	16.42	14.1	17.22	17.22	NA	NA	NA	13.37	18.04	19.64	13.23	18.26	20.22
	130	11.84	11.84	11.84	14.76	16.42	16.42	14.8	17.22	17.22	NA	NA	NA	14.54	18.69	20.09	14.47	18.99	20.31
	140	11.75	11.75	11.75	15.26	16.42	16.42	15.36	17.22	17.22	NA	NA	NA	15.47	19.21	20.46	15.47	19.56	20.37
	150	NA	NA	NA	15.67	16.42	16.42	15.82	17.22	17.22	NA	NA	NA	16.25	19.64	20.78	16.29	20.02	20.4
		ISOBUTANE			IPENTANE			PENTANE			TOLUENE			CYCLOHEXANE			CYCLOPENTANE		

Table 50: Parameter study for basic ORC: Thermal efficiency for 220, 280 and 300 ℃ flue gas inlet tem perature

In certain cases when using Isobutane and Toluene as a working fluid, no results are obtainable. If a flue gas outlet temperature of 150 ℃ is applied for Isobutane, the optimisation will take place along the 20 bar pressure isoline. The corresponding saturation temperature to that pressure level is around 100 ℃. If 10 ℃ are added because of the pinch point at the evaporator/preheater to thermal oil, the thermal oil temperature should be around 110 ℃. If minimum allowable temperature difference between flue gas outlet temperature and thermal oil inlet temperature is defined by 40 ℃ the thermal oil will not able to heat up (alm ost horizontal line in h,T diagram) due to the model set up in these cases. In the case of Toluene the condenser pressure level is far below 5 kPa and therefore the results have been excluded. In either case neither Isobutane nor Toluene would have shown optimum performance for those chosen temperature configurations. It has been mentioned in chapter 7 that the same settings except cooling temperatures have been applied for those parameter studies.

11.5.2 Parameter study for ORC with IHE

	ηth [%]	Tflue,in [°C]																
ALL FLUIDS	Tflue,out [°C]	220	280	300	220	280	300	220	280	300	220	280	300	220	280	300	220	280	300
	110	13.08	13.67	13.67	12.91	18.67	18.67	12.74	19.45	19.45	11.04	15.22	16.99	11.53	16.43	18.53	11.54	16.77	19.24
	120	13.67	14.3	14.3	14.26	19.4	19.4	14.14	20.12	20.24	12.73	16.73	18.38	13.18	17.81	19.76	13.15	18.1	20.4
	130	14.33	14.89	14.89	15.36	19.93	20.09	15.29	20.45	20.94	14.17	18	19.54	14.57	18.96	20.78	14.49	19.18	21.33
	140	13.03	13.03	13.03	16.27	20.31	20.72	16.23	20.82	21.6	15.43	19.09	20.55	15.77	19.95	21.65	15.64	20.08	21.93
	150	NA	NA	NA	17.06	20.72	21.24	17.05	21.22	21.95	16.69	20.06	21.44	16.85	20.8	22.4	16.82	20.83	22.4
		ISOBUTANE			IPENTANE			PENTANE			TOLUENE			CYCLOHEXANE			CYCLOPENTANE		

Table 51: Parameter study for ORC with IHE: Thermal efficiency for a flue gas inlet temperature of 220, 280 and 300 ℃

In the case of Isobutane no values for 150 ℃ flue gas outlet temperatures are returned again. The evaluations of Toluene are displayed in Table 51, but even these results are minor lower than the condenser pressure limit of 5 kPa. It can be noticed that Toluene does not supply best performance regardless of what kind of temperature configuration has been chosen for the evaluation.